Antigens of diagnostic relevance in autoimmunity: characterization, production strategies and immunoassays development .

UNIVERSITÀ
DEGLI STUDI
FIRENZE

DOTTORATO DI RICERCA IN

SCIENZE FARMACEUTICHE

CICLO XXVII

COORDINATORE Prof.ssa Teodori Elisabetta

Antigens of diagnostic relevance in autoimmunity: characterization, production strategies and immunoassays development

Settore Scientifico Disciplinare CHIM/08

Dottorando

Dott.ssa Pacini Giulia

Tutore

Prof. Rovero Paolo

Coordinatore

Prof.ssa Teodori Elisabetta

Anni 2012/2014

CONTENTS

CHAPTER 1: AUTOIMMUNITY & BIOMARKERS 1

AUTOIMMUNE DISEASES 2

Role of aberrant post translational modifications in autoimmunity 4

Relevance of biomarkers in autoimmunity 5

Strategies for antigenic probes production: recombinant versus synthetic 7

Strategies for auto-Ab detection: Enzyme-Linked ImmunoSorbent Assays (ELISA) 11

Chemical Reverse Approach applied to Multiple Sclerosis: CSF114(Glc) 12

AIM OF THE WORK 14

CHAPTER 2: MYELIN OLIGODENDROCYTE GLYCOPROTEIN 17

STRUCTURE AND FUNCTION OF MYELIN OLIGODENDROCYTE GLYCOPROTEIN 18

THE CONTROVERSIAL ROLE OF MOG IN AUTOIMMUNITY 21

Central nervous system autoimmune diseases in which MOG is putatively involved 21

Multiple Sclerosis (MS) 21

Experimental Autoimmune Encephalomyelitis (EAE) 22

Neuromyelitis Optica (NMO) 23

Role of MOG in central nervous system autoimmunity: first hypothesis and animal models contribution 24

MOG as putative auto-Ag in human CNS AID: an issue open to discussion 26

AIM OF THE WORK 32

PART I: IMMUNOLOGICAL ROLE OF MOG IN THE EAE MICE MODEL OF MS 36

Results & Discussion 37

First cohort: preliminary SP-ELISA screening on $rMOG_{1-117}(His)_6$, CSF114 and CSF114(Glc) 37

Second cohort: anti-$rMOG_{1-117}(His)_6$ IgM screening 38

Third cohort: $rMOG_{1-117}$ epitope mapping 39

Materials & Methods 41

Serum samples 41

Antigens 41

Enzyme-Linked Immunosorbent Assay (ELISA) 41

PART II: EVALUATION OF MOG-IgG AND CSF114(Glc)-IgG AS ADDITIONAL NMO BIOMARKERS 42

***Results & Discussion* 42**

***Materials & Methods* 44**

Serum samples 44

Antigens 44

Enzyme-Linked Immunosorbent Assay (ELISA) 44

PART III: IMMUNOLOGICAL ROLE OF MOG IN NMO-LIKE EAE RAT MODELS 45

***Results & Discussion* 45**

***Materials & Methods* 51**

Serum samples 51

Antigens 51

Enzyme-Linked Immunosorbent Assay (ELISA) 51

PART IV: OPTIMIZATION OF rMOG$_{1-117}$ PRODUCTION PROCESS 52

***Results & Discussion* 52**

***Materials & Methods* 54**

rMOG$_{1-117}$(His)$_6$ expression and purification protocol 54

pET-22rMOG$_{1-117}$(His)$_6$ plasmid 54

ER2566 cells transformation with pET-22rMOG$_{1-117}$(His)$_6$ 54

Precultures and Expression Test 55

Large-scale protein expression 55

Cell lysis and IB solubilization 55

Purification and refolding by affinity chromatography 56

rMOG$_{1-117}$(His)$_6$ expression and purification protocol optimization 57

BL21(DE3) cells chemical transformation with pET-22rMOG$_{1-117}$(His)$_6$ 57

Precultures and Expression Test 57

Large-scale protein expression 57

Evaluation of the best strategy for cell lysis and IB solubilization 58

Method #1 58

Method #2 58

Purification and refolding by affinity chromatography 59

PART V: SEMI-SYNTHESIS OF ABERRANTLY N-GLUCOSYLATED $hMOG_{1-117}$ 60

Results & Discussion ***60***

Materials & Methods ***64***

Chemical Transformation of DH5α cells with pET-22b and pMAT-(TEVconsensus)-(Cys^{35})$hMOG_{1-117}(His)_6$ *64*

Precultures and Midiprep of pET-22b and pMAT-(TEVconsensus)-(Cys^{35})$hMOG_{1-117}(His)_6$ *64*

Double Digestion of pET-22b and pMAT-(TEVconsensus)-(Cys^{35})$hMOG_{1-117}(His)_6$ *65*

Ligation of the digested fragments *66*

Chemical Transformation of DH5α and XL-10 cells with ligation products *67*

Colony picking and Colony PCR *67*

Miniprep of the ligation product *68*

Ligation validation: Double digestion and PCR of the prepped plasmids *69*

Ligation validation: Sequencing of the amplicons *70*

Chemical transformation of BL21Gold(DE3) cells with pET-22b-(TEVconsensus)-(Cys^{35})$hMOG_{1-117}(His)_6$ *70*

Colony picking and Colony PCR *71*

Precultures and Expression Test *71*

Evaluation of the best large-scale expression strategy *72*

Cell Lysis and IB Disruption *72*

Recombinant protein purification *73*

Mass Spectrometry analyses of the purified fractions *73*

$hMOG_{35-117}(His)_6$ cleavage trials with TEV *74*

(TEVconsensus)-(Cys^{35})$hMOG_{1-117}(His)_6$ cleavage trials with TEV: MALDI-MS analyses *74*

(TEVconsensus)-(Cys^{35})$hMOG_{1-117}(His)_6$ cleavage trials with TEV: HPLC analyses *75*

HPLC analyses on (TEVconsensus)-(Cys^{35})$hMOG_{1-117}(His)_6$ 75

HPLC analyses on cleavage reaction samples 75

$hMOG_{35-117}(His)_6$ cleavage trials with TEV: Buffers composition *76*

GENERIC METHODS **77**

Molecular Biology Generic Methods ***77***

Sodium Dodecyl Sulphate PolyAcrilamide Gel Electrophoresis (SDS-PAGE) *77*

Tricine-PAGE *78*

Agarose gel *79*

CHAPTER 3: ROLE OF PTM IN PRIMARY BILIARY CIRRHOSIS 81

PRIMARY BILIARY CIRRHOSIS 82
PBC immunopathogenesis: the key role of anti-mitochondrial Ab 83
Significance of lipoic acid cofactor in Ab recognition 87
AIM OF THE WORK 91
RESULTS & DISCUSSION 94
Importance of lipoyc acid and its chiral center 94
Role of lipoyl-K^{173} and the relevance of K^{173} exposition on the tip of the β-turn 95
Relevance of N-glucosylation in PBC autoimmunity 96
Search of an antigenic probe able to recognize disease-specific auto-Ab in PBC pts sera 98
CONCLUSIONS 101
MATERIALS & METHODS 105
Serum samples 105
Antigens 105
Enzyme-Linked Immunosorbent Assay (ELISA) 105
SUPPLEMENTARY DATA 106

BIBLIOGRAPHY 108

ABBREVIATIONS 120

CHAPTER 1: AUTOIMMUNITY & BIOMARKERS

AUTOIMMUNE DISEASES

The immune system is an extraordinary integrated network of chemical and cellular mediators, delegated to the organism defense against any form of external agent. As summarized in Figure 1, under normal conditions the immune system exhibits tolerance to self-molecules, and thus does not respond to elements expressed in endogenous tissues. When self-tolerance is lost, the immune system reacts against one or more of the body's own components, triggering a set of mechanisms that represent the hallmark of autoimmune diseases (AID).

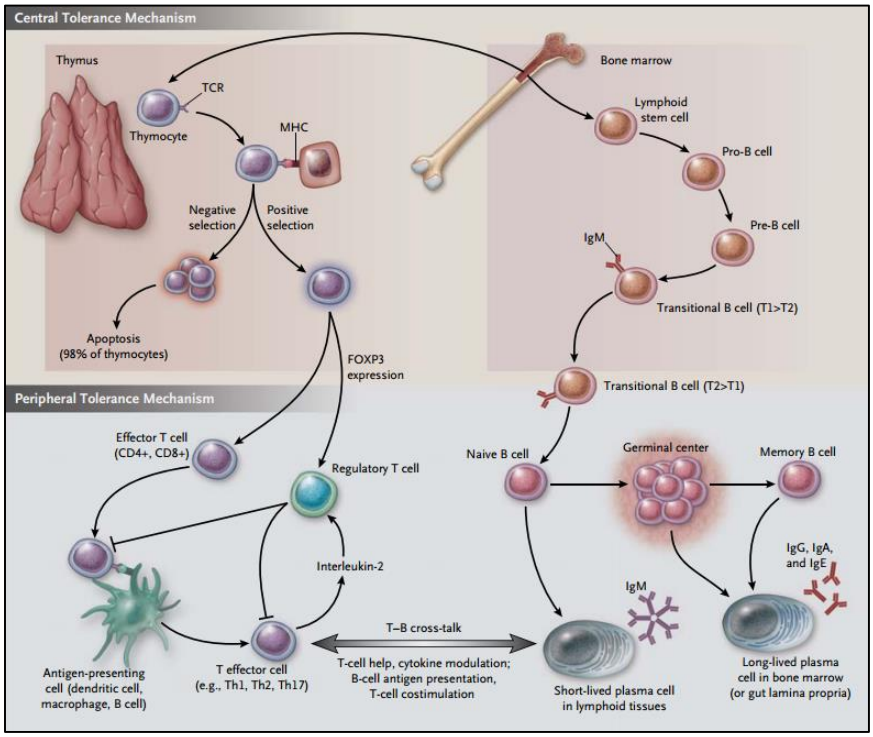

Figure 1: Central and Peripheral Tolerance Mechanisms[1].

AID are a collection of many complex and heterogeneous disorders, characterized by the aberrant reaction of the immune system against self. Such pathologies are classified as organ-specific, in which the immune response is predominantly or exclusively directed toward tissue-specific elements, or systemic, in which the loss of immune tolerance is directed toward systemic antigens (Ag) and disease manifestations can occur at a variety of different sites. It is estimated that AID afflict more than 8% of people worldwide[2], but the actual prevalence is predicted to be even higher because the extent of less common AID is possibly miscalculated due to the scarcity of epidemiological data[3]. Nearly 75% of AID patients (pts) are women[3], and the risk of developing an AID is about tenfold higher for women than for age-matched men, although there are exceptions (e.g. several autoimmune renal disorder)[4].

Even if the etiology of AID is still unknown, it is widely demonstrated that both onset and development are consequence of interaction between genetic and environmental factors[5]. It is known for decades that genetic predisposition to most AID involves genes within the major histocompatibility complex (MHC), reflecting the essential immunoregulatory effects of the human leukocyte Ag (HLA), but the exact mechanism that underlie these effects is still matter of debate. Recently, genome-wide association studies (GWAS) permitted to take remarkable steps forward in the genetics of AID: it was shown that more than 200 loci are associated with one or more AID. In many cases, the precise causal alleles or genes driving the associations were not identified, but it was demonstrated that some loci belong to categories of genes involved in: intracellular signaling regulating T- and B-cells activation; signaling by cytokines and cytokines receptors; pathways mediating innate immunity and microbial response[1]. Despite these recent progresses, much of the heritability of AID remains unaccounted for, disclosing that genes, alone, are not sufficient to trigger the disease, and that environmental factors play a key role in the autoimmune process. This hypothesis is supported by the largely incomplete concordance of AID in monozygotic twins[6].

Environmental risk factors associated with AID are numerous, as well as their possible mechanisms of action (summarized in Figure 2). In particular, both chemical and infectious agents are able to induce aberrant post-translational modifications (PTM) in self-Ag, contributing to tolerance breakdown.

Environmental factors that have been associated with autoimmune diseases
- Infectious agents (bacteria, viruses)
- Chemicals/xenobiotics
- Adjuvants
- Physical elements (ultraviolet radiation)

Possible mechanisms
- Polyclonal B cell activation;
- Direct effect impairing the immune response (*Th17 cells*);
- Effects on innate immunity (*TLR, adjuvants*);
- Direct interaction with regulatory cells (*T regulatory cells*);
- Modification of self antigens (*post-translational modifications*);
- Alterations of DNA methylation (*epigenetics*)

Figure 2: Environmental factors associated with AID and putative mechanisms involved in the breakdown of immune tolerance[7].

Role of aberrant post translational modifications in autoimmunity

As just mentioned, it was demonstrated that one of the mechanisms able to elicit the autoimmune reaction is represented by PTM, described as covalent addition of functional groups, or amino acids (Aa) conversions, that can be driven by enzymes or occur spontaneously (Table 1)[8,9]. PTM are frequently required for the biological function of numerous proteins, and occur during many physiological cellular events, e.g. ageing and cell replication: indeed, it is estimated that 50-90% of the human proteins are post-translationally modified[9]. The presence of aberrant PTM can result to changes in both functionality and immunogenicity of the protein, leading to the formation of neo-Ag. Effectively, PTM could induce immune tolerance breakdown through different mechanisms. Concerning T-cells autoimmune response, some PTM could not be present at the time of selection within the thymus, allowing autoreactive T-cells to migrate to the periphery, or else, proteins containing PTM could encounter a different Ag processing compared with the unmodified analog (Figure 3). In any case, T-cells response leans toward specificity to the modified self-Ag[10]. Conversely, B-cells response tends to be promiscuous, since antibodies (Ab) could be able to bind not only the modified but also the native self-Ag, leading to cross-reactivity. This is probably due to the conservation of the Aa flanking the modified site[10].

Modification	Aa altered
Additions	
Acetylation	Lys, Ser
Glycosylation	Asn, Ser
Hydroxylation	Pro, Lys
Methylation	Arg, Hys, Lys
Phosphorilation	Ser, Thr, Tyr
Conversions	
Deamidation/Isoaspartylation	Asp, Asn
Citrullination/Deamidation	Arg

Table 1. Example of common PTM.

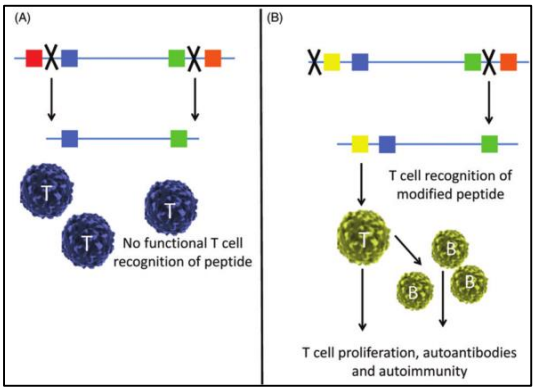

Figure 3: alteration of Ag processing by aberrant PTM. (A) Native proteins are cleaved by proteases (represented by X) into peptides. T and B cells do not recognize self-peptides. (B) Proteins bearing aberrant PTM are not properly cleaved by proteases, creating neo-Ag for T cells [11].

The differences between T- and B-response to post-translationally modified self-proteins was elucidated by Mamula M.J. *et al.*[12], in a study on the Ag of human systemic lupus erythematosus (SLE), the small nuclear ribonucleoprotein particle D. The authors showed that mice immunized with isoaspartyl-modified form (isoAsp) of the peptide Ag develop T-response only against isoAsp peptide, and not against the Asp form. On the other hand, auto-Ab generated by the same immunization procedure were able to bind both isoAsp and Asp form of the Ag. Therefore, it could be hypothesized that the introduction of an aberrant PTM is able to promote the epitope spreading process, by which the immune response diversifies to include epitopes beyond the site(s) inducing the initial reaction[13]. This phenomenon can be both intra-molecular and inter-molecular[12,14].

In a nutshell, a putative PTM-induced autoimmune mechanism could be the following (Figure 4): proteins are aberrantly post-translationally modified e.g. during cellular stress, and then are released from apoptotic/necrotic cells where they are phagocytized by Ag presenting cells (APC). The presence of PTM can affect the Ag processing and presentation on MHC class II. At that point, modified peptide is presented to autoreactive T- and B-cells that have escaped negative selection, leading to autoimmune response[11].

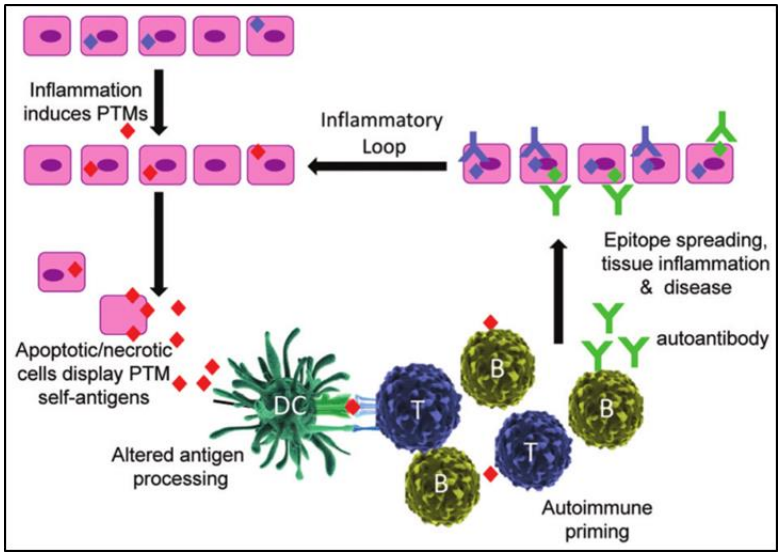

Figure 4. Aberrant PTM on self-proteins initiate the autoimmune response.

Relevance of biomarkers in autoimmunity

AID are generally thought as being relatively rare[2], but actually are among the leading causes of death among young and middle-aged women (age < 65 years) in the United States[15]. The chronic nature of many AID results in a significant impact in terms of quality of life, medical care utilization, and both direct and indirect economic costs[16]. Therefore, it is crucial to carry out an early diagnosis and to follow the progress of the disease, ideally with a test characterized by low-invasivity, low-cost, and easy execution. Unfortunately, to date, in most cases the diagnostic and prognostic methods used for AID do not meet these criteria.

In order to develop a diagnostic or prognostic tool able to satisfy the previously mentioned properties, it could be useful to take advantage of biomarkers (BM), objectively measurable and evaluable biological indicator of normal physiological events, pathogenic processes or pharmacological responses to a therapeutic intervention. Indeed, BM can provide numerous information about the disease of interest, reflecting and summarizing easily all the complex agents and processes that are needed to produce it[17]. This reduction of biological complexity makes BM important and strong "decision-making tools" in clinical and diagnostic[18]. Consequently, BM field is arousing great attention, and both diagnostic and prognostic research is moving toward the design of methodologies that allow the simultaneous measurement of multiple markers (the so-called "profiling methods"), in order to have a more comprehensive view and to follow different aspects of the disease.

As already noted, the autoimmune mechanism is characterized by the presence of a response against self-proteins, which could lead to the appearance of circulating auto-Ab. Interestingly, several studies showed that some disease-specific auto-Ab can precede clinical symptoms by years[19,20], while others can fluctuate with disease exacerbations or remissions[21] (as summarized in Figure 5[22]). In such cases, auto-Ab may represent useful and valuable BM for both diagnostic and prognostic purposes. One of the greatest advantages in using auto-Ab as disease BM is exemplified by the possibility to detect them in biological fluids with simple immunoenzymatic assays, using antigenic probes consisting of the native Ag, or molecules able to mimic its structure. In the latter case, it is essential not only to identify the biological target(s) of auto-Ab, but also to produce suitable probes.

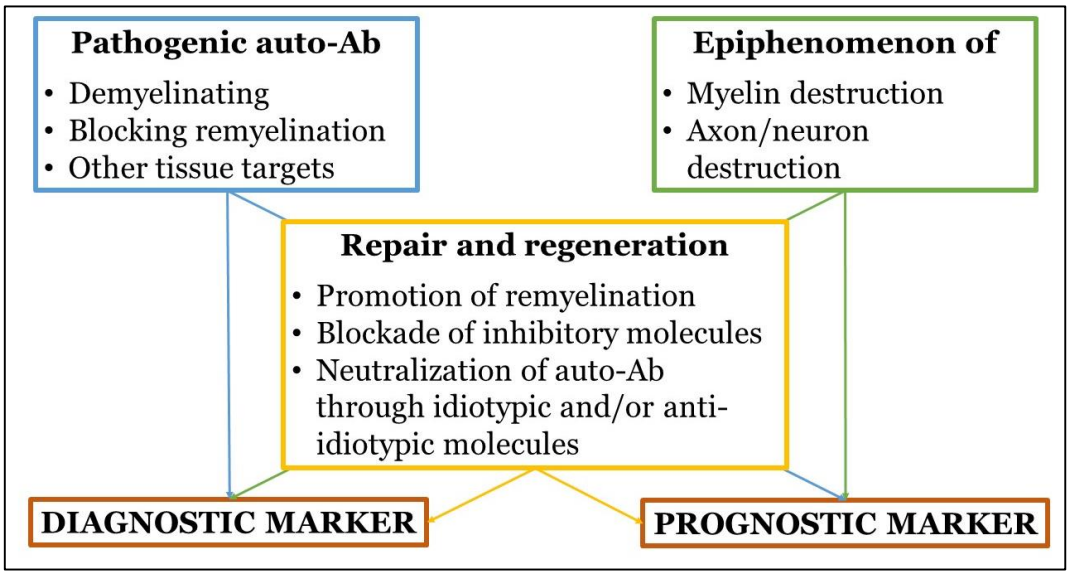

Figure 5: Potential role of Ab as biomarkers in the case of central nervous system demyelinating AID.

Strategies for antigenic probes production: recombinant versus synthetic

The antigenic probe source is a crucial variable, as it affects reproducibility, specificity and sensitivity of the detection assay. The necessity to satisfy these criteria makes difficult to use native Ag isolated from natural sources (e.g. animal tissues), because of their significant limitations in terms of yield, purity and reproducibility. Therefore, it is essential to overcome this problem identifying an antigenic probe able to mimic the native Ag and to detect specific auto-Ab.

One of the most used strategies to produce antigenic probes is represented by the **molecular cloning of the auto-Ag**. This procedure consists in the isolation of the messenger RNA (mRNA) corresponding to the gene of interest, the conversion of mRNA to complementary DNA (cDNA) by reverse transcriptase and the insertion of the cDNA in an expression vector. Then the obtained vector is transferred in the selected expression host, which will produce the recombinant protein encoded by the cloned gene (Figure 6). The choice of the expression host is decisive to obtain the protein provided with the desired physicochemical characteristics. For example, *Escherichia coli* (*E.coli*) represents a very efficient protein production machinery, which permits to achieve a stable, easy and relatively low-cost recombinant protein production. Furthermore, the use of inducible promoter expression plasmids allows to obtain large amounts of product. The recombinant protein can be easily purified by affinity chromatography adding an N- or C-terminus-tag (e.g. 6 residues of Histidine, 6-His): this technique enables to obtain highly purified final products, and also to perform on-column reactions, as cleavage to remove the tag or refolding.

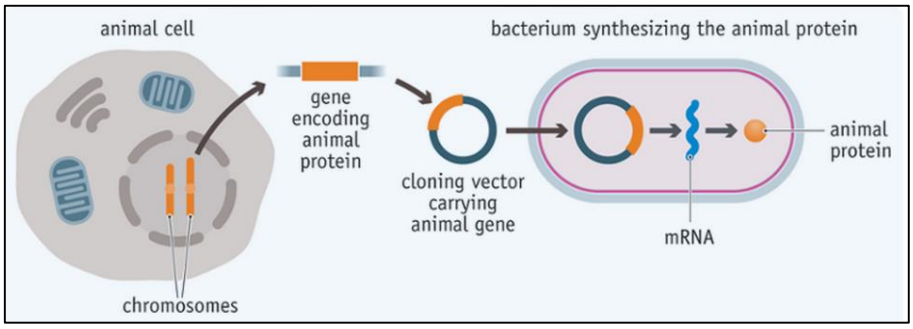

Figure 6: Outline of molecular cloning in bacteria.

However, the use of *E.coli* as expression host has some limitations. First, the size of the protein should be comprised within the range of 100-300 Aa. Larger proteins are poorly expressed, while smaller need to be stabilized by a fusion partner. Second, bacteria often recognize the recombinant protein as foreign, and therefore isolate it into inclusion bodies (IB), insoluble aggregates of misfolded, neo-synthesized recombinant protein. The purification of the protein from IB requires a time-consuming procedure that includes sonication, mechanical and/or physical homogenization, and the use of strong denaturant conditions (e.g. 6 M Urea or Guanidinium Hydrochloride, GuaCl). Moreover, since the protein folding is often fundamental for the Ag-Ab recognition, the recombinant probe has to be refolded at a later stage. However, the IB expression

can be considered also a kind of advantage: IB are often formed only by the protein, are non-toxic for the host and can be accumulated in the cytoplasm in larger amounts compared with soluble proteins. Third, recombinant proteins expressed in bacteria are lacking in PTM, because the biological machinery required for the modification process is absent in prokaryotes. In the last few years, some advanced molecular biology techniques were developed to overcome this issue. In particular, the attention was focused on transferring bacteria N-glycosylation systems to expressing *E.coli* strains, allowing the *in vivo* production of glycosylated proteins in an easy-to-manipulate and fast-growing host[23]. In 2002 Wacker *et al.*[24] discovered an N-linked glycosylation system in *Campylobacter jejuni* (*C. jejuni*), a Gram-negative bacterium, and fully reconstituted this pathway in *E.coli*. The *C. jejuni* glycosylation machinery is based on a block transfer mechanism, which involves the addition of an undecaprenyl pyrophosphate-linked heptasaccharide to the amino group of an Asn in the protein consensus sequence Asp/Glu-X1-Asn-X2-Ser/Thr (X1 and X2 are any amino acid except Pro)[25,26] (Figure 7a). The oligosaccharide is assembled in the cytosol by the addition of the indicated sugars from nucleotide-activated donors, and is subsequently translocated across the inner membrane into the periplasm by the protein glycosylation K protein. Another N-glycosylation system was defined in the Gram-negative gammaproteobacterium *Haemophilus influenzae* (*H. influenzae*), providing the sequential transfer of sugars to the conventional eukaryotic consensus sequence for N-linked glycosylation[27,28] (Figure 7b). In particular, it was disclosed that sugars from nucleotide-activated donors are transferred to the Asn-X-Ser/Thr sequon of high-molecular-weight adhesin 1 (HMW1) by the glycosyltransferase HMW1C in the cytoplasm, and are elongated by the same enzyme. This mechanism was confirmed with purified components *in vitro*, demonstrating the ability of HMW1C to transfer both glucose and galactose residues derived from common sugar precursors. Furthermore, it was shown that HMW1C exhibits both oligosaccharyltransferase activity, adding N-linked sugars to HMW1, and glycosyltransferase activity, generating hexose–hexose bonds. Even if these *in vivo* glycosylation methods are still quite challenging, they open up the possibility to produce proteins provided with the desired glycans using molecular cloning tools[29].

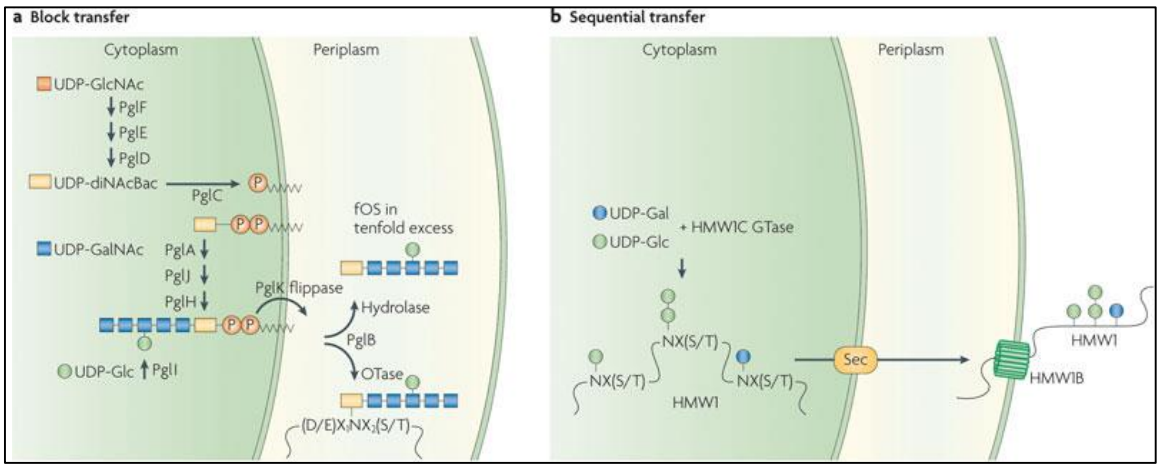

Figure 7: Overview of bacterial N-linked pathways for protein glycosylation. a) Block transfer (*C. jejuni*) and b) Sequential transfer (*H. influenzae*).

In addition to the bacteria system, also numerous eukaryotic expression systems are yet available (yeast, plants, insects and mammalian). These methodologies allow the obtainment of proteins provided with the host usual PTM, which may not correspond to the desired one. Compared with the bacteria system, yields are often lower, costs of production are higher and cell culturing is noticeably more complicated.

Another methodology used to produce antigenic probes is represented by the **synthesis of peptides**, short chains of Aa linked by amide bond. The most widely used technique to obtain peptides is solid-phase peptide synthesis (SPPS), which consists in the elongation of a peptide chain anchored to a solid matrix by successive additions of Aa, taking advantage of the formation of an amide bond between the carboxyl group of the incoming Aa and the amino group of the Aa bound to the matrix. The procedure can be fully automated. The presence of a covalent bond between the growing chain and the support permits an easy separation of the peptide from any excess of unused Aa and other by-products. Peptides are stable in time, and by SPPS they can be obtained in large amount, with high purity and reproducibility, using a rather simple procedures. SPPS represent a promising tool for antigenic probes production, essentially for two reasons:

- It can be used to obtain peptides containing both linear and conformational epitopes;
- It allows the univocal inclusion of the desired PTM in the peptide, using both a building block and a convergent approach.

On the other hand, there are several drawbacks:

- Peptides are designed according to the native auto-Ag, and then it is mandatory to identify the exact Aa sequence of interest;
- The size of the molecules accessible by this technique is limited (up to 50 Aa);
- Peptides with incorrect, truncated or modified sequences can occur due to technical failure;
- Peptide separation and characterization methods are required.

A methodology inspired by the necessity to overcome some of the synthetic and recombinant approaches issues is the **native chemical ligation (NCL)**, a chemoselective reaction between a C-terminal thioester and an N-terminal Cys residue to produce a peptide bond at the site of ligation (Figure 8)[30]. The first step is a transthioesterification between the thiol side-chain of the Cys and the C-terminal acyl donor to generate an intermediate thioester-linked adduct; then a spontaneous intramolecular S→N acyl shift produces a native amide bond between the two fragments. NCL allows to introduce the desired modification in a controlled fashion in the C-terminal peptide fragment, which subsequently will be connected with the N-terminal recombinant portion. The ligation occurs specifically at the N-terminal Cys, even if additional Cys residues are present in either segment, and no protecting groups are necessary for any of the Aa side-chain functional groups[31]. The NCL reaction is performed in aqueous solution, and chaotropes as GuaCl or Urea can be added to increase the solubility of the fragments without affecting the success of the ligation.

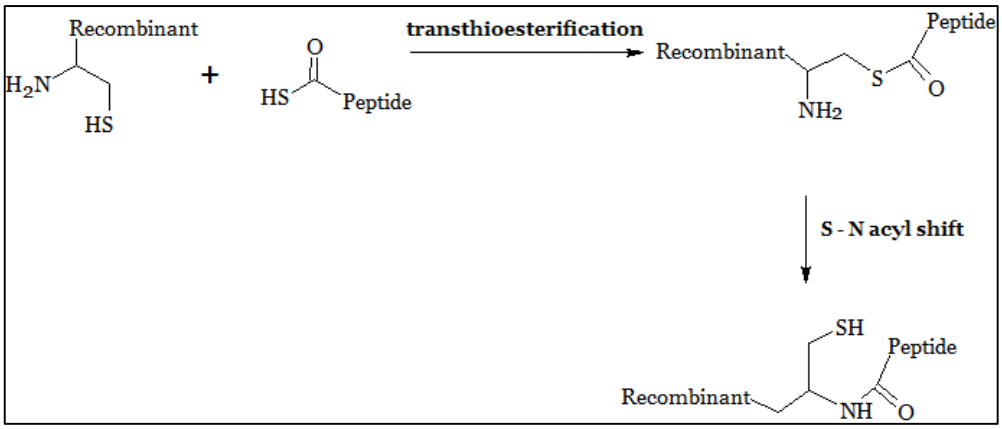

Figure 8: Native Chemical Ligation scheme

NCL can be carried out using two unprotected peptide fragments, or a peptide and a recombinant protein. The latter strategy enables to obtain larger proteins, and requires (1) a recombinant protein provided with an N-terminal free Cys, and (2) a synthetic peptide with a C-terminal thioester, prepared according to the specifications reported below:

(1) To produce a recombinant protein with an N-terminal free Cys, it is necessary to introduce a pre-Cys sequence that will be proteolitically cleaved after the protein purification. One of the most commonly used technique to produce the free-Cys involves the use of *Tobacco Etch Virus* (TEV) protease, a highly specific Cys endopeptidase able to recognize an ENLYFQ\S (where '\' denotes the cleaved peptide bond) consensus sequence. The recombinant cleavage represents a key step, and therefore has to be optimized to obtain the maximum amount of pure, N-terminal free Cys protein.

(2) The obtainment of C-terminal thioester is a critical step, which can be accomplished using SPPS and avoiding basic conditions that destabilize the thioester group. The efficiency of NCL reaction is heavily dependent on the nature of the C-terminal thioester acyl donor (Xaa-SR). Even if it was reported that all the 20 natural Aa are compatible with the NCL reaction, the kinetics depends on the steric and electronic properties of the C-terminal residue Xaa[32].

This NCL variant is a laborious, time-consuming method, because it requires mastery of both SPPS and molecular cloning, and then includes the disadvantages of either. Nevertheless, NCL combines also the benefits of the previously mentioned techniques, and is one of the few approaches enabling the obtainment of homogeneous and consistent samples of full-length protein provided with the modification of interest.

Strategies for auto-Ab detection: Enzyme-Linked ImmunoSorbent Assays (ELISA)

Enzyme-linked immunosorbent assays (ELISA) are biochemical plate-based assays designed for detecting and quantifying substances in a given sample, based on the primary immunology concept of Ag binding to specific Ab. ELISA are widely used in diagnostic field and analytical biomedical research, as they allow both quantitative and qualitative detection of specific Ag or Ab in biological fluids. The greatest advantage of these techniques lies in the immobilization of one of the reactants to a solid surface: this feature makes ELISA easy to design and to perform, and enables to separate bound from non-bound material during the assay, allowing to measure specific analytes within a crude preparation.

The general ELISA procedure (shown in Figure 9) involves the immobilization of the Ag on a solid phase (coating), usually on a 96-well microtiter plate, and the consequent blocking of any un-coated areas of the well with a solution of non-reactive protein (e.g. fetal bovine serum, FBS). Then the given biological sample is applied, allowing the binding of the coated Ag to a specific Ab, which is subsequently detected bound by a secondary enzyme-coupled Ab. Detection is accomplished by assessing the conjugated enzyme activity via incubation with a substrate to produce a measureable product. Secondary Ab are commonly labeled with alkaline phosphatase or horseradish peroxidase, and a large selection of substrates is available. The choice depends upon the required assay sensitivity and the instrumentation available for signal-detection.

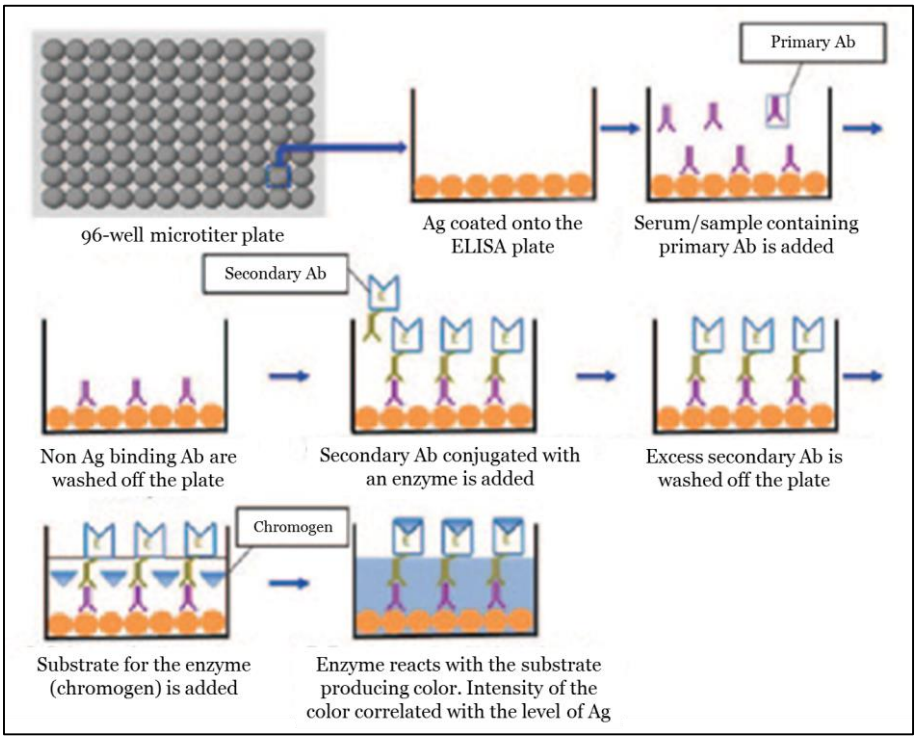

Figure 9: General ELISA technique summary[33].

Starting from ELISA basic procedure, numerous variations of the assay were developed (Figure 10):

- Direct assay (the Ag is detected by a labeled primary Ab).
- Solid-phase (SP-ELISA), or direct assay (the Ag is detected using a conjugate secondary Ab, which binds the primary Ab). This variation represents the best compromise between ease of execution, costs and reliability of the results.
- Capture assay, or sandwich ELISA (the Ag is bound between two primary Ab, one of which is coated on the plate. Detection occurs using a conjugate secondary Ab).
- Competitive ELISA (primary Ab is incubated with the Ag, and the resulting complexes are added to wells coated with the same Ag, or with another Ag).

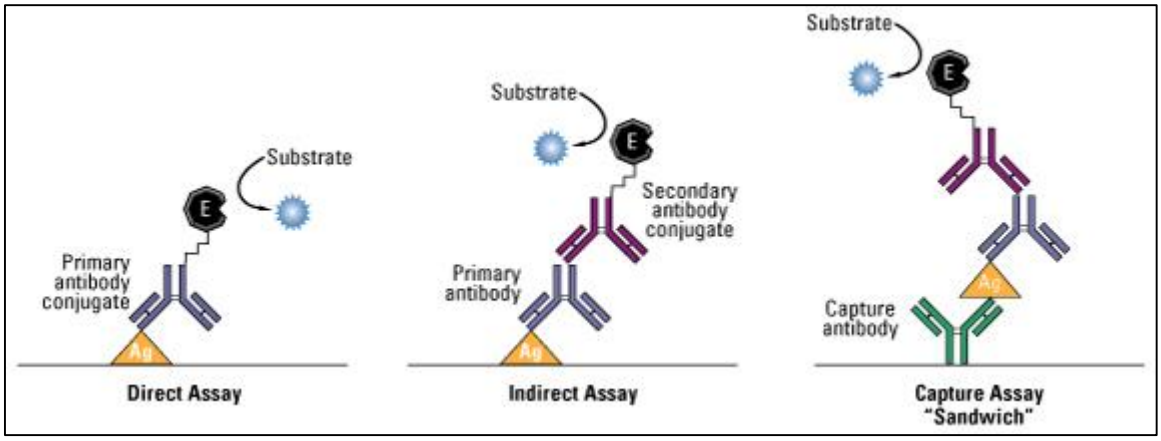

Figure 10: ELISA variations.

Chemical Reverse Approach applied to Multiple Sclerosis: CSF114(Glc)

The necessity to identify new candidate BM of disease in AID led to the use of new discovery tools. A promising strategy to detect auto-Ab as disease-specific BM is represented by the chemical reverse approach, a methodology based on the use of pts sera to screen focused libraries of Ag[18]. The approach is defined "reverse" because it enables the identification of auto-Ag through the ELISA screening of dedicated antigenic probes libraries with a large group of pts sera. The recognition of specific probes by serum Ab drives the selection and the optimization of the "chemical" structure of the library, e.g. through the evaluation of different PTM. By the use of the chemical reverse approach it is possible to identify molecules able to recognize selectively and specifically auto-Ab as disease BM, and therefore to develop diagnostic and/or prognostic tools.

The chemical reverse approach proved to be interesting in the case of Multiple Sclerosis (MS), allowing the identification of the N-glucosylated peptide CSF114(Glc) as antigenic probe, able to recognize disease-specific auto-Ab as BM of MS. This finding is based on the previous results achieved by Mazzucco *et al.*, which demonstrated that a glucosylated peptide analogue of the immunodominant epitope of human Myelin Oligodendrocyte Glycoprotein (hMOG), [Asn[31](Glc)]hMOG(30-50), is able to recognize auto-Ab in MS pts sera[34]. Subsequently, it was

demonstrated that the un-glucosylated analogue hMOG(30-50) is inactive, despite its conformation in solution is similar to the one adopted by [Asn3[1](Glc)]hMOG(30-50). Therefore, the authors concluded that the ability of [Asn[31](Glc)]hMOG(30-50) to detect auto-Ab is not conformation-dependent, but is related to the N-glucose moiety[35]. Starting from this point, our research group synthesized a series of peptides and glycopeptide sequences unrelated to MOG to further investigate the relevance of glycosylation in MS autoimmunity[36,37]. We found out that all glycopeptides containing glucose identified high Ab titers, but that a completely MOG-unrelated sequence, termed CSF114(Glc), was able to detect the highest auto-Ab titers in MS pts serum. CSF114(Glc) is a structure-based designed type I' β-turn sequence, characterized by the propensity to optimally expose the sugar moiety[38]. The relevance of glucose was confirmed testing a small focused library of CSF114 analogues with glyco-Aa diversity, as glycopeptides lacking Asn(Glc) displayed irrelevant inhibitory activity in competitive ELISA and failed to detect IgG in SP-ELISA. Therefore, it was assumed that the minimal epitope is represented by Asn(Glc). Furthermore, through the use of another peptides library, it was also demonstrated the importance of type I' β-turn structure for minimal epitope exposure. At the clinical level, the CSF114(Glc) value was established testing it as antigenic probe in SP-ELISA. It was shown that CSF114(Glc) is able to detect high titer IgM in 30% of the examined relapsing-remitting subtype MS population compared with healthy and pathological controls. Conversely, the anti-CSF114(Glc) IgG determination has a prognostic value, as it parallels the occurrence of magnetic resonance imaging lesions and disease progression in 40% of analyzed pts. These findings on CSF114(Glc) uncovered the importance of N-glucosylation in the case of MS immunopathogenesis, paving the way for further investigation on the link between this aberrant PTM and AID.

The interest in CSF114(Glc) was boosted by the hypothesis of a mimicry between the peptide and aberrantly N-glucosylated self-Ag, triggering the MS specific immunological response. In order to identify the native Ag mimicked by CSF114(Glc), we used anti-CSF114(Glc) auto-Ab isolated from MS pts sera as primary Ab in Western Blot (WB) experiments on whole rat brain proteins. Immunoreactive bands were identified with alpha fodrin, alpha actinin 1, creatine kinase, and CNPase by proteomic analyses. CSF114(Glc) purified auto-Ab were subsequently tested against the commercially available version of the previously mentioned proteins, disclosing that only alpha actinin 1 was specifically recognized, whereas the other three proteins were not consistently detectable. It is interesting to note that alpha actinin 1 is implicated in other inflammatory and degenerative AID, such as lupus nephritis and autoimmune hepatitis[39]. These results give grounds for additional studies on the role of alpha actinin 1 in MS[40] §.

§ Pandey, S., Dioni, I., Lambardi, D., Real-Fernandez, F., Peroni, E., **Pacini, G.**, Lolli, F., Seraglia, R., Papini, A. M., Rovero, P. Alpha actinin is specifically recognized by Multiple Sclerosis autoantibodies isolated using an N-glucosylated peptide epitope. *Mol. Cell. Proteomics* **12,** 277–82 (2013).

AIM OF THE WORK

AID represent a group of chronic and heterogeneous diseases, whose common trait is the immune system reaction against self-components of the organism. Most of the AID have unknown etiology, but it was demonstrated that both genetic and environmental factors are involved in triggering the pathologic mechanism[5]. Because of their chronicity and their debilitating complications, AID have high medical and socioeconomic costs[16], leading to the crucial necessity to perform an early diagnosis and to monitor the disease follow up. Unfortunately, the available diagnostic and prognostic instruments are often complicated and invasive. In order to develop diagnostic and/or prognostic tools marked by low-invasivity, low-cost, and easy execution, it is crucial to detect trustworthy BM. The BM characterization has a significant importance also because it represents a powerful instrument to disclose the molecular mechanisms involved in the ethiopathogenesis of the disorder of interest.

In this context, the main goal of this work is to identify the target(s) of the humoral autoimmune response using the chemical reverse approach, which involves the screening of focused Ag libraries with pts serum[18]. Indeed, in the case of autoimmunity, an easily detectable and reliable BM may be represented by the titer of a specific auto-Ab. A key feature of this study is the evaluation of the role of aberrant PTM in autoimmunity, as it was hypothesized that environmental agents may induce the occurrence of non-natural PTM on self-proteins, uncovering neo-epitopes and triggering the autoimmune response[11].

For this purpose, the experimental workflow of this project is the following:

1. Auto-Ag selection: the Ag to be studied was chosen through an in-depth bibliographical research on the AID of interest.
2. Evaluation of putative aberrant PTM: depending on Ag structure, Aa sequence and localization, it is possible to hypothesize the most probable aberrant PTM. The eventual involvement of disease-correlated enzymatic reactions and the presence of modifications dependent on exposure to environmental agents were taken into account.
3. Antigenic probe production: once the native Ag is known, and the presence of aberrant PTM was evaluated, one has to select the best strategy to produce an antigenic probe able to mimic the desired Ag. The selection is guided by the characteristics of the antigenic probe (e.g. presence of PTM, protein length, importance of folding, Aa sequence, etc.). In this project, depending on the characteristic of the desired antigenic probe, different approaches were used to produce it: SPPS, NCL and molecular cloning.

4. Auto-Ab detection: according to the chemical reverse approach, the obtained antigenic probes were tested with pts sera or with sera from animal models of the disease of interest, in order to verify their ability to reveal auto-Ab as specific pathological BM. The selected detection methodology is SP-ELISA, which is characterized by adequate specificity and reproducibility as well as ease of execution and moderate cost.

In particular, the attention was focused on two main topics, which will be treated separately within this presentation:

- The role of Myelin Oligodendrocyte Glycoprotein (MOG) as putative auto-Ag in central nervous system AID (Chapter 2);
- Investigation of the involvement of aberrant PTM in the ethiopathogenesis of Primary Biliary Cirrhosis (Chapter 3).

CHAPTER 2: MYELIN OLIGODENDROCYTE GLYCOPROTEIN

STRUCTURE AND FUNCTION OF MYELIN OLIGODENDROCYTE GLYCOPROTEIN

Myelin Oligodendrocyte Glycoprotein (MOG) is a 218 Aa (28 kiloDalton, kDa) member of the immunoglobulin (Ig) superfamily exclusively expressed in the central nervous system (CNS). In particular, it is a minor component of myelin (0,05%), and its localization is on the outermost surface of myelin sheath and the plasma membrane of oligodendrocytes[41] (Figure 11). The specific function of the protein still has to be clarified: it was shown that it is an important surface marker of oligodendrocyte maturation, and it was suggested that it might act as cell adhesion molecule, regulator of microtubule stability and mediator of interactions between myelin and immune system[42]. The *MOG* gene maps to the region encoding the MHC in both humans and rodents, and the protein is highly conserved between species[43].

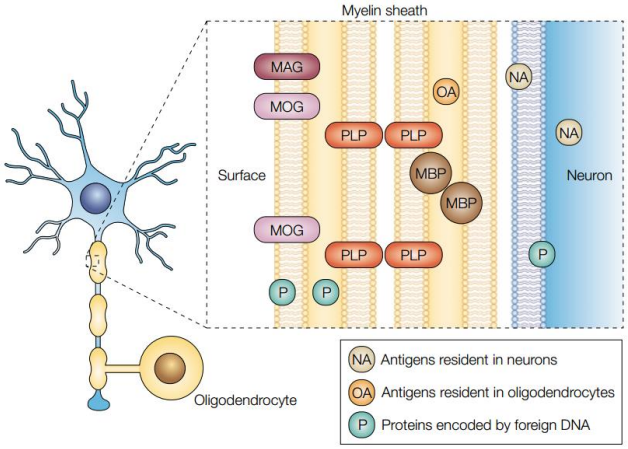

Figure 11: Proteins of the myelin sheath, oligodendrocytes and neurons.
MAG, Myelin-Associated Glycoprotein; MBP, Myelin Basic Protein; PLP, Proteo-Lipid Protein[44].

In 1996, Kroepfl *et al.* proposed a pattern of MOG topology (Figure 12)[45], hypothesizing that the protein contains the following domains:

- an extracellular domain (MOG_{ED}) that comprises an Ig-like portion and the N-linked carbohydrate moiety (N-terminal);
- a first typical transmembrane domain;
- a second hydrophobic domain, which is probably associated with the membrane but not spanning it. In this region there are two Cys that appear to be targets for palmitoylation;
- a small intracellular domain (C-terminal).

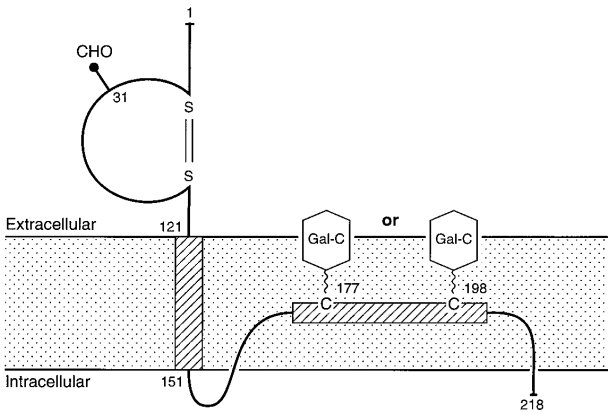

Figure 12: Proposed model for MOG membrane topology[42].

Crystal structure of $rMOG_{ED}$[46] and $mMOG_{ED}$[47] were resolved with X-ray crystallography in 2003 (Figure 13). These studies proved that the overall structure of MOG_{ED} adopts a topology of an Ig-V domain structure, which consists of a compact β-sandwich domain with one antiparallel β-sheet (strands A, B, E, and D) packing against a mixed β-sheet (strands A, G, F, C, C, and C). The N and C termini are at opposite ends of the molecule. In addition to the β-strands, there are four 3_{10} helices at the periphery of the molecule. The core packing residues of MOG_{ED} is represented by a canonical disulfide bond (Cys24–Cys98) that packs against the consensus residue (Trp39), and a salt bridge between Arg68 and Asp92. The glycosylation site of MOG (Asn31) is located in the BC loop, exposed at the top, membrane-distal side of MOG_{ED}.

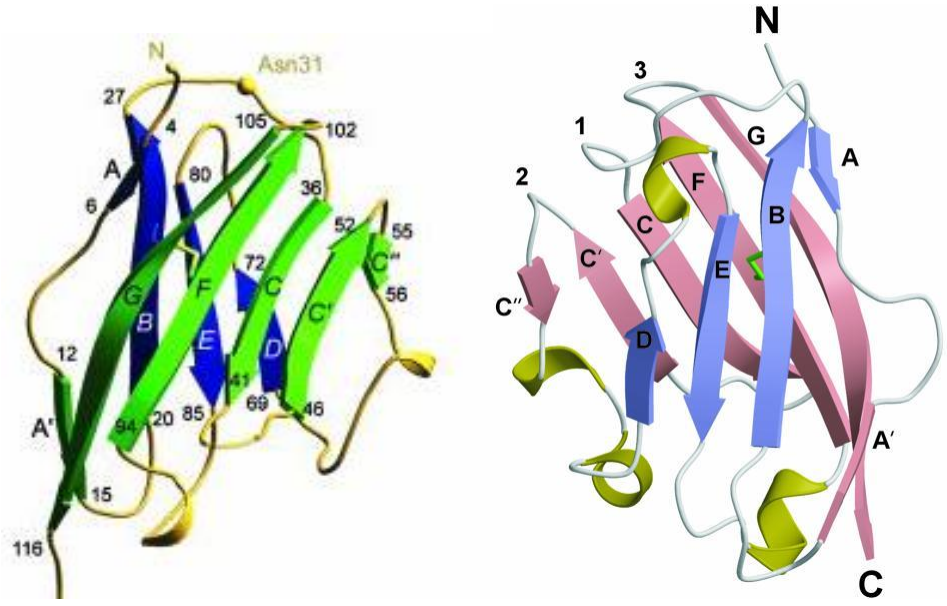

Figure 13: X-ray crystal structure of $rMOG_{ED}$ (on the left) and $mMOG_{ED}$ (on the right).

MOG_{ED} was crystallized as a monomer, but the observed interactions within the crystalline lattice were suggestive of a biologically relevant MOG_{ED} dimer. Indeed, there are three regions of crystal contacts observed within the lattice of MOG, and only one of these was observed to lie on a crystallographic twofold, forming an antiparallel, head-to-tail dimer within the lattice. The shape complementarity index at the dimer interface is high, representing a value that is comparable to that observed in Ab–Ag interactions. The dimer interface runs along the long axis of the molecule, with interactions predominantly involving the extreme N terminus, the A-A' loop (residues 8–11), the C–C' loop (residues 40–46), and the F–G strand β-hairpin (residues 95–112) (Figure 14). The interface is dominated by van der Waals interactions and hydrogen bonds, and all the residues mediating the dimeric contacts are conserved among species.

These findings confirmed that native MOG exist as a mixture of monomeric and dimeric species, as repeatedly reported [42,48,49]. It was demonstrated that the monoclonal Ab (mAb) 8-18C5, which is able to mediate demyelination *in vitro* and *in vivo*, and to augment clinical EAE in rats[50], is capable to recognize proteins with relative mass of 26–28 kDa (monomeric MOG) and 54 kDa (dimeric MOG) in CNS myelin from mouse and human brain as well as native hMOG purified from brain. It was also confirmed that the observed dimer was not merely due to crystal packing artifacts using several biochemical techniques (e.g. native gel electrophoresis).

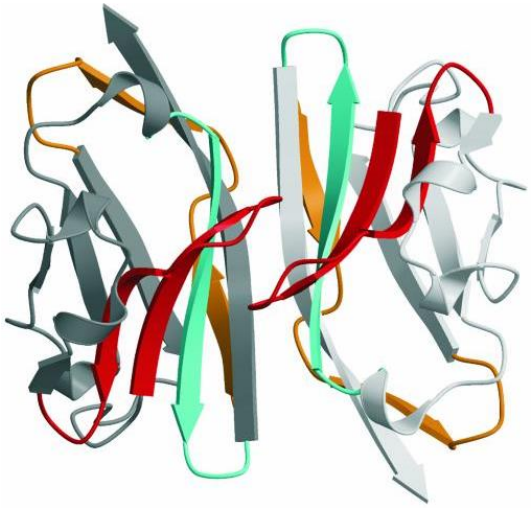

Figure 14: Schematic representation of the MOG_{ED} head-to-tail dimer

THE CONTROVERSIAL ROLE OF MOG IN AUTOIMMUNITY

Central nervous system autoimmune diseases in which MOG is putatively involved

Multiple Sclerosis (MS)

MS is the major inflammatory demyelinating disease of CNS[51]. The disorder represents a prime cause of neurological disability in young adults[52], resulting in wide health, psychological, and socio-economic consequences. MS is marked by inflammatory infiltrates, both axonal and neuronal damage, destruction of myelin sheath and oligodendrocytes, and glial proliferation, leading to the formation of large confluent plaques of demyelination in white and grey matter[51]. While most of the immune mechanisms associated with demyelination and tissue damage in MS are present in other CNS pathologies, it has to be stressed that widespread demyelination with preservation of axons is highly specific for MS, with the exception of viral infection of oligodendrocytes[53] or the presence of toxins affecting myelin or oligodendrocytes[54].

The course of this chronic pathology usually starts with a clinically isolated syndrome (CIS) that evolves in clinically definite MS in 63% of cases[55]. The majority of MS pts (85-90%) develop relapsing-remitting MS (RRMS), in which worsening of clinical symptoms alternate with periods of remission[51,56]. About 40% of RRMS pts develop secondary progressive MS (SPMS), a form characterized by a progression of the disease associated with decrease or absence of relapses. In 10-20% of pts, MS manifests with a slow and progressive exacerbation of symptoms without remission (primary progressive MS, PPMS)[56] (Figure 15).

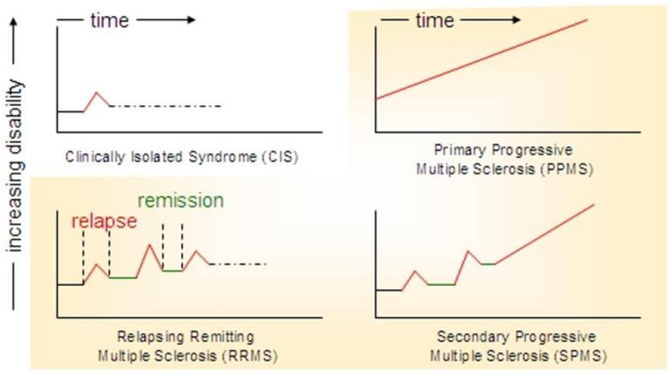

Figure 15: Time course of the different MS subgroups.

As immune mechanisms are at the core of the disease, MS is widely regarded as autoimmune. However, MS triggering events still have to be clarified, as both genetic and environmental factors are involved[57]. The extremely heterogeneous pattern of symptoms and disease course makes challenging to both diagnose and predict the pathology progression[58].

In the last decades, much efforts were made to characterize the auto-Ab response in MS[59,60], as the presence of oligoclonal Ig bands in the CSF of most MS pts uncovered the potential involvement of an autoimmune humoral reaction in MS pathogenesis[61]. Auto-Ab may have different biological functions in MS, ranging from a mere bystander phenomenon to primary involvement at different stages of the immunopathogenic cascade (e.g. demyelination), facilitation of repair mechanisms (e.g. remyelination) and balancing of the natural autoimmunity system. Therefore, a precise characterization of the auto-Ab response in MS may enable the identification of BM for diagnosis, clinical classification, monitoring of disease activity and follow-up prediction (Figure 16)[62].

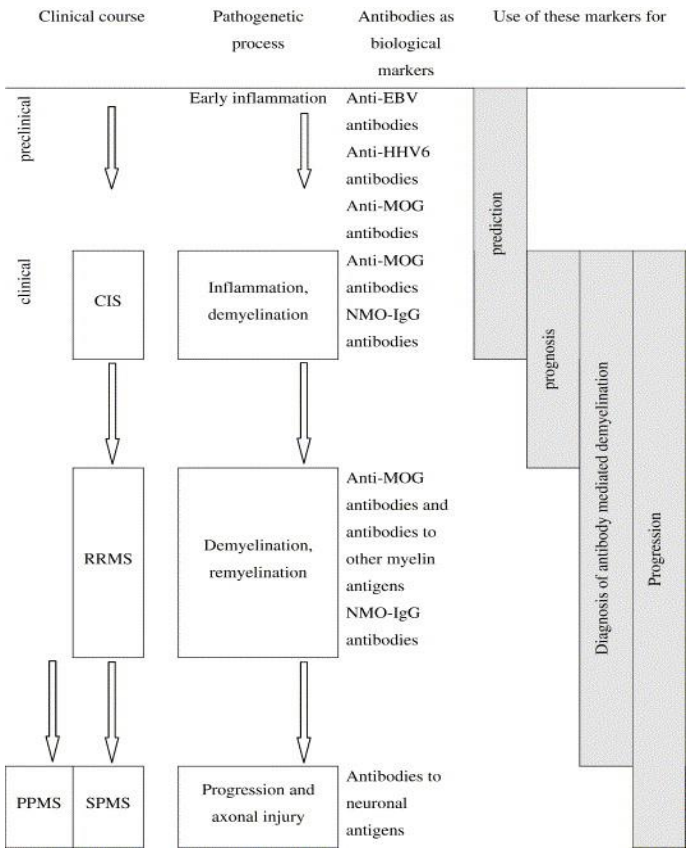

Figure 16: Potential use of Ab as BM in MS.

Myelin Ag were longtime considered as the primary targets of humoral autoimmune response in MS, and recently the focus was shifted to the entire CNS cells[58], but unfortunately the Ag involved in the disorder have not been clearly identified yet.

Experimental Autoimmune Encephalomyelitis (EAE)

As the access to MS tissue and biological fluids samples is often restricted, and the modification of experimental conditions is limited in human studies, it is necessary to employ animal models to understand the immunopathological mechanisms of the disease. Due to the extreme complexity of MS, a single animal model is not representative of all the clinical features of the disease[53]. Large part of the MS pathophysiology was uncovered using EAE, which is the most extensively used MS model. Initially, EAE induction was performed using brain or spinal cord homogenates, or purified myelin proteins, added with an adjuvant. To date, the model is obtained immunizing the animals with an emulsion of adjuvant and recombinant or synthetic myelin proteins (or peptides deriving

from them) by subcutaneous injection. The disease can be achieved also by cell transfer from EAE donors to naïve recipient[53], whereas spontaneous disease can be obtained in transgenic mice[63].

Concerning MS, EAE closely parallels key features of the human disease, as inflammation, demyelination and gliosis[64]. Nevertheless, EAE differs from MS in several remarkable aspects. First, EAE requires an external immunization step to develop[65], typically with adjuvant containing bacterial components highly capable of activating the innate immune system[66]. Second, EAE represents the prototype T cell-mediated model, whereby CD4+ T cells are the major effector of the disease, while MS immunopathology is characterized by both humoral and cellular mechanisms[51]. Third, in EAE the inducing Ag are known, while the triggering event of MS is still matter of debate. It is evident that usage of different immunizing agents, protocols, or animals (mice, rats, primates, etc.) will lead to a different subtype of immune response, and therefore to a particular CNS inflammatory disorder. Therefore, the use of one of the EAE model variation should be guided by a rational selection based on a specific research question.

Neuromyelitis Optica (NMO)

NMO is a severe inflammatory demyelinating disease characterized by severe attacks of neuritis and myelitis. The pathology affects selectively optic nerves and spinal cord (but not necessarily with co-occurrence), typically spares the brain in the early stages, and generally follows a relapsing course[67,68]. Until recently, NMO was considered an MS variant, as both are featured by optic neuritis, myelitis and inflammatory demyelination[69,70], but currently it is known that the disorders have distinct clinical, neuroimaging and laboratory features[67,71] (summarized in Table 2).

	Multiple sclerosis	Neuromyelitis optica
Definition	Central nervous system symptoms and signs that indicate the involvement of the white-matter tracts Evidence of dissemination in space and time on the basis of clinical or MRI findings No better explanation	Transverse myelitis and optic neuritis At least two of the following: brain MRI, non-diagnostic for multiple sclerosis; spinal cord lesion extending over three or more vertebral segments; or seropositive for NMO-IgG
Clinical onset and course	85% remitting-relapsing 15% primary-progressive Not monophasic	Onset always with relapse 80–90% relapsing course 10–20% monophasic course
Median age of onset (years)	29	39
Sex (F:M)	2:1	9:1
Secondary progressive course	Common	Rare
MRI: brain	Periventricular white-matter lesions	Usually normal or non-specific white-matter lesions; 10% unique hypothalamic, corpus callosal, periventricular, or brainstem lesions
MRI: spinal cord	Short-segment peripheral lesions	Longitudinally extensive (≥3 vertebral segments) central lesions
CSF white-blood-cell number and differential count	Mild pleocytosis Mononuclear cells	Occasional prominent pleocytosis Polymorphonuclear cells and mononuclear cells
CSF oligoclonal bands	85%	15–30%

Table 2: Definitions and characteristics of MS and NMO[75]

The real breakthrough in NMO field was achieved in 2004 by Lennon *et al.*, with the discovery of NMO-IgG, an auto-Ab to aquaporin-4 (AQP4) present in more than 70% NMO pts[72]. NMO-IgG recognizes aquaporin-4 (AQP4), the main channel responsible for water homeostasis regulation in the CNS. AQP4 is located in astrocyte membranes, and the areas where its expression is normally

higher coincide with the sites of brain lesions in 10% of pts[73,74]. The identification of a specific serological disease BM enabled to simplify the diagnosis and to investigate the molecular immune-mechanisms. Nevertheless, the role of NMO-IgG and AQP4 has yet to be clarified. Despite the NMO-IgG identification as disease BM, a small percentage of pts remains seronegative. In this context, the presence and significance of anti-MOG auto-Ab in NMO is matter of debate.

Role of MOG in central nervous system autoimmunity: first hypothesis and animal models contribution

Inflammatory demyelinating diseases of CNS include numerous and heterogeneous pathologies, such as MS and NMO. The evidence of an Ab-dependent mechanism contributing to at least a subset of pts affected by these disorders is highlighted by both histopathological investigations and clinical response to plasma exchange[76]. First studies aimed at understanding the mechanism(s) that induces demyelination dates back to the period between '800 and the early '900. In 1906, Marbourg proposed the existence of a soluble myelinolytic factor, while Babinski hypothesized that myelin was attacked by inflammatory cells[77]. By the use of EAE animal model, today it is well known that both mechanisms are possible, and that selective primary demyelination can be induced either by cytotoxic T-cells recognizing an oligodendrocyte Ag[78,79], or by specific demyelinating auto-Ab[80]. The advent of myelinating tissue culture models in the 60s allowed to discover that sera and cerebrospinal fluid (CSF) from MS pts contain a soluble factor able to induce demyelination *in vitro*[81,82]. This phenomenon was observed predominantly in pts with active disease[83], but rarely in control sera[82,83]. A similar demyelinating factor was found in the sera of EAE animals after sensitization with CNS homogenate[81,84–87]. Later, it was discovered that this soluble factor was an Ig able to induce demyelination through complement activation both *in vitro*[88] and *in vivo*[89,90]. The target Ag of demyelinating Ab was identified as MOG[91] using the mouse mAb 8-18C5 directed against rat cerebellar glycoproteins[49]. Since then, MOG became the most extensively studied putative Ag in CNS AID. The encephalitogenic properties of MOG are believed to result from the extracellular localization of its IgV-like domain on the outermost myelin lamellae, which makes it an exposed target accessible to autoimmune attack even on intact myelinated axons[92,93].

The attention in MOG was further encouraged by the demonstration of the association between demyelinating activity of guinea pig EAE serum and anti-MOG Ab titers[91]. The presence of demyelinating Ab anti-MOG was then confirmed in both rodent and primates EAE models[50,80,94], and it was shown that anti-MOG Ab are capable to induce widespread plaque-like demyelination in the white matter[95] and in the cerebral cortex[96] *in vivo*. In MOG-induced EAE models, the subpial demyelinating cortical lesions were identical to those present in MS pts[96], while these lesions are absent in Ab-independent EAE models[97].

In 2004, von Büdingen *et al.*[98] demonstrated, using an EAE marmoset model, that only auto-Ab directed against conformational epitopes of MOG are responsible for demyelination worsening.

Indeed, they observed the occurrence of IgG deposition and complement activation only in association with the presence of conformational auto-Ab. In the same publication, they reported that conformational auto-Ab are also an essential factor for disease dissemination within CNS, a typical hallmark of human MS. A year later, Marta *et al.*[99] obtained an EAE model immunizing C57BL/6 mice with either rat (rMOG) or hMOG. Although anti-MOG Ab were generated in both cases, only immunization with hMOG led to a B-cells dependent disorder. In particular, they showed that the mutation of Pro at position 42 with Ser in hMOG (as in rMOG) results in a change in the mechanism of encephalitogenicity from B-cell dependent to independent, reflecting the close connection between Ag conformation and Ab pathogenicity. They established also that only Ab from mice immunized with unmodified hMOG were encephalitogenic in primed B cell-deficient mice. Furthermore, they demonstrated the capability of encephalitogenic anti-hMOG Ab to bind properly glycosylated MOG. Based on these data, they hypothesized that non-pathogenic Ab bind linear MOG determinants, while pathogenic Ab recognize only conformational, glycosylation-dependent epitopes.

Understanding the three-dimensional structure of MOG_{ED} allowed the identification of solvent-exposed surfaces that may be involved in Ab-mediated demyelination. As previously mentioned, Ab demyelinating activity is strictly dependent on epitope conformation, with the exception of a minor subset of murine mAb able to bind also peptides containing the 63-87 region. This sequence includes the DE loop, which forms part of a protruding surface at the top of BED sheet and comprises highly exposed residues[100]. Additionally, it was shown that Lewis rats immunized with MOG(35-55) develop a demyelinating variant of EAE, leading to the hypothesis that also this fragment encompasses a B-epitope[101]. This assumption is supported by MOG(35-55) localization into the surface-exposed and highly flexible CC' loop (Aa residues 41-46). Furthermore, MOG_{ED} was crystallized in complex with a chimeric fragment Ag-binding (Fab) derived from 8-18C5 (Figure 17)[46].

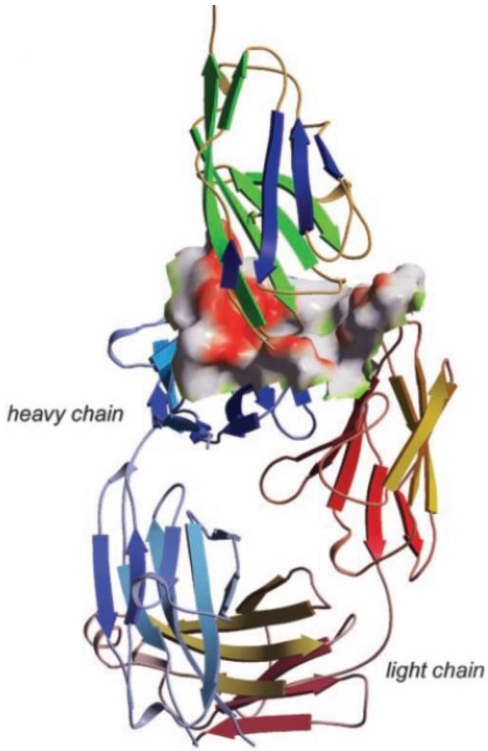

Figure 17: Overall structure of Fab-MOG_{ED} complex. The binding site of Fab is shown with surface representation, and atoms contacting MOG_{ED} are colored in red.

The capacity of 8-18C5 to detect MOG from different species and to inhibit the binding MOG-specific mAb to the protein indicate that 8-18C5 recognizes a central conserved epitope. The crystal structure of MOG-Fab complex disclosed that 8-18C5 binds the upper, membrane-distal surface of MOG_{ED}, namely the N terminus and the BC, C'C" and FG loops. The major interaction site is formed by the three complementarity determining regions (CDR) of the mAb heavy chain and both residues in the G strand and in the FG loop (Aa residues 101-108), which represent 65% of the total MOG_{ED} interaction surface. The highly specific interaction with the 101-108 region is also supported by presence of van der Waals bonds between MOG residues and Fab in the periphery of the binding site.

The discovery of the crucial relevance of MOG conformation and glycosylation in the occurrence of EAE pathogenesis represents a concrete breakthrough in the CNS autoimmunity field.

MOG as putative auto-Ag in human CNS AID: an issue open to discussion

Despite the interesting and grounded results achieved in animal models, the demonstration of anti-MOG Ab pathogenicity in humans is still lacking. The main reason for the inhomogeneous and controversial data on the role of MOG in MS autoimmune response is the use of different assays testing different MOG preparations (summarized in Table 3). Namely, the causes of this debatable circumstance concern:

1. sequence, conformation and origin of MOG used as Ag;
2. technique used to measure anti-MOG Ab;
3. Ig isotype detected;
4. absence of standardized MS subtype definition;
5. nature of negative controls (normal blood donors, NBD; other neurological disease, OND; etc.).

Some of these aspects were summarized in the following table:

Type of MOG	recombinant MOG (different portions) expressed: – in mammalian cells – in *E.coli* – by *in vitro* translation synthetic peptides (1 to 125 Aa) purified from human myelin tetramer cell-based assays (human or murine cells expressing hMOG on their surface)
MOG sequence	human, rat, mouse
Ig isotype	IgG, IgM, IgA
Immunossay	ELISA, Immunoblot, Fluid Phase, Elispot, Fluorescence-activated flow cytometry (FACS)

Table 3: MOG preparations and immunoassays used for anti-MOG Ab detection[102]

Since 1991, the role of anti-MOG Ab in MS and in other CNS AID was extensively investigated (results are reviewed in Table 4 [62,103,104]). The first studies were carried out employing hMOG purified from brain white matter as Ag in ELISA testing MS pts sera and CSF. This methodology enabled the detection of anti-MOG Ab in the CSF of a subset of MS pts, but also in the control cohort[105]. Afterwards, comparable results were obtained using not-refolded hMOG extracellular domain expressed in *E.coli*[106]. The use of full-length glycosylated mouse MOG (mMOG) expressed in mammalian cells allowed the identification of high IgM titers in MS pts during the first demyelinating event, and elevated IgG during relapses and secondary chronic progressive MS. The results obtained with MS subgroups were compared with NBD and remission pts[107]. These findings permitted to hypothesize the importance of epitope glycosylation and conformation also in human MS. Later studies confirmed the theory of a pathogenic role of anti-MOG Ab[108–113], while others denied it[114–118]. Additionally, in the recent years the focus partially shifted to pediatric MS[119–122] and other neurological AID (e.g. NMO and acute disseminated encephalomyelitis, ADEM), leading to an even more intricate situation.

In this context, our research group focused on the detection of serum IgG and IgM directed against the extracellular domain of MOG, with an emphasis on the protein conformation. To do this, Gori *et al.*[118] developed a method to produce recombinant $rMOG_{1\text{-}125}(His)_6$ centered on the on-column refolding and affinity purification of the protein produced in *E.coli*. MOG folding was verified by circular dichroism spectroscopy, then the protein was used as antigenic probe in SP-ELISA. Results obtained disclosed that $rMOG_{1\text{-}125}(His)_6$ is not able to detect serum Ab neither in MS pts nor in controls using an immunoenzymatic solid-phase assay.

Study	**Method**	**Ag**	**Ig isotype**	**Sample tested**	**Results & Discussion**
Xiao 1991[105]	ELISA	hMOG from white matter	IgG	Plasma and CSF	Anti-MOG IgG were detected in 7/30 MS pts (compared with controls). No anti-MOG IgG Ab were demonstrable in plasma.
Karni 1999[123]	ELISA	hMOG expressed in *E.coli*	IgG	Plasma and CSF	Anti-MOG Ab are elevated in MS, but also in other neurologic diseases.
Lindert 1999[124]	WB	hMOG expressed in *E.coli*	IgG	Serum	The frequency of anti-MOG seropositive samples was significantly higher in MS than in normal random controls (positivity percentages: MS 54%; controls 22%).
Reindl 1999[106]	WB ELISA	hMOG expressed in *E.coli*	IgG	Serum	38% of MS are seropositive for anti-MOG IgG (persistent response). Similar % were found in OND, but the response is transient.
Egg 2001[125]	Immunoblot	hMOG expressed in *E.coli*	IgG, IgM, IgA	Serum	72% of MS have anti-MOG Ab, and the dominating one is anti-MOG IgM. A significant relationship between anti-MOG IgA and a progressive disease course was found.
Berger 2003[126]	WB	hMOG expressed in *E.coli*	-	Serum of CIS patients	Analysis of anti-MOG (and MBP) Ab enables to predict early conversion to clinically definite MS.
Vojdani 2003[127]	ELISA	Syntethic MOG peptides	IgG, IgM, IgA	Serum	Detection of anti-MOG peptides Ab, together with the measurement of other serological parameters, could be used for the confirmation of MS diagnosis.
Kennel de March 2003[128]	ELISA, ELISPOT	Synthetic MOG(35-55), recombinant MOG	IgG, IgM, IgA	Serum	MS patients had significantly higher levels of anti-MOG IgA and MOG-specific spot-forming cells than controls.

Study	**Method**	**Ag**	**Ig isotype**	**Sample tested**	**Results & Discussion**
Gaertner 2004[107]	ELISA	mMOG transfected AG8 cells	IgG, IgM	Serum	Anti-MOG IgM were elevated during the first demyelinating event, while higher MOG-specific IgG were found during relapses and in secondary chronic progressive MS compared to pts in remission and controls.
Lampasona 2004[129]	Liquid-phase radiobinding assay	hMOG *in vitro* translated	IgG, IgM	Serum	The frequency of positive samples with low titers of anti-MOG IgG (≤5.7%) and IgM (≤8.3%) was similar in both MS and control, disclosing that anti-MOG Ab are not disease specific.
Mantegazza 2004[130]	ELISA	hMOG expressed in *E.coli*	IgG	Serum and CSF	Serum anti-MOG Ab were detectable in 13.7% of MS pts, mainly in SPMS (25%), in 13.7% of OND pts and in 6.2% of controls. A direct correlation between disease severity and anti-MOG titer was found only in PPMS and SPMS pts. Anti-MOG Ab were present in the CSF of 11.4% MS patients and 18.9% OND pts.
Zhou 2006[109]	Cell-based assay	hMOG transfected LN18 cells	IgG, IgM	Serum	IgG but not IgM Ab-titers to native MOG were significantly higher in MS compared with different control group (highest prevalence in PPMS). The presence of a pathogenic Ab response to native MOG in a subgroup of MS patients was suggested.

Study	**Method**	**Ag**	**Ig isotype**	**Sample tested**	**Results & Discussion**
Lalive 2006[110]	Cell-based assay	hMOG transfected CHO cells	IgG	Serum	Compared with healthy controls, native MOG-specific IgGs were most frequently found in serum of CIS and RRMS, only marginally in secondary progressive SPMS PPMS. Therefore, cell-based assay provides a practical serologic marker for early detection of CNS autoimmune demyelination.
	ELISA (only on CIS cohort)	hMOG expressed in *E.coli*	IgG		
Kuhle 2007[114]	WB	hMOG expressed in *E.coli*	IgG, IgM	Serum of CIS patients	No associations were found between the presence of anti-MOG Ab and progression to MS.
Pelayo 2007[115]	WB	hMOG expressed in *E.coli*	ND	Serum of CIS patients	No associations were found between the presence of anti-MOG Ab and CIS-to-MS conversion.
O'connor 2007[116]	ELISA (DELFIA)	hMOG expressed in *E.coli* (refolded)	IgG, IgM	Serum and CSF	It was shown that tetramer RIA is the most sensitive methodology for MOG auto-Ab. MOG-specific auto-Ab were identified in a subset of ADEM but only rarely in adult-onset MS cases, indicating that MOG is a more prominent target antigen in ADEM than MS.
	Solution phase radioimmuno-assay (RIA)	hMOG *in vitro* translated (self-assembling radiolabeled tetramers)			
Menge 2007[111]	ELISA LiPhELIA	hMOG expressed in *E.coli*	IgG	Serum	SP methods are superior in measuring anti-MOG Ab, but do not have the discriminative power to isolate only the disease-relevant ones. Indeed, anti-MOG IgG reactivity of MS and controls are comparable.

Study	Method	Ag	Ig isotype	Sample tested	Results & Discussion
Wang 2008[131]	ELISA	hMOG expressed in *E.coli*	IgG, IgM	Serum	The presence of anti-MOG IgG was related with an increase in risk of developing MS. This association may in part reflect cross-reactivity between MOG and Epstein-Barr nuclear antigen.
Klawiter 2010[113]	ELISA	hMOG produced using baculovirus and insect cell-mediated expression system	IgG	Serum and CSF	Serum and CSF anti-MOG Ab, together with albumin levels, were used to calculate s a marker of intrathecal MOG Ab production, the rMOG index, which was found to be elevated in MS compared to controls. Results obtained display that intrathecal anti-MOG Ab production may be more pronounced in progressive than relapsing forms of MS.
Gori 2011[118]	ELISA	Refolded rMOG expressed in *E.coli*	IgG, IgM	Serum	Anti-MOG Ab are not detectable in both MS and controls.
Menge 2011[132]	ELISA Denaturing ELISA	Recombinant refolded hMOG1-125, hMOG1-118 and rMOG1-125 produced in *E.coli*	IgG	Serum	High-titer of anti-MOG Ab were identified in ≈8% of tested samples, and are highly specific for certain epitopes of hMOG. In RRMS, high-titer anti-MOG IgG correlate with disability.

Table 4: Summary of the most relevant studies on anti-MOG Ab response in MS.

AIM OF THE WORK

MOG is one of the most studied Ag candidate in the case of demyelinating AID, especially in MS[102,104]. The hypothesis of MOG involvement in the autoimmune reaction is due to the exposition of its Ig-like extracellular domain on the outermost surface of myelin sheaths, allowing the access of potential auto-Ab to the protein[41]. Despite the presence of numerous studies based on MOG, the role of the protein in CNS AID is still controversial. Indeed, the use of inhomogeneous protein preparations and different immunological protocols to reveal anti-MOG Ab led to the presence of contrasting and debatable data. In this context, we decided to study the involvement of MOG in different CNS AID using the refolded recombinant rat extracellular domain of the protein, $rMOG_{1-117}$. The choice of a shortened protein fragment compared with the so-called standard extracellular domain MOG_{1-125} was inspired by an attempt to avoid the solubility issues characterizing $rMOG_{1-125}$. Indeed, $rMOG_{1-125}$ sequence comprises also a small transmembrane portion, which is highly hydrophobic ($F^{119}YWI^{122}$). The removal of these Aa residues may lead a more soluble recombinant product, which is more appropriate to be employed as Ag in immunological solid-phase assays. The initial decision of our research group to work with rMOG as antigenic probe dates back to the early 2000, and was guided by the fact that the protein was used in studies with animal model, aimed to understand the molecular mechanisms of MS. Furthermore, one of our primary focus was to restore the native protein conformation through the refolding procedure, in order to preserve MOG conformational epitopes. This feature supported the employment of rat protein because the reference conformational studies were carried out on the rat isoform[46] (together with the mice one[47]). However, the use of the rat protein in studies on human pathology may lead to confusing data: hMOG and rMOG share a >90% homology, but rMOG has a Ser in position 42, while hMOG has a Pro (Figure 18). As already speculated by Marta *et al.*[99], this single Aa difference could lead to structural differences, with consequent alteration of the immunogenicity of the probe.

rMOG1-117 – hMOG1-117 BLAST alignment

Identities: 106/117 (91%)

```
rMOG1-117           GQFRVIGPGHPIRALVGDEAELPCRISPGKNATGMEVGWYRSPFSRVVHLYRNGKDQDAE
                    GQFRVIGP HPIRALVGDE ELPCRISPGKNATGMEVGWYR PFSRVVHLYRNGKDQD +
hMOG1-117           GQFRVIGPRHPIRALVGDEVELPCRISPGKNATGMEVGWYRPPFSRVVHLYRNGKDQDGD

rMOG1-117           QAPEYRGRTELLKESIGEGKVALRIQNVRFSDEGGYTCFFRDHSYQEEAAVELKVED
                    QAPEYRGRTELLK++IGEGKV LRI+NVRFSDEGG+TCFFRDHSYQEEAA+ELKVED
hMOG1-117           QAPEYRGRTELLKDAIGEGKVTLRIRNVRFSDEGGFTCFFRDHSYQEEAAMELKVED
```

Figure 18: $rMOG_{1-117}$ – $hMOG_{1-117}$ BLAST alignment.
In red, Aa differences. + indicates a conservative mutation.
Ser^{42} and Pro^{42} are highlighted in yellow.

Based on the foregoing, recombinant $rMOG_{1-117}$ was used as antigenic probe in SP-ELISA aimed to disclose different aspects of MOG immunogenicity in several pathologies. In particular, we evaluated the role of MOG in:

- EAE mice model of MS;
- NMO;
- NMO-like EAE rat models.

Furthermore, as the Ag production step is crucial in the BM research field, part of the work was focused on MOG production through molecular biology techniques. In particular, we worked on:

- Optimization of $rMOG_{1-117}$ productive process;
- Semi-synthesis of aberrantly N-glucosylated $hMOG_{1-117}$.

The previously mentioned aspects will be treated separately in this presentation. Specifically, the work is structured as follows:

- **Part I: Immunological role of MOG in the EAE mice model of MS**
  The EAE mice model was obtained by Dr. Rina Aharoni (Weizmann Institute, Rehovot, Israel) immunizing C57BL/6 mice with commercial mMOG(35-55) peptide. We tested sera samples of mice with various clinical course (active disease with different disease score; spontaneous recovery; immunized mice that have not developed any clinical sign), comparing them with naïve mice. We tested three temporally distinct cohorts of sera, to assess different hypothesis:
  1. <u>First cohort: preliminary SP-ELISA screening on $rMOG_{1-117}(His)_6$, CSF114 and CSF114(Glc).</u>
     17 EAE active disease, 1 spontaneous recovery and 8 naïve mice sera samples were tested in SP-ELISA to assess the presence of Ab response against MOG. The N-glucosylated peptide CSF114(Glc) was also tested, together with its un-glucosylated analog, to assess the role of N-glucosylation in the mice model.
  2. <u>Second cohort: anti-$rMOG_{1-117}(His)_6$ IgM screening.</u>
     16 EAE active disease, 3 spontaneous recovery, 6 immunized mice that that have not developed any clinical sign ("no disease") and 12 naïve mice sera samples were tested in SP-ELISA to verify the hypothesis of a protective role of anti-MOG IgM.
  3. <u>Third cohort: $rMOG_{1-117}$ epitope mapping</u>.
     33 EAE active disease, 12 spontaneous recovery, 2 "no disease" and 9 naïve mice sera samples were tested to determinate the presence of an epitope spreading mechanism against MOG portions different from the immunizing peptide mMOG(35-55). For this purpose, the MOG(1-117) sequence was divided in 6 peptide fragments (1-34, 35-55, 56-75, 76-95 and 96-117), which were subsequently used as antigenic probe in SP-ELISA. Results obtained were compared with the one achieved on the full-length recombinant protein.

- **Part II: Evaluation of MOG-IgG and CSF114(Glc)-IgG as additional BM in NMO**
  NMO is an inflammatory demyelinating disorder of CNS that affects spinal cord and optic nerve. In 2004, Lennon *et al.* discovered a specific disease BM, NMO-IgG, that is an auto-Ab of the IgG class directed against AQP4[72]. As NMO-IgG is present in approximately 70% of NMO pts, the evaluation of other NMO BM may be useful to perform a more accurate diagnosis. Recently, the role of MOG as auto-Ag in NMO was extensively studied, but the relevance of anti-MOG Ab in this pathology still needs clarifications. These findings disclosed the potential of anti-MOG IgG as additional NMO BM, but to date the involvement of MOG in NMO is still matter of debate. In this context, we assessed the presence of a specific IgG reactivity against MOG testing 21 NMO pts sera in SP-ELISA. As NMO is an MS-related disorder, we tested the same sera on CSF114(Glc), and results obtained for both Ag were compared with a cohort of 20 NBD using a cutoff calculated as (mean value of NBD)+3*(standard deviation of NBD).

- **Part III: Immunological role of MOG in NMO-like EAE rat models**
  Several attempts to obtain a specific *Rattus Norvegicus* NMO-like model were made by Prof. Jerome De Seze group (*Hôpitaux universitaires de Strasbourg*, France) immunizing Brown Norway rats with recombinant, not-refolded $rMOG_{1-117}(His)_6$ produced in our lab. In particular, it was studied the possibility to reproduce the disorder administering two doses of immunizing agent, or using an IgG passive-transfer strategy. In this context, we evaluated the Ab response elicited in the NMO-like model to disclose the correlation between anti-MOG Ab titer and disease progression. A first attempt to evaluate the model obtained immunizing Brown Norway rats with $rMOG_{1-117}(His)_6$ was made studying the time-course of IgM and IgG anti-MOG Ab response. Subsequently, it was assessed the correlation between Ab titer against refolded MOG and both time- and disease-course in four different immunization protocols. The same animal cohort was examined to verify the presence of a response against unfolded MOG and CSF114(Glc).

- **Part IV: Optimization of $rMOG_{1-117}$ production process**
  Ag production process is a key step of the BM research in both diagnostic and prognostic fields. As mentioned several times during this presentation, MOG is the most studied candidate Ag in the case of CNS AID, and therefore the production of this protein as antigenic probe is of crucial relevance to study the immunopathogenesis of disorders such as MS or NMO. In our lab, we decided to employ recombinant $rMOG_{1-117}$, which was obtained through the expression and purification protocol published by Gori *et al.*[118]. This methodology includes numerous laborious and time-consuming phases that invalidate productivity. Therefore, the aim of this project was to improve $rMOG_{1-117}$ production process, focusing on the optimization of both expression in *E.coli* and purification/on-column refolding of the protein.

- **Part V: Semi-synthesis of aberrantly N-glucosylated $hMOG_{1-117}$**

  The involvement of aberrant PTM on MOG in triggering CNS autoimmunity is a crucial topic. In this context, we hypothesized that an aberrant N-glucosylation on the MOG native site of glycosylation (Asn^{31}) may be involved in the immunopathogenesis of CNS demyelinating disorders. This assumption is supported by the presence of a preliminary study proving that [Asn^{31}(Glc)]hMOG(30-50) is capable to recognize auto-Ab in MS pts sera, while the corresponding un-glycosylated hMOG(30-50) is inactive[34]. Furthermore, it is well documented that the N-glucosylated type I' β-turn peptide CSF114(Glc) is able to detect specific and high affinity Ab in MS patients, disclosing the relevance of N-glucosylation in MS autoimmunity[36,37]. Therefore, we decided to develop a NCL semi-synthetic strategy to produce [Asn^{31}(Glc)]$hMOG_{1-117}$, which will be compared with both un-glucosylated $hMOG_{1-117}$ and CSF114(Glc) from an immunological point of view. The chosen protocol provides the formation of an amide bond between a recombinant protein bearing an N-terminal Cys and a peptide with a C-terminal thioester. For this purpose, it was decided to produce the hMOG fragment (35-117) using molecular biology tools, engineering the sequence to obtain the N-terminal free Cys. Specifically, a selective point mutation was introduced at the 35 residue (M35C) and the sequence was extended at the N-terminus with the TEV-protease consensus sequence. The C-terminal active ester of the peptide fragment [Asn^{31}(Glc)]hMOG(1-34) was prepared at the SOSCO Laboratory (*Universitè de Cergy Pontoise, France*).

PART I: IMMUNOLOGICAL ROLE OF MOG IN THE EAE MICE MODEL OF MS

As stated in the previous section, the aim of this study concerns the evaluation of the immunological role of MOG in an EAE mice model of MS obtained immunizing C57BL/6 mice with a commercial mMOG(35-55) peptide. We tested sera samples of mice with various clinical courses (active disease with different disease score; spontaneous recovery; immunized mice that have not developed any clinical sign), comparing them with naïve mice. In particular, we assessed different hypothesis testing three temporally distinct cohorts of sera:

1. First cohort: preliminary SP-ELISA screening on $rMOG_{1-117}(His)_6$, CSF114 and CSF114(Glc): we evaluated the presence of Ab response against MOG, together with the role of N-glucosylation in the MS mice model.
2. Second cohort: anti-$rMOG_{1-117}(His)_6$ IgM screening: we investigated a putative protective role of anti-MOG IgM.
3. Third cohort: $rMOG_{1-117}$ epitope mapping: we explored the possible presence of Ab directed against MOG epitopes different from the immunizing peptide mMOG(35-55), i.e. a phenomenon known as epitope spreading. MOG(1-117) sequence was divided in 6 peptide fragments (1-34, 35-55, 56-75, 76-95 and 96-117), which were subsequently used as antigenic probe in SP-ELISA. Results obtained were compared with the one achieved on full-length recombinant protein.

Results & Discussion

First cohort: preliminary SP-ELISA screening on $rMOG_{1-117}(His)_6$, CSF114 and CSF114(Glc)

Results are summarized in Figure 19. No response to peptide Ag was detected in EAE mice compared with naïve. In the case of IgG, EAE mice showed high response to $rMOG_{1-117}(His)_6$, while only the recovery mice displayed a high and consistent response to $rMOG_{1-117}(His)_6$ compared with both EAE and naïve mice. The latter finding allowed us to hypothesize a protective role for anti-MOG IgM.

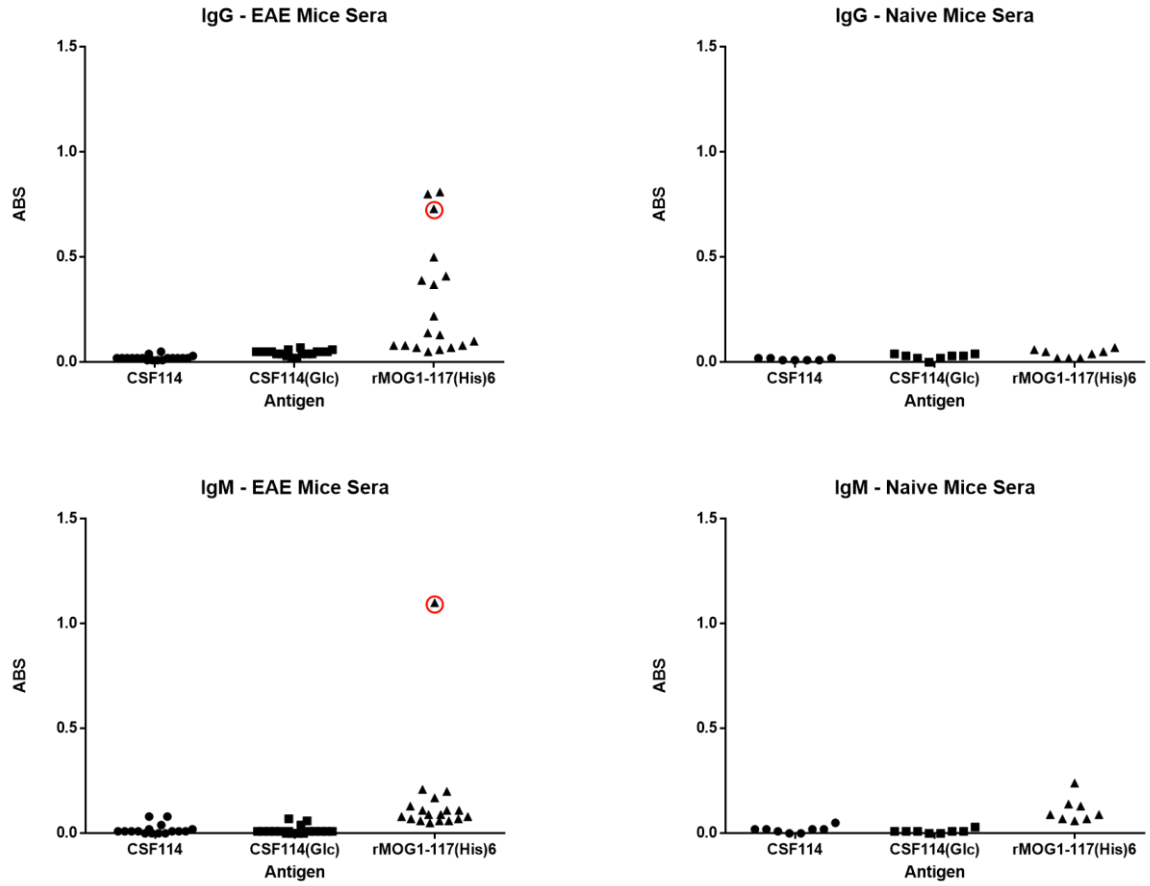

Figure 19: Data distribution for IgG (top) and IgM (bottom) in EAE (left) and naïve mice (right). Recovery mice is highlighted with a red circle.

Second cohort: anti-rMOG$_{1-117}$(His)$_6$ IgM screening

Results obtained are shown in Figure 20. Cutoff value was calculated as (mean of naïve)+ 3*(standard deviation of naïve). Tests on the new cohort displayed that most of recovery and "no disease" mice have anti-MOG IgM titers, confirming the hypothesized anti-MOG IgM protective role. However, anti-MOG IgM are present also in the active disease group.

A limitation of these data concerns the small recovery and "no disease" cohorts. Therefore, the obtained results have to be considered as preliminary. The small size of the cohort and the difficulty in the model management (most of the mice do not survive beyond day 22) prevented us to perform a time-course and a disease-course analysis of the Ab response against rMOG.

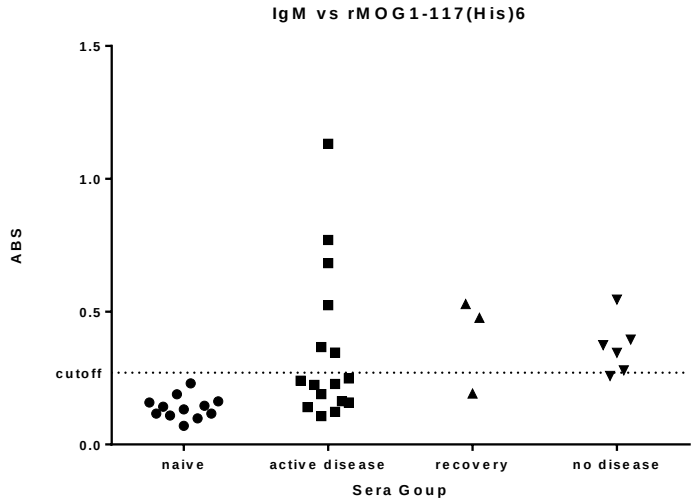

Figure 20: Data distribution of IgM against rMOG$_{1-117}$(His)$_6$ tested the second cohort. Cutoff value is shown with the dotted line.

Third cohort: $rMOG_{1-117}$ epitope mapping

Results obtained are shown in Figure 21. No significant response was detected against any Ag in the case of IgM comparing EAE with naïve mice. On the contrary, EAE active disease mice displayed high and specific IgG response against mMOG(35-55) and recombinant $rMOG_{1-117}$, while no response was detected against the other Ag. The higher response against the recombinant full-length protein compared with the immunizing peptide allowed us to speculate the presence of a MOG conformational epitope recognized by auto-Ab. Indeed, the recombinant protein is able to reproduce both Aa sequence and conformation of the native Ag, which is probably stable during the coating phase. The peptide probe instead is able to mimic only a linear, short portion of the protein, and due to its flexibility may display a random conformation on the plate. Therefore, it can be hypothesized the presence of two distinct families of auto-Ab: one directed against a linear peptide reproduced by both mMOG(35-55) and the recombinant protein, and one able to detect conformational epitope(s) on $rMOG_{1-117}$. To verify this assumption, it will be necessary to test both Ag in a competitive ELISA test.

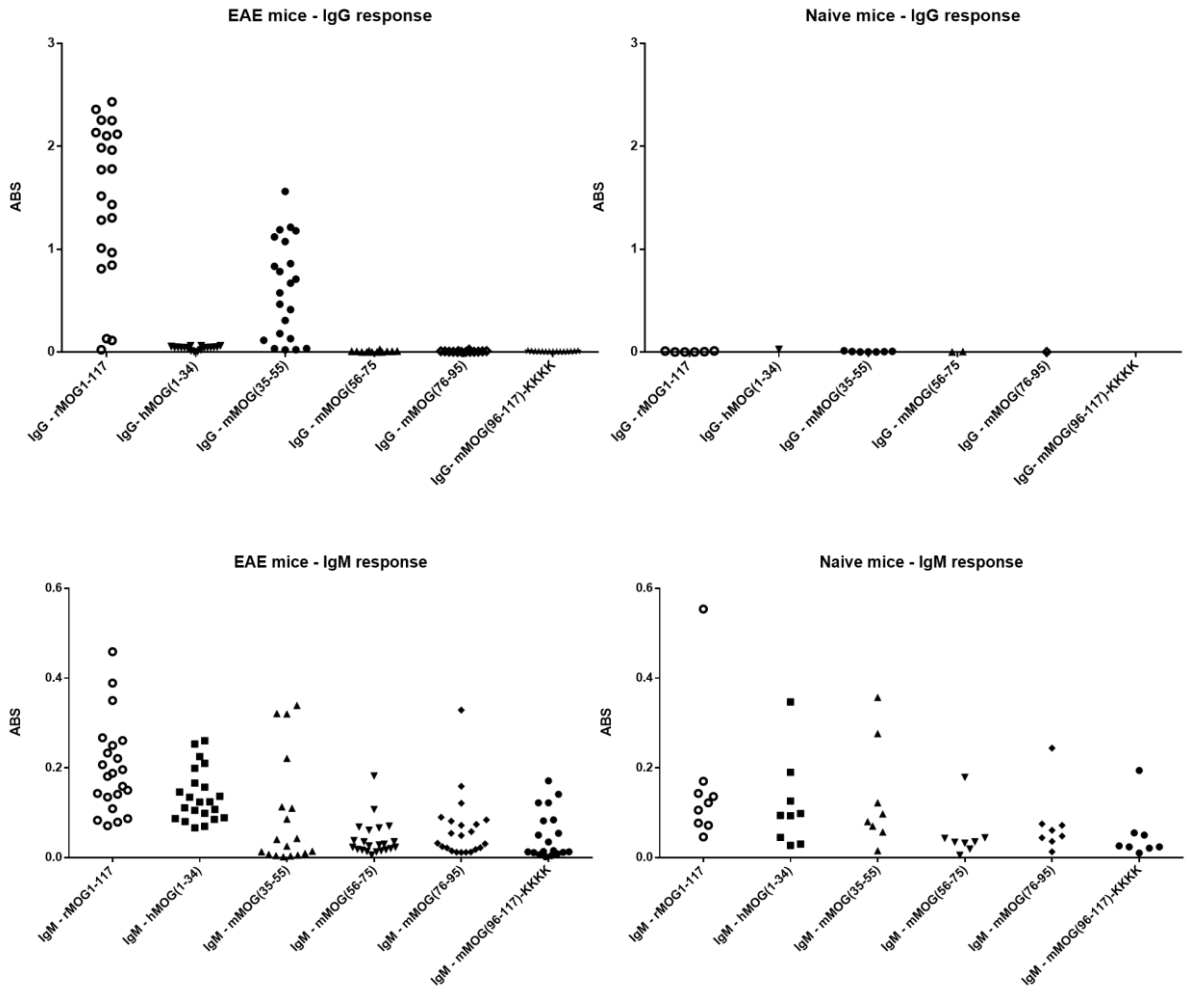

Figure 21: Data distribution for IgG (top) and IgM (bottom) in EAE (left) and naïve mice (right).

The possibility to investigate MS using an animal model is remarkably advantageous, as it enables to study in depth the disorder from a clinical point of view, and also to have a large number of biological samples. Conversely, both development and management of a proper disease model is complicated. For example, the use of the EAE mice model of MS allows to examine immunopathological and molecular aspect characterizing the acute phase of the disorder, because the animals did not survive long after immunization. Furthermore, blood draws are difficult and often lead to the death of the animal.

In conclusion, the obtained results boost the interest in using recombinant MOG to assess the presence of Ab in the mice model of MS. The use of a proven animal model has numerous advantages, as it enables to plan the desired experiments aimed to explore a peculiar aspect of the disorder, and to have a large number of samples to be analyzed. The results presented are preliminary and therefore will require further investigations to better understand the molecular mechanisms underlying the immunological response to MOG in MS. A limitation of this study is represented by the execution of tests on temporally distinct cohorts, making the obtained data not entirely homogeneous. However, we demonstrated the lack of evidence of an epitope spreading mechanism related to MOG sequence. Based on these findings, future developments of this work will include focused and detailed studies aimed to disclose the putative pathologic role of the anti-MOG immunological response. Specifically, the existence of a correlation between anti-MOG Ab and disease course, or response to pharmacological therapy, will be evaluated. Furthermore, the intriguing theory of a protective role of anti-MOG IgM response will be deepened.

Materials & Methods

Serum samples

90 EAE induced mice serum samples (provided by Dr. Rina Aharoni, Weizmann Institute, Rehovot, Israel) were analyzed, divided according to disease status. 29 naïve mice serum samples were used as healthy control group. Samples were tested in triplicate with a single dilution (1:100) in FBS Buffer.

Antigens

Recombinant $rMOG_{1-117}$ was produced according to the protocol published by Gori *et al*[118]. Peptide probes were synthesized at the French-Italian Laboratory of Peptide and Protein Chemistry & Biology (PeptLab), University of Florence and University of Cergy-Pontoise.

Enzyme-Linked Immunosorbent Assay (ELISA)

1 microgram (ug)/well of Ag (peptide or protein) were dissolved in Coating Buffer (12mM Na_2CO_3, 35mM $NaHCO_3$, pH 9.6), then 100 microliter (ul) of solution were dispensed in each well of 96-well Maxisorp plates. Plates were incubated @4°C ON. Subsequently, plates were washed 3 times with Washing Buffer (0,9% NaCl, 0,01% Tween 20), and blocked 1 h at room temperature (RT) with 100ul/well of FBS Buffer (10% FBS in Washing Buffer). FBS Buffer were removed, and 100ul/well of diluted sera sample (1:100 in FBS Buffer) were dispensed. Blank wells were included in all the plates, and were obtained using FBS Buffer instead of serum. Plates were incubated @4°C ON, and then washed 3 times with Washing Buffer. 100ul/well of secondary Ab diluted in FBS Buffer (mIgG 1:30000 and mIgM 1:7500) were dispensed, and plates were incubated 3 h at RT. Plates were washed 3 times with Washing Buffer, then 100ul/well of Substrate Solution (1mg/ml p-PNP in Substrate Buffer: 1M Diethanolamine, 1mM MgCl2, pH 9.8) were dispensed. Plates were incubated for 15'-40', and then ABS at 405 nm of each well was red with a spectrophotometer. ABS value for each serum was calculated as (mean ABS of triplicate) – (mean ABS of blank triplicate).

PART II: EVALUATION OF MOG-IgG AND CSF114(Glc)-IgG AS ADDITIONAL NMO BIOMARKERS

As already noted, NMO is an inflammatory demyelinating disorder of CNS, characterized by the presence a specific disease BM (an auto-Ab of the IgG class directed against AQP4), which is present in approximately 70% of NMO pts[72]. Therefore, the evaluation of other NMO BM may be useful to perform a more accurate diagnosis. The potential role of anti-MOG IgG as additional NMO BM was taken into account, but the studies done so far failed to give definitive results on this topic.

In this context, we assessed the presence of a specific IgG reactivity against MOG testing NMO pts sera in SP-ELISA. As NMO is an MS-related disorder, we tested the same sera on CSF114(Glc), which is an antigenic probe able to detect disease-specific Ab response in RRMS. Results obtained for both Ag were compared with NBD.

Results & Discussion

IgG reactivity to $rMOG_{1-117}(His)_6$ is shown in Figure 22. Results obtained indicate that IgG reactivity to MOG is not increased in pts compared with NBD, disclosing that anti-MOG IgG is not a reliable BM in the case of NMO. However, we noted that Ab titer in AQP- pts is higher than in AQP+ (Figure 23), even if both the NMO groups have lower anti-MOG IgG values compared with NBD.

Results obtained testing the antigenic probe CSF114(Glc) on both NMO and NBD sera (Figure 24) show that there is no significant difference between pts and healthy controls, disclosing that anti-CSF114(Glc) IgG is not a BM in the case of NMO. This finding further confirms that NMO and MS are two distinct pathologies, characterized by different serological profiles.

Concluding, our study demonstrates that anti-MOG IgG are not present in NMO pts. The use of the properly refolded rat isoform of the extracellular domain of the protein, which shares a >90% homology with the human one, could represent a limitation of this work. Indeed, rMOG has a Ser in position 42, while hMOG has a Pro: this could lead to both structural and immunogenicity differences. It may be useful to repeat the test comparing anti-rMOG and anti-hMOG Ab titer. Furthermore, the absence of anti-CSF114(Glc) IgG in NMO pts provides an additional evidence of the different pathological profile of MS and NMO. One of the further developments of this work may be represented by the enlargement of both NMO and NBD cohorts, in order to obtain more reliable data, to be compared with the one previously achieved for MS.

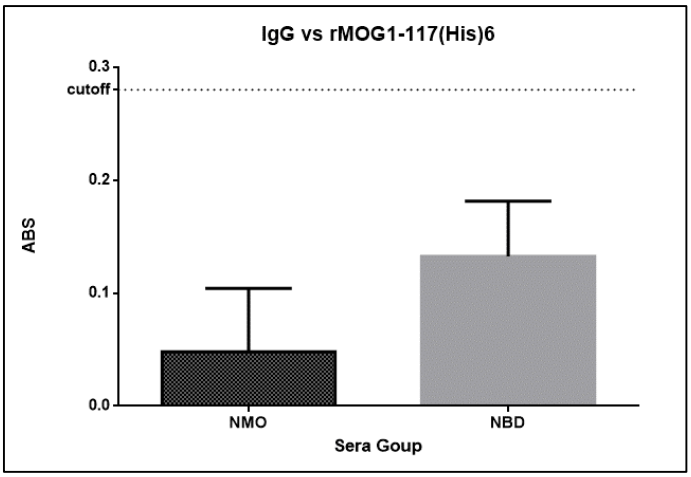

Figure 22: IgG reactivity to $rMOG_{1-117}(His)_6$ in NMO (left) and NBD (right). Cutoff value is represented with a dotted line.

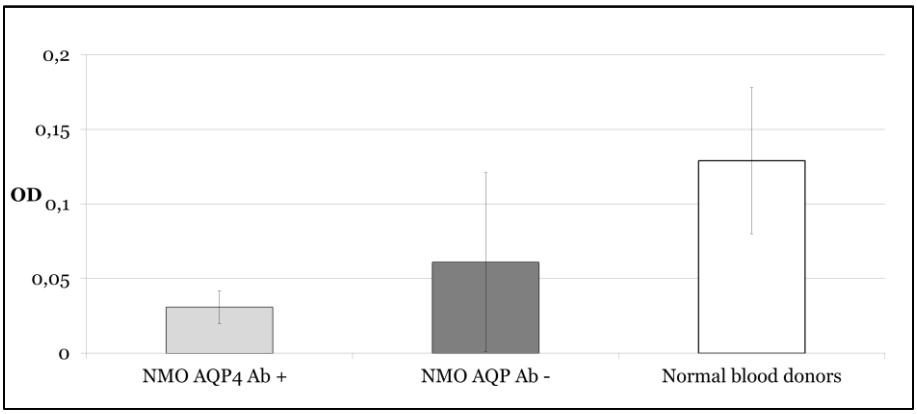

Figure 23: IgG reactivity to $rMOG_{1-117}(His)_6$ in the tested sera group. From left: AQP4+ NMO pts, AQP4- NMO pts, NBD.

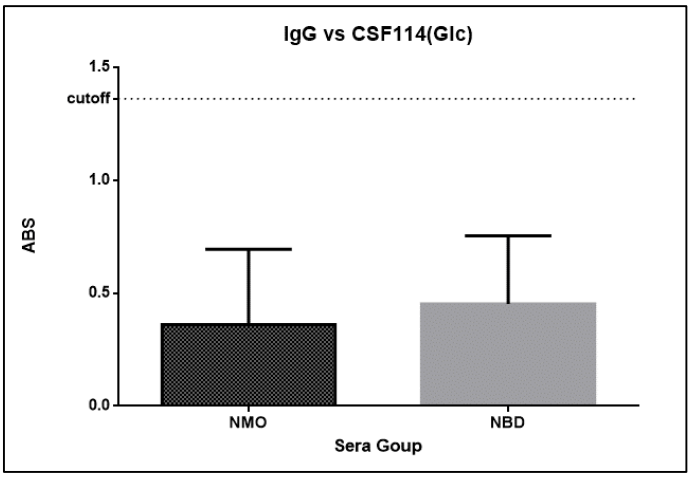

Figure 24: IgG reactivity to CSF114(Glc) in NMO (left) and NBD (right). Cutoff value is represented with a dotted line.

Materials & Methods

Serum samples

21 NMO pts serum samples (provided by Prof. Jerome De Seze, *Hôpitaux universitaires de Strasbourg*, France) were analyzed, divided according to disease status. 20 NBD serum samples were used as healthy control group. Samples were tested in triplicate with a single dilution (1:100) in FBS Buffer.

Antigens

Recombinant $rMOG_{1-117}$ was produced according to the protocol published by Gori *et al*[118]. Peptide probe was synthesized at the French-Italian Laboratory of Peptide and Protein Chemistry & Biology (PeptLab), University of Florence and University of Cergy-Pontoise.

Enzyme-Linked Immunosorbent Assay (ELISA)

1ug/well of Ag (peptide or protein) were dissolved in Coating Buffer (12mM Na_2CO_3, 35mM $NaHCO_3$, pH 9.6), then 100 ul of solution were dispensed in each well of 96-well Maxisorp plates. Plates were incubated @4°C ON. Subsequently, plates were washed 3 times with Washing Buffer (0,9% NaCl, 0,01% Tween 20), and blocked 1 h at RT with 100ul/well of FBS Buffer (10% FBS in Washing Buffer). FBS Buffer were removed, and 100ul/well of diluted sera sample (1:100 in FBS Buffer) were dispensed. Blank wells were included in all the plates, and were obtained using FBS Buffer instead of serum. Plates were incubated @4°C ON, and then washed 3 times with Washing Buffer. 100ul/well of secondary Ab diluted in FBS Buffer (hIgG 1:8000 and hIgM 1:1200) were dispensed, and plates were incubated 3 h at RT. Plates were washed 3 times with Washing Buffer, then 100ul/well of Substrate Solution (1mg/ml p-PNP in Substrate Buffer: 1M Diethanolamine, 1mM MgCl2, pH 9.8) were dispensed. Plates were incubated for 15'-40', and then ABS at 405 nm of each well was red with a spectrophotometer. ABS value for each serum was calculated as (mean ABS of triplicate) – (mean ABS of blank triplicate).

PART III: IMMUNOLOGICAL ROLE OF MOG IN NMO-LIKE EAE RAT MODELS

As previously noted, the obtainment of a specific *Rattus Norvegicus* NMO-like EAE model was achieved immunizing Brown Norway rats with recombinant, not-refolded $rMOG_{1-117}(His)_6$ produced in our lab. In particular, it was analyzed the possibility to reproduce the disorder administering two doses of immunizing agent (together with adjuvant). The aim of this study was to evaluate the Ab response elicited in the NMO-like model to disclose the correlation between anti-MOG Ab titer and disease progression. A first attempt to evaluate the model obtained immunizing Brown Norway rats with $rMOG_{1-117}(His)_6$ was made studying the time-course of IgM and IgG anti-MOG Ab response. Subsequently, it was assessed the correlation between Ab titer against refolded MOG and both time- and disease-course in four different immunization protocols. The same cohort was examined to verify the presence of a response against unfolded MOG and CSF114(Glc).

Results & Discussion

11 EAE rat serum samples collected in different days post immunization (DPI) were tested in SP-ELISA against $rMOG_{1-117}(His)_6$. Results obtained were compared with 3 naïve rat samples (Figure 25). Data obtained confirmed the presence of a canonical Ab response, with the IgM peak at day 10 and the IgG peak around day 45.

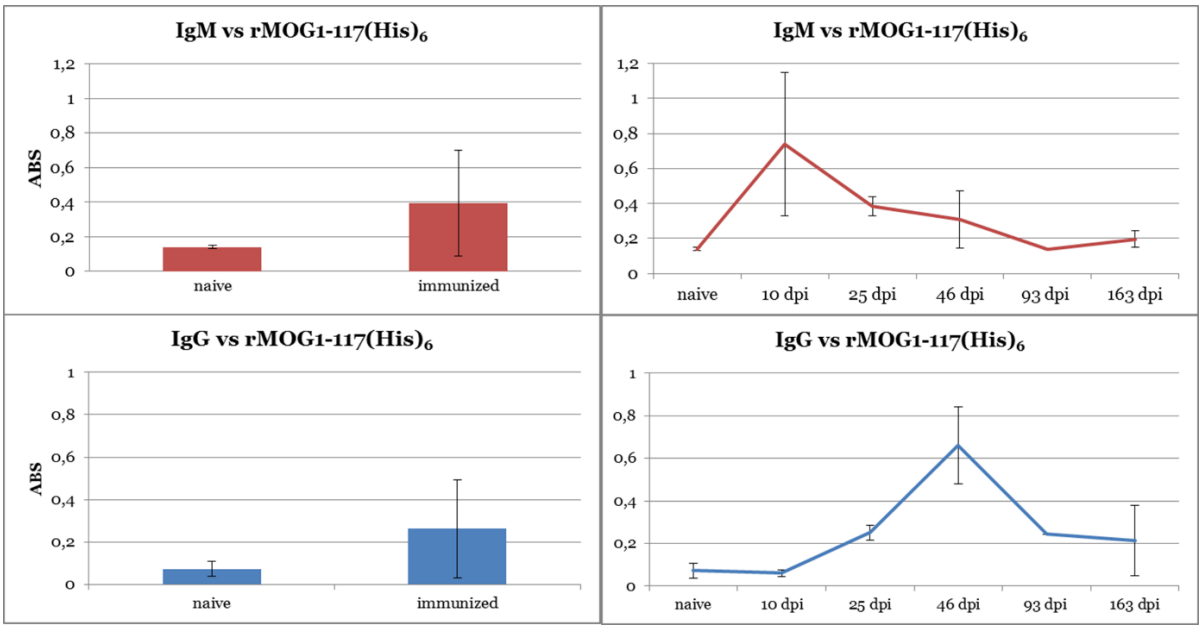

Figure 25: IgM and IgG response to $rMOG_{1-117}(His)_6$. Anti-MOG Ab time-course is shown on the right.

A second rat cohort was tested to assess the correlation between anti-MOG titer and disease progression in four distinct models. Animals were immunized with recombinant, unfolded $rMOG_{1-117}(His)_6$, then divided in 4 groups:

1. No further immunization;
2. Boost at day 39 with PBS;
3. Boost at day 39 with $rMOG_{1-117}(His)_6$;
4. Boost at day 50 with $rMOG_{1-117}(His)_6$.

Serum samples were collected from at day 42, 51 and 77 post immunization, and tested against $rMOG_{1-117}(His)_6$. Results obtained are shown in Figure 26 and Figure 27 .

Rats that received one single immunization with the protein have a disease score = 0 throughout the observation period, and developed a stable anti-MOG Ab response (both IgM and IgG) after the administration of the protein. These findings indicate that the first immunization with the protein triggers a strong humoral response, which however is not correlated with disorder occurrence or progression. Similar results were achieved in the animals boosted with PBS alone, which in turn did not exhibit pathological signs.

In the case of double-immunization, rats developed a disease score = 4-5 after the boost. We observed that IgG titers are high and stable in time, in agreement with the previously mentioned results that disclose the IgG peak around day 45 post-immunization (Figure 25). Therefore, the anti-MOG IgG detected still refers to the first immunization step. In the case of IgM, we noticed a high increase in the Ab titer in 3/5 animals.

From a molecular point of view, it appears that a single immunization with the recombinant is $rMOG_{1-117}(His)_6$ is not sufficient to induce the disease in Brown Norway rats, even if it is able to elicit an Ab response. Conversely, animals boosted with a second dose of protein develop a severe NMO-like disorder, corresponding to a rise of the anti-MOG IgM titer. Based on these findings, we can hypothesize two different scenarios:

- the anti-MOG response is not correlated with disease progression, and therefore the detected Ab have not a pathologic role;
- there are two families of anti-MOG Ab, and only one is responsible for disease occurrence. We are not able to distinguish them because we used a full-length recombinant protein, which contains different epitopes, both conformational and linear.

In the latter case, it would be interesting to investigate the epitope of the two families through an epitope mapping study, using both solid phase and competitive ELISA. Summarizing, we demonstrated that a NMO-like model can be obtained immunizing Brown Norway rats with recombinant $rMOG_{1-117}(His)_6$. This result allows us to speculate a role of this protein in the disorder, even if we obtained contrasting data in human NMO. As already stated, this may be due to the use of recombinant rMOG as Ag in the tests with human sera: the two isoforms share a high degree of homology in terms of sequence, but some of the not conserved Aa may be crucial for both

conformation and immunogenicity, affecting the Ab recognition. The relevance of this difference in the primary sequence will be elucidated testing in parallel rMOG and hMOG as Ag, and comparing the obtained data. However, it must be kept in mind that both the results achieved studying NMO and the rat NMO-like model are preliminary, and therefore further clarifications and investigations are needed.

The same sera cohorts were tested also against unfolded $rMOG_{1\text{-}117}(His)_6$ and CSF114(Glc). Preliminary results are show in Figure 28 (IgM response) and Figure 29 (IgG response). The Ab response detected against refolded and unfolded recombinant protein is slightly different, indicating that the conformation is maintained during the ELISA coating step. However, this difference is not statistically relevant, and does not allow us to speculate the presence of conformational epitopes. Concerning CSF114(Glc), we have not detected any IgG response against this probe, coherently with the data obtained in the human NMO pathology (Figure 24). Conversely, the anti-CSF114(Glc) IgM response is detectable in the model regardless of the immunization protocol, with a trend mirroring that of MOG. This pattern of Ab response against the glucosylated peptide (namely, presence of IgM and absence of IgG) may indicate a sort of epitope spreading starting from the immunizing agent.

As stressed also in the case of EAE mice model of MS, the use of animal models in both clinical and immunological field is of crucial relevance, as it enables to understand numerous aspects that would otherwise be out of reach. The obtainment of a suitable NMO-like EAE animal model may allow to disclose the molecular mechanisms characterizing this CNS AID, and in particular to clarify the immunopathogenic role of both AQP4 and MOG. However, further investigations on the Ab response of the NMO-like model are required to formulate a precise hypothesis of immunopathogenic molecular mechanism characterizing the disorder.

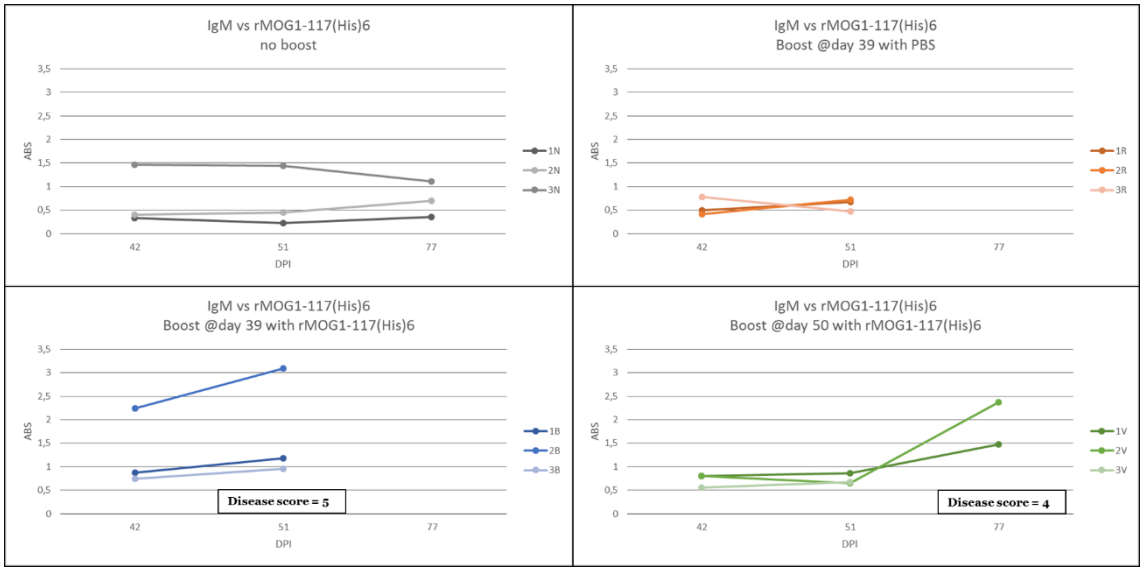

Figure 26: IgM response to rMOG$_{1-117}$(His)$_6$ in the different cohorts: not boosted rats (black); boosted at day 39 with PBS (red); boosted at day 39 with rMOG$_{1-117}$(His)$_6$ (blue); boosted at day 50 with rMOG$_{1-117}$(His)$_6$.

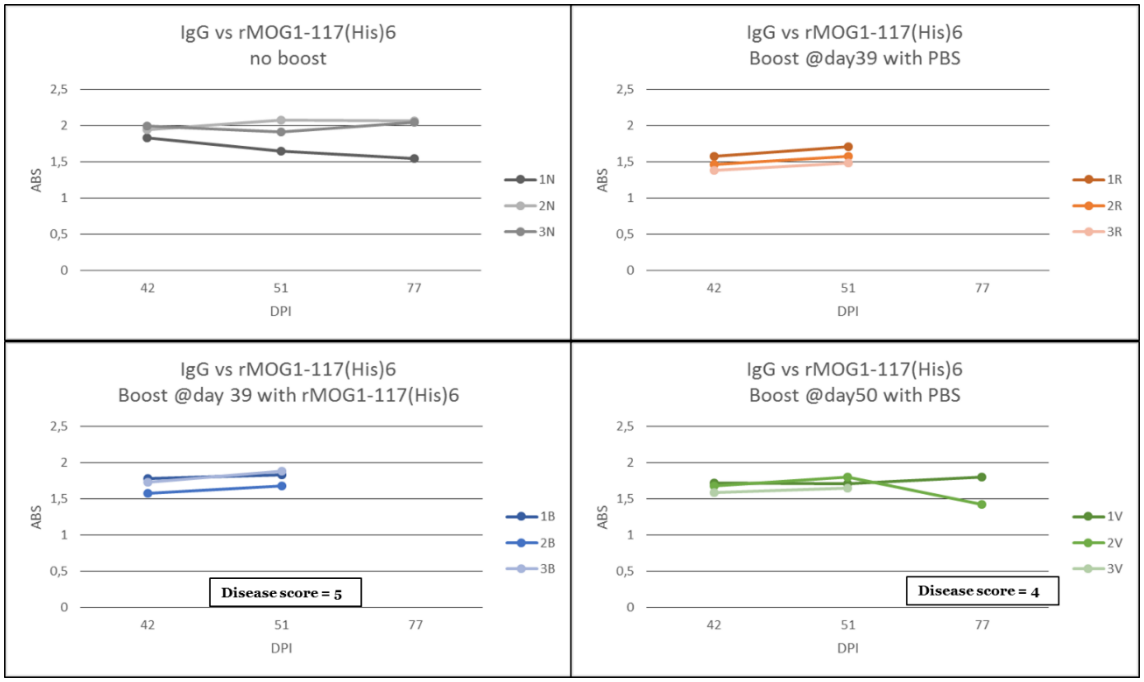

Figure 27: IgG response to rMOG$_{1-117}$(His)$_6$ in the different cohorts: not boosted rats (black); boosted at day 39 with PBS (red); boosted at day 39 with rMOG$_{1-117}$(His)$_6$ (blue); boosted at day 50 with rMOG$_{1-117}$(His)$_6$.

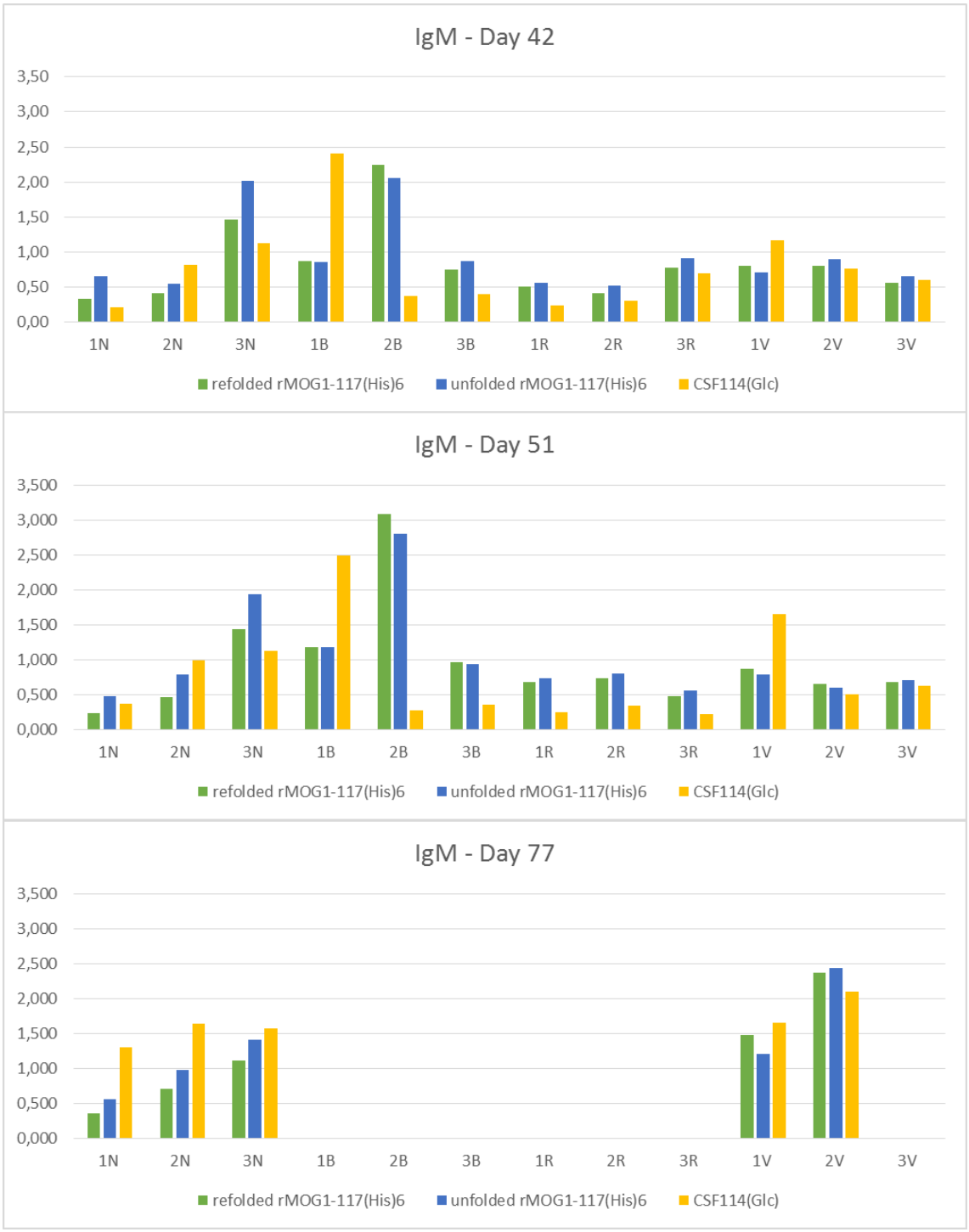

Figure 28: IgM titers against refolded $rMOG_{1-117}(His)_6$ (green), unfolded $rMOG_{1-117}(His)_6$ (blue) and CSF114(Glc) (yellow) in the 4 different immunization protocols: not boosted (1N, 2N, 3N), boosted at day 39 with $rMOG_{1-117}(His)_6$ (1B, 2B, 3B), boosted at day 39 with PBS (1R, 2R, 3R), boosted at day 50 with $rMOG_{1-117}(His)_6$ (1V, 2V, 3V).

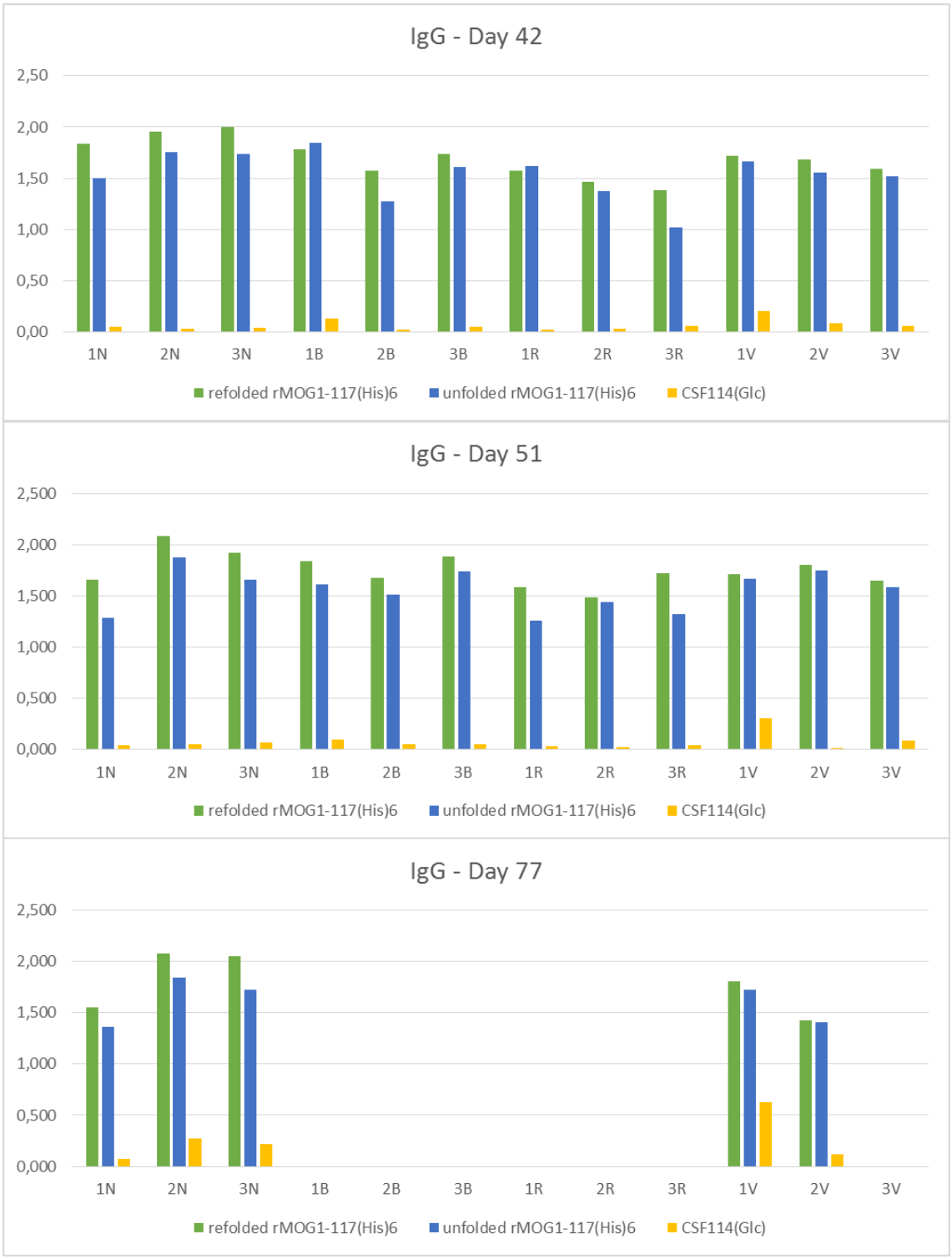

Figure 29: IgG titers against refolded $rMOG_{1-117}(His)_6$ (green), unfolded $rMOG_{1-117}(His)_6$ (blue) and CSF114(Glc) (yellow) in the 4 different immunization protocols: not boosted (1N, 2N, 3N), boosted at day 39 with $rMOG_{1-117}(His)_6$ (1B, 2B, 3B), boosted at day 39 with PBS (1R, 2R, 3R), boosted at day 50 with $rMOG_{1-117}(His)_6$ (1V, 2V, 3V).

Materials & Methods

Serum samples

50 EAE induced rat serum samples (provided by Prof. Jerome De Seze group (*Hôpitaux universitaires de Strasbourg*, France) were analyzed, divided according to the immunization protocol. Samples were tested in triplicate with a single dilution (1:100) in FBS Buffer.

Antigens

Recombinant refolded $rMOG_{1-117}$ was produced according to the protocol published by Gori *et al*[118]. Recombinant unfolded $rMOG_{1-117}$ was obtained modifying the purification protocol as follows. Solubilized IB sample was loaded in column and washed with:

1. 50 ml Buffer A (100 mM NaH_2PO_4, 10 mM Tris, 6M GuaCl) pH 8;
2. 50 ml Buffer A pH 6;
3. 50 ml Buffer A pH 5.2.

Elution was performed using Buffer A pH 4.5.

Peptide probes were synthesized at the French-Italian Laboratory of Peptide and Protein Chemistry & Biology (PeptLab), University of Florence and University of Cergy-Pontoise.

Enzyme-Linked Immunosorbent Assay (ELISA)

1ug/well of Ag (peptide or protein) were dissolved in Coating Buffer (12mM Na_2CO_3, 35mM $NaHCO_3$, pH 9.6), then 100 ul of solution were dispensed in each well of 96-well Maxisorp plates. Plates were incubated @4°C ON. Subsequently, plates were washed 3 times with Washing Buffer (0,9% NaCl, 0,01% Tween 20), and blocked 1 h at RT with 100ul/well of FBS Buffer (10% FBS in Washing Buffer). FBS Buffer were removed, and 100ul/well of diluted sera sample (1:100 in FBS Buffer) were dispensed. Blank wells were included in all the plates, and were obtained using FBS Buffer instead of serum. Plates were incubated @4°C ON, and then washed 3 times with Washing Buffer. 100ul/well of secondary Ab diluted in FBS Buffer (rIgG 1:5000 and rIgM 1:5000) were dispensed, and plates were incubated 3 h at RT. Plates were washed 3 times with Washing Buffer, then 100ul/well of Substrate Solution (1mg/ml p-PNP in Substrate Buffer: 1M Diethanolamine, 1mM MgCl2, pH 9.8) were dispensed. Plates were incubated for 15'-40', and then ABS at 405 nm of each well was red with a spectrophotometer. ABS value for each serum was calculated as (mean ABS of triplicate) – (mean ABS of blank triplicate).

PART IV: OPTIMIZATION OF rMOG$_{1-117}$ PRODUCTION PROCESS

As stated in the introductive chapter, Ag production process is a key step of the BM research in both diagnostic and prognostic fields. As mentioned several times during this presentation, MOG is the most studied candidate Ag in the case of CNS AID, and therefore the production of this protein as antigenic probe is of crucial relevance to study the immunopathogenesis of disorders such as MS or NMO. In our lab, we decided to employ recombinant rMOG$_{1-117}$, which was obtained through the expression and purification protocol published by Gori *et al.*[118]. This methodology includes numerous laborious and time-consuming phases that invalidate productivity. Therefore, the aim of this project was to improve rMOG$_{1-117}$ production process, focusing on the optimization of both expression in *E.coli* and purification/on-column refolding of the protein.

Results & Discussion

The recombinant rat protein rMOG$_{1-117}$ was primarily expressed, purified and refolded according to the protocol published by Gori *et al.*[118]. This methodology was very effective, but included some laborious and lengthy steps. Therefore, the method was improved optimizing the following steps:

1. *E.coli* cells

   The previous protocol was carried out employing ER2566 electrocompetent *E.coli* cells, which give high transformation efficiencies using a quick method. However, the procedure requires specialized apparatus and cuvettes, and is salt-sensitive. The use of chemically competent cells leads to both simplification of the protocol and cost reduction, as no special equipment is necessary and cells are less expensive. Furthermore, the selected BL21(DE3)-Gold cells are ultra-competent, thus allowing the obtainment of transformation efficiencies comparable with the one achieved using electrocompetent cells.

2. IB solubilization

   The original protocol provided 5 steps of sonication-centrifugation-resuspension with Potter. In particular, the resuspension part is laborious, time-consuming and requires skills with the instrument. Additionally, the final product has to be resuspended by a ≈90' stirring and then centrifuged again before the purification.

   A first attempt for improvement was made changing resuspension buffer composition (which consisted of Tris and NaCl) by the addition of a denaturant (GuaCl) and a detergent (Triton X-100), in order to facilitate the solubilization. Furthermore, the number of sonication-centrifugation-resuspension steps was reduced from 5 to 3. Unfortunately, the new method was still disadvantageous, as the Potter resuspension was still required, and

the final stirring step was not removed. Furthermore, the obtained sample was viscous, leading to overpressure problems of and column clogging during the purification.
Both duration and complexity of the process were considerably reduced using the next measures:

- Longer sonication for time (1' instead of 10");
- Longer and at higher-rpm speed (from 17,000 to 25,000 rpm) centrifugation steps;
- Use of Urea 8M and ≈30' stirring for solubilization.

These modifications enable to obtain a soluble sample to be purified with only 2 centrifugation steps and 1 resuspension by stirring. Being liquid, the lysate can be loaded directly into the purification system without needing dilution, and causes no problems to the column or to the instrument.

3. Purification method
   The previously reported method used a Precision Column Holder to be packed with Chelating Sepharose Fast Flow resin and then added with $NiSO_4$. This procedure requires two incubation steps of the column: the first, to facilitate the Ni^{2+} binding to the resin (30') and the second to allow the protein sample binding to Ni^{2+} (2h). Furthermore, an approximate calculation of the protein concentration is needed, in order to estimate the amount of resin and $NiSO_4$ to be loaded in column. To avoid the manual packing, which is laborious and time-consuming, the HisTrap FF pre-packed column was selected. This column is pre-charged with Ni Sepharose 6 Fast Flow, has high binding capacity (approximately 40 mg/ml medium) and is compatible with a wide range of additives (reducing agents, detergents, denaturants, ecc.). The price of the product is moderate, and can be further reduced recharging the exhausted column with fresh $NiSO_4$ after an easy cleaning-in-place procedure.
   Another improvement concerns the use of a Superloop to introduce the lysate in the purification system. This step enables to fully automate the procedure, as the sample is injected in the column directly by the instrument. Moreover, up to 50 ml of solubilized IB can be purified at one time, significantly reducing the process time.

Materials & Methods

$rMOG_{1-117}(His)_6$ expression and purification protocol

<u>$pET\text{-}22rMOG_{1-117}(His)_6$ plasmid</u>

$pET\text{-}22rMOG_{1-117}(His)_6$ plasmid (Figure 30) was obtained amplifying the 1-117 portion of MOG from $pQE12rMOG_{ED}(His)_6$ plasmid and inserting it into a pET-22b vector (Novagen).

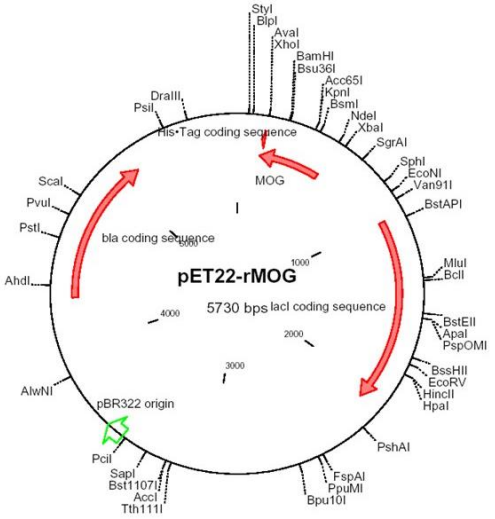

MRGSGQFRVIGPGHPIRALVGDEAELPCRI
SPGKNATGMEVGWYRSPFSRVVHLYRNGK
DQDAEQAPEYRGRTELLKESIGEGKVALRI
QNVRFSDEGGYTCFFRDHSYQEEAAVELKV
EDLEHHHHHH

Figure 30: pET-22rMOG1-117(His)$_6$ plasmid structure (left) and recombinant rMOG1-117(His)$_6$ sequence (right). In red, Aa added during the amplification step. In blue, the 6-His tag.

<u>ER2566 cells transformation with $pET\text{-}22rMOG_{1-117}(His)_6$</u>

ER2566 electrocompetent cells were transformed with $pET\text{-}22rMOG_{1-117}(His)_6$ using the electrophoretic transformation protocol. Briefly, 70 ul of cells were added to 1 ul of plasmid (120 ng/ul), then the suspension was transferred into a 1 mm cuvette and electroporated (2000 V, 5 ms). Immediately, 300 ul of SOC medium were added to the cells. The obtained suspension was incubated at 37°C for 1 h with vigorous shaking, then 50 or 100 ul were plated on pre-warmed selective plates (LB Amp+) and incubated overnight (ON) at 37°C. Single colonies were picked and inoculated in 2 ml of LB each. The precultures (PC) were incubated ON at 37°C with vigorous shaking.

Precultures and Expression Test

Colonies were chosen to prepare PC. 5 ml of LB medium containing Ampicillin were inoculated with one single colony and incubated ON at 37°C with vigorous shaking. Then 6 ml of LB medium containing Ampicillin were inoculated with 6 ul of PC, and incubated at 37°C with vigorous shaking until an OD_{600nm} between 0.4 and 0.8 (log-phase) was reached. Afterwards, 1 ml of each suspension was collected as not-induced sample (NI) and the remaining culture was induced with 5 ul of IPTG (final concentration: 1 mM) and incubated ON at 37°C with vigorous shaking. 1 ml of each induced culture was collected (I). NI and I samples were centrifuged at 17000 rpm for 30' at 4°C, then the pellet was resuspended in 50 ul of Laemmli Buffer, heated at 100°C for 10' and loaded on 16% SDS-PAGE (Sodium Dodecyl Sulphate PolyAcrilamide Gel Electrophoresis).

Large-scale protein expression

1 ml of PC was inoculated in 1 L of LB medium containing Ampicillin, then incubated at 37°C with vigorous shaking until an OD_{600nm} between 0.4 and 0.8 (log-phase) was reached. Afterwards, 1 ml of each suspension was collected as not-induced sample (NI) and the remaining culture was induced with 5 ul of IPTG (final concentration: 1 mM) and incubated ON at 37°C with vigorous shaking. 1 ml of each induced culture was collected (I). NI and I samples were centrifuged at 17000 rpm for 30' at 4°C, then the pellet was resuspended in 50 ul of Laemmli Buffer, heated at 100°C for 10' and loaded on 16% SDS-PAGE.

Cell lysis and IB solubilization

The ON 1 L culture was centrifuged for 30' at 4°C, 4000 rpm. The pellet was resuspended in 10 ml of Soni Buffer pH 8 (50 mM Tris, 300 mM NaCl) containing protease inhibitor (500 ul of a solution obtaining dissolving a tablet of Complete, EDTA-free protease inhibitor in 2 ml of milliQ H_2O), then stored at -20°C if not immediately used for the following steps. The suspension was added with a tip of lysozyme, then stirred for at least 30' at RT. LDAO was added (0,83 ml/50 ml of culture), then:

1. The suspension was sonicated on ice (10x30'', power=50%) and centrifuged for 30' at 4°C, 17000 rpm.
2. The pellet was resuspended* in 10 ml of Soni Buffer + LDAO 0,5%.
3. The suspension was sonicated on ice (10x30'', power=50%) and centrifuged for 20' at 4°C, 17000 rpm.
4. The pellet was resuspended* in 10 ml of Soni Buffer + LDAO 0,5%.
5. The suspension was sonicated on ice (10x30'', power=50%) and centrifuged for 20' at 4°C, 17000 rpm.
6. The pellet was resuspended* in 10 ml of Soni Buffer + LDAO 0,5%.

7. The suspension was sonicated on ice (10x30", power=50%) and centrifuged for 20' at 4°C, 17000 rpm.
8. The pellet was resuspended* in 10 ml of Soni Buffer.
9. The suspension was sonicated on ice (10x30", power=50%) and centrifuged for 20' at 4°C, 17000 rpm.
10. The pellet was resuspended* in 10 ml of Soni Buffer.
11. The suspension was sonicated on ice (10x30", power=50%) and centrifuged for 20' at 4°C, 17000 rpm.

* Resuspension steps are performed with Potter.

The obtained pellet (IB) was solubilized adding 500 ul of Soni Buffer and then 5 ml of Buffer A + 40 mM β-mercaptoethanol, βME, pH 8 (100 mM NaH_2PO_4, 10 mM Tris, 6M GuaCl, 40 mM βME) and stirring for 30-90' at RT. The suspension was centrifuged at 17000 rpm for 30' at RT.

Purification and refolding by affinity chromatography

Precision Column Holder XK16 was packed with Chelating Sepharose Fast Flow resin, then connected with ÄktaBasic chromatograph system. The column was washed with milliQ H_2O, disconnected and added with $NiSO_4$, then stirred for 30' at RT. The column was connected again with ÄktaBasic chromatograph system and washed with milliQ H20, then equilibrated with Buffer A + 1 mM βME pH 8 (100 mM NaH_2PO_4, 10 mM Tris, 6M GuaCl, 1 mM βME).

Previously obtained sample was diluted with Buffer A pH 8 (100 mM NaH_2PO_4, 10 mM Tris, 6M GuaCl), in order to obtain a 2-3 mM βME final concentration. Sample was loaded into the column, then stirred for 2 h at RT. The column was packed by gravity and connected with ÄktaBasic chromatograph system. Purification and refolding method is the following (flow: 1 ml/min):

a) Refolding. Gradient (600'): 100% Buffer A → 100% Buffer B + GSH pH 8 (100 mM NaH_2PO_4, 10 mM Tris, 3mM GSH)
b) Gradient (120'). 100% Buffer B + GSH → 100% Buffer B (100 mM NaH_2PO_4, 10 mM Tris)
c) Elution. 100% EluBuffer pH 8 (100 mM NaH_2PO_4, 10 mM Tris, 200 mM NaCl, 500 mM Imidazole).

$rMOG_{1-117}(His)_6$ expression and purification protocol optimization

BL21(DE3) cells chemical transformation with pET-22r$MOG_{1-117}(His)_6$

BL21(DE3) cells were transformed with pET-22r$MOG_{1-117}(His)_6$ using the chemical transformation protocol. Briefly, 100 ul of cells were added to 1-50 ng of plasmid and incubated on ice for 30', then heat shocked for 20"-1' in a 42°C water bath without shaking and incubated on ice again for at least 2'. 900 ul of pre-warmed LB medium were added to each cell aliquot, and then the suspensions were incubated at 37°C for 1 h at 225 rpm. 100 ul of each suspension were plated on pre-warmed selective plates (LB Amp+) and incubated ON at 37°C.Single colonies were picked and inoculated in 2 ml of LB each. The PC were incubated ON at 37°C with vigorous shaking.

Precultures and Expression Test

Colonies were chosen to prepare PC. 5 ml of LB medium containing Ampicillin were inoculated with one single colony and incubated ON at 37°C with vigorous shaking. Then 6 ml of LB medium containing Ampicillin were inoculated with 6 ul of PC, and incubated at 37°C with vigorous shaking until an OD_{600nm} between 0.4 and 0.8 (log-phase) was reached. Afterwards, 1 ml of each suspension was collected as not-induced sample (NI) and the remaining culture was induced with 5 ul of IPTG (final concentration: 1mM) and incubated ON at 37°C with vigorous shaking. 1 ml of each induced culture was collected (I). NI and I samples were centrifuged at 17000 rpm for 30' at 4°C, then the pellet was resuspended in 50ul of Laemmli Buffer, heated at 100°C for 10' and loaded on 16% SDS-PAGE.

Large-scale protein expression

1 ml of PC was inoculated in 1 L of LB medium containing Ampicillin, then incubated at 37°C with vigorous shaking until an OD_{600nm} between 0.4 and 0.8 (log-phase) was reached. Afterwards, 1 ml of each suspension was collected as not-induced sample (NI) and the remaining culture was induced with 5 ul of IPTG (final concentration: 1 mM) and incubated ON at 37°C with vigorous shaking. 1 ml of each induced culture was collected (I). NI and I samples were centrifuged at 17000 rpm for 30' at 4°C, then the pellet was resuspended in 50ul of Laemmli Buffer, heated at 100°C for 10' and loaded on 16% SDS-PAGE.

Evaluation of the best strategy for cell lysis and IB solubilization

Method #1

The ON 1 L culture was centrifuged for 30' at 4°C, 4000 rpm. The pellet was resuspended in 10 ml of Tris 20 mM pH 8 containing protease inhibitor (500ul of a solution obtaining dissolving a tablet of Complete, EDTA-free protease inhibitor in 2 ml of milliQ H_2O), then stored at -20°C if not immediately used for the following steps. The suspension was sonicated on ice (4 x 10", power=60%) and centrifuged for 10' at 4°C, 17000 rpm. The pellet was resuspended* in 10 ml of cold IB Solubilization Buffer pH 8 (2M GuaCl, 20 mM Tris, 0.5 M NaCl, 2% Triton X-100) then sonicated on ice (4 x 10", power=60%) and centrifuged for 10' at 4°C, 17000 rpm. The pellet was resuspended* in 10 ml of cold IB Solubilization Buffer pH 8 then sonicated on ice (4 cycles of 10", power=60%) and centrifuged for 10' at 4°C, 17000 rpm. The pellet was resuspended* in 10 ml of cold IB Solubilization Buffer pH 8 without GuaCl (20 mM Tris, 0.5 M NaCl, 2% Triton X-100) then sonicated on ice (4 x 10", power=60%) and centrifuged for 10' at 4°C, 17000 rpm. The pellet obtained can be used immediately for purification or conserved at -20°C. The IB pellet was resuspended in 10 ml of Binding Buffer pH 8 with βME (GuaCl 6M, NaH_2PO_4 0.1 M, 10 mM Tris, 0.5 M NaCl, 20 mM Imidazole, 20 mM βME) by stirring for 60-90' at RT, then centrifuged for 15' at RT, 17000 rpm

* The resuspension steps are performed with Potter.

Method #2

The overnight cultures were centrifuged at 4000 rpm for 30' at 4°C. The pellet was resuspended in 10 ml of 20 mM Tris pH 8 containing protease inhibitor (500 ul of a solution obtaining dissolving a tablet of Complete, EDTA-free protease inhibitor in 2 ml of milliQ H_2O), then stored at -20°C if not immediately used for the following steps. The suspension was sonicated (3 x 1', 40% amplitude, repeated twice) and centrifuged at 25000 rpm for 65' at 4°C. The supernatant (called "1st supernatant") was collected to evaluate the possible presence of the protein, and the pellet was resuspended in the same amount of Urea 8M. The sample was sonicated and centrifuged again. The supernatant (called "2nd supernatant") was collected to evaluate the possible presence of the protein, and the pellet was resuspended in the same amount of Urea 8M. The sample obtained was called "Solubilised IB". 20 ul of each sample were added with 5 ul of 5X Laemmli Buffer, heated at 100°C for 10' and loaded on 16% SDS-PAGE. After the SDS-PAGE run, is evident that the protein is absent in the 1st supernatant, while the largest amount is located in the 2nd wash. This sample was used for the purification step.

Purification and refolding by affinity chromatography

The purification steps are performed using ÄktaBasic chromatograph system and the HisTrap FF 1 ml column (GE Healthcare). Purification and refolding method is the following:

1) Column equilibration. 15 CV Binding Buffer pH 8 (6 M GuaCl, 0.1 M NaH_2PO_4, 10 mM Tris, 0.5 M NaCl, 20 mM Imidazole)
2) Sample Injection
3) Conditioning. 15 CV Binding Buffer pH 8. The UV signal must be stable
4) Refolding. Gradient (600'): 100% Binding Buffer pH 8 → 100% GSH Buffer pH 8 (6 M GuaCl, 0.1 M NaH_2PO_4, 10 mM Tris, 0.5 M NaCl, 20 mM Imidazole, 3 mM GSH)
5) Wash (60'). GSH Buffer pH 8
6) Gradient (150'). 100% GSH Buffer pH 8 → 100% Washing Buffer (0.1 M NaH_2PO_4, 10 mM Tris, 0.5 M NaCl, 20 mM Imidazole)
7) Wash. 5 CV Washing Buffer
8) Elution. Gradient (20 CV): 100% Washing Buffer → 100% Elution Buffer (6 M GuaCl, 0.1 M NaH_2PO_4, 10 mM Tris, 0.5 M NaCl, 500 mM Imidazole)
9) Continue the Elution with 100% Elution Buffer.

PART V: SEMI-SYNTHESIS OF ABERRANTLY N-GLUCOSYLATED $hMOG_{1-117}$

As stated above, the involvement of aberrant PTM on MOG in triggering CNS autoimmunity is a crucial topic. In this context, we hypothesized that an aberrant N-glucosylation on the MOG native site of glycosylation (Asn^{31}) may be involved in the immunopathogenesis of CNS demyelinating disorders. For this purpose, it was decided to produce the $hMOG_{35-117}$ fragment using molecular biology tools, engineering the sequence to obtain the N-terminal free Cys. Specifically, a selective point mutation was introduced at the 35 residue (M35C) and the sequence was extended at the N-terminus with the TEV-protease consensus sequence. The C-terminal active ester of the peptide fragment [Asn^{31}(Glc)]hMOG(1-34) was prepared at the SOSCO Laboratory (*Universitè de Cergy Pontoise, France*).

Results & Discussion

To perform NCL, the native sequence of $hMOG_{35-117}$, reported on data bank, was modified with a selective point mutation ($M^{35}\rightarrow C^{35}$) and extended with the consensus sequence of TEV at the N-terminus. Furthermore, a 6-His tag was added at the C-terminus to enable Ni-affinity chromatography purification (Figure 31). The designed sequence was successfully cloned in a pET-22b expression vector (Figure 32. Cloning steps are displayed in Materials & Methods section), as demonstrated by PCR (Figure 33) and sequencing (data not shown). Further confirmation was obtained performing a specific digestion on the purified PCR fragment (Figure 33).

Recombinant protein expression and purification protocols were developed and selected in order to optimize both protein yield and process timing. In particular:

- Expression was carried out in BL21(DE3)-Gold chemically competent *E.coli* cells, which enable a high efficiency expression level under the control of a T7 promoter.
- It was determined that the best strategy to obtain an acceptable amount of soluble protein is the post-induction ON growth at RT with vigorous shaking. Classical 37°C ON growth after induction enables to obtain higher protein concentrations, which precipitates after purification.
- Recombinant protein is expressed in IB. The chosen strategy to obtain solubilized IB provides two sonication-high speed centrifugation steps (Figure 34). The developed methodology is not time-consuming and enable the obtainment of the protein sample directly in solution after the last centrifuge. The latter feature is particularly important because it allows to easily manipulate the sample during the purification step and avoid column clogging.

Purification was performed on large-scale cultures using an Äktabasic system. The selected affinity columns are the prepacked HisTrap FF 1ml, which enable to perform a rapid and efficient process. The developed protocol allows to purify the recombinant from the lysate through a 4-step process, which leads to the obtainment of partially refolded protein in non-denaturing conditions. The identity of the purified protein was assessed by MALDI-MS (Figure 35), performed in collaboration with Toscana Biomarkers srl (Siena), and SDS-PAGE (Figure 36). The latter analysis enabled to notice that a fraction of the protein is not retained in column during the wash step, as it is present also in the column flow-through. Therefore, the column flow was always collected, checked by SDS-PAGE to verify the presence of MOG, and eventually loaded in column for a second purification round.

MENLYFQCEVGWYRPPFSRVVHLYRNGKD
QDGDQAPEYRGRTELLKDAIGEGKVTLRI
RNVRFSDEGGFTCFFRDHSYQEEAAMELK
VEDLEHHHHHH

Figure 31: Engineered hMOG$_{35-117}$ sequence, (TEVconsensus)-(Cys^{35})hMOG$_{1-117}$(His)$_6$.
In green, the TEV consensus sequence. In red, the mutated residue (M35C).In blue, the 6-His tag.

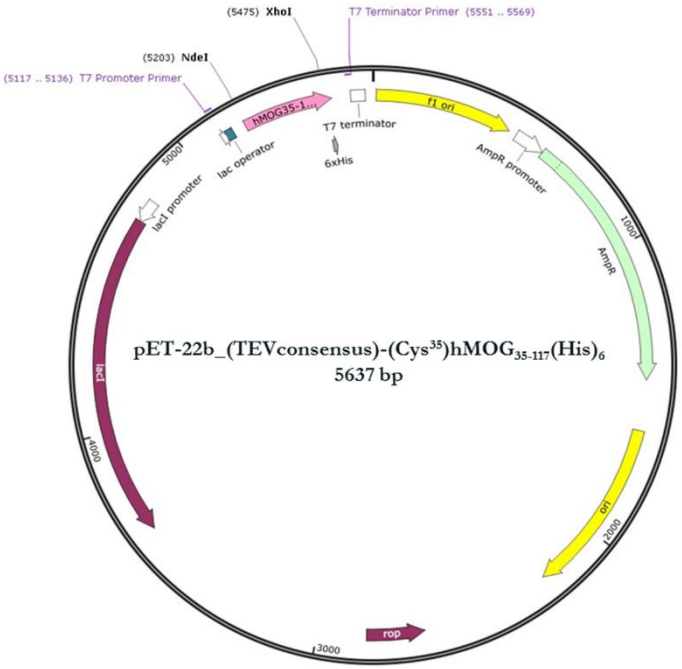

Figure 32: pET-22b_(TEVconsensus)-(Cys^{35})hMOG$_{1-117}$(His)$_6$ vector scheme.

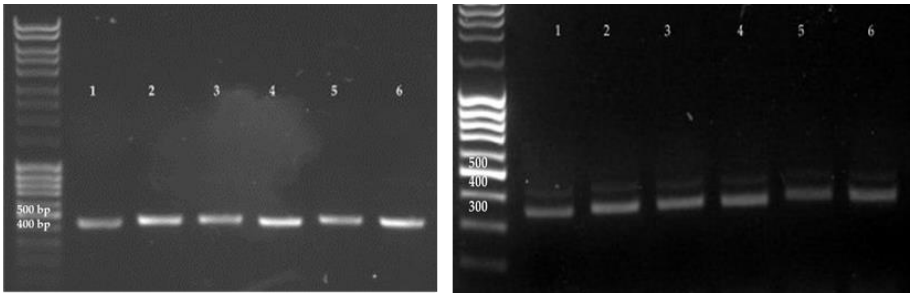

Figure 33: 1,5% agarose gels: on the left, PCR fragments obtained amplifying the plasmid with T7 promoter and terminator primers (desired fragment =453 bp); on the right PCR fragments digested with XhoI (desired fragment = 359 bp).

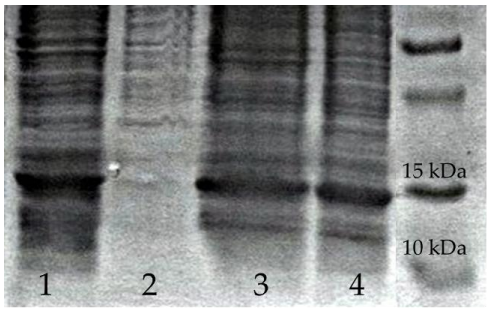

16% SDS-PAGE
1. Large scale expression pellet
2. 1st wash: supernatant after sonication and centrifugation
3. 1st pellet, resuspended in Urea 8M
4. 2nd wash: supernatant after 2nd round of sonication and centrifugation. Sample loaded in column

Figure 34: 16% SDS-PAGE of different fractions obtained during cell lysis and IB solubilization. The protein is present in solution after 2 sonication-centrifugation steps.

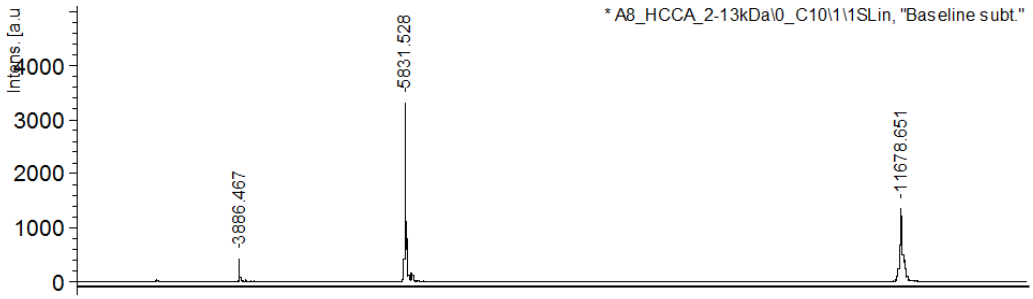

Figure 35: MALDI-MS analysis of (TEVconsensus)-(Cys^{35})hMOG$_{1\text{-}117}$(His)$_6$ protein. (MW = 11678 Da).

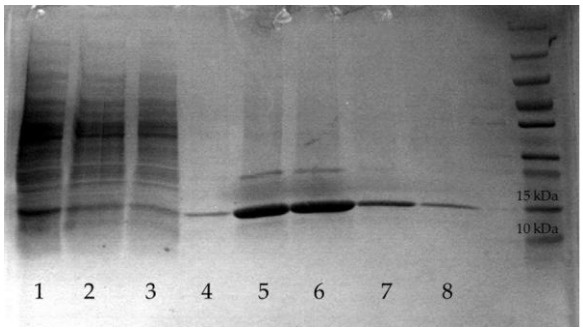

1. Sample loaded
2. 1st column flowthrough
3. 2nd column flowthrough
4. Purified fraction 1
5. Purified fraction 2
6. Purified fraction 3
7. Purified fraction 4
8. Purified fraction 5

Figure 36: 16% SDS-PAGE of (TEVconsensus)-(Cys^{35})hMOG$_{1\text{-}117}$(His)$_6$ protein. In the first lane, the solubilized IB sample loaded in column, then the column flow-throughs and the purified fractions.

To obtain the free N-terminal Cys^{35} required for NCL, several TEV-cleavage attempts were performed. In particular, the following variables were adjusted to maximize the amount of cut protein: units of enzyme (U), cleavage buffer composition, incubation time and temperature. Samples obtained after cleavage reaction were run on 16%-4% SDS or 18%-5% Tricine PAGE, in order to verify the cleavage. Since gels have not enabled the detection of two distinct bands (cut and uncut protein), it was necessary to perform MALDI-MS analyses on the samples. Another useful methodology to monitor the cleavage reaction is analytical HPLC-MS. This technique requires small sample volume, is fast and relatively inexpensive. Furthermore, it allows to follow the reaction course observing the protein molecular weight, provided by MS. Using both MALDI-MS and HPLC, we established that the best cut protein yield was obtained using 200 U of TEV/100 ug of protein, and incubating the reaction ON at 20°C in a buffer containing 2 M Urea and 14 mM βME. In spite of the numerous different reaction conditions tested, we have not obtained high yield of (Cys^{35})-$hMOG_{35-117}$. Indeed, all the samples analyzed are composed by a mixture of cut and uncut protein, and the latter was always the most abundant. To overcome this problem, we decided to purify selectively the cut protein (Cys^{35})-$hMOG_{35-117}$ using semi-preparative HPLC.

Further developments of this work include:

- ligation reaction implementation;
- purification of the semi-synthetic protein;
- use of the semi-synthetic construct as antigenic probe in SP-ELISA tests aimed to clarify the role of aberrant N-glucosylation on MOG.

The development of a methodology allowing the obtainment of N-glucosylated MOG is crucial to investigate the involvement of aberrant PTM in the ethiopathogenesis of CNS AID, and to elucidate the role of MOG as putative auto-Ag. The use of NCL enables to combine the advantages of *E.coli* expression and SPPS, but requires considerable skills in both techniques. Furthermore, the large number of steps and the significant time necessary to execute and setup the method may invalidate the feasibility of this technique. To overcome these issues, preliminary tests were performed using advanced molecular biology tools. In particular, a plasmid encoding the *H. influenza* glycosyltransferase HMW1C (kindly provided by Prof. Barbara Imperiali, Massachusetts Institute of Technology, Cambridge) was employed to perform a double chemical transformation on BL21(DE3)-Gold *E.coli* cells, together with pET-22r$MOG_{1-117}(His)_6$ plasmid. Indeed, rMOG sequence includes the consensus sequence sequon Asn-X-Thr required for *in vivo* glycosylation operated by HMW1C. Unfortunately, the attempts performed using the HMW1 N-glucosylation standard protocol have not succeeded, possibly because of the protein expression at the IB level.

Materials & Methods

Chemical Transformation of DH5α cells with pET-22b and pMAT-(TEVconsensus)-(Cys^{35})hMOG$_{1-117}$(His)$_6$

50 ul of chemically competent cells were transformed using two different plasmids, pET-22b (Novagen) and pMAT-(TEVconsensus)-(Cys^{35})hMOG$_{1-117}$(His)$_6$ (Life Technologies). Specifically, 2 different mixes were prepared:

1. DH5α cells + 10 ng of pET-22b
2. DH5α cells + 10 ng of pMAT-(TEVconsensus)-(Cys^{35})hMOG$_{1-117}$(His)$_6$

Reactions were incubated on ice for 30', then heat-shocked at 42°C for 20" and incubated again on ice for 2'. 950 ul of LB medium was added to each reaction, and then the suspensions were incubated at 37°C for 1 hour with vigorous shaking. 100 ul of each suspension were plated on LB-Agarose plates containing Ampicillin. Plates were incubated at 37°C overnight.

Precultures and Midiprep of pET-22b and pMAT-(TEVconsensus)-(Cys^{35})hMOG$_{1-117}$(His)$_6$

Colonies are visible on all the plates. 2 colonies for each plasmid were chosen for PC. Briefly, each colony was inoculated in 3 ml of LB medium containing Ampicillin and incubated at 37°C for 8h with vigorous shaking. Then 50 ml of fresh medium were inoculated with 100 ul of the starter culture and incubated ON at 37°C for 8h with vigorous shaking. Both plasmids were purified from cell cultures using NucleoBond® PC100 kit (Macherey-Nagel). According to the manufacturer's protocol, the cultures were centrifuged @4000 g for 30' @4°C. The pellets were carefully resuspended in buffer S1+RNase A, then buffer S2 was added. The suspension were mixed by inverting the tubes 6-8 times. Pre-cooled buffer S3 was added, and the lysates were immediately mixed by inverting the tubes until a homogenous suspension containing an off-white flocculate is formed. Suspensions were incubated on ice for 5'. Meanwhile, NucleoBond® columns were equilibrated with buffer N2. Lysates were clarified using the provided folded filters, then each solution was loaded into a column. After the columns have emptied by gravity, buffer N3 was added to wash the columns. Flow-throughs were discarded. Plasmids were eluted from the columns using buffer N5. Each plasmid was precipitated adding RT carefully discarded, then 70% RT ethanol was added to each pellet. Solutions were centrifuged @15000 g for 10' @RT, then ethanol was carefully removed. Pellets were allowed to dry @RT for 10', then reconstituted with water.

Double Digestion of pET-22b and pMAT-(TEVconsensus)-(Cys^{35})hMOG$_{1-117}$(His)$_6$

pET-22b (cloning vector, V) and pMAT-(TEVconsensus)-(Cys^{35})hMOG$_{1-117}$(His)$_6$ (plasmid containing insert, I) were double-digested using NdeI and XhoI (NEB), using the following protocol:

	pET-22b (V)	pMAT-(TEVconsensus)-(Cys^{35})hMOG$_{1-117}$(His)$_6$ (I)
Reagent	Volume (ul)	Volume (ul)
Buffer 4 (10X)	2.5	2.5
BSA (100X)	0.25	0.25
NdeI	0.5	0.5
XhoI	0.5	0.5
pET-22b (V)	2.5 (1 ng)	-
pMAT-(TEVconsensus)-(Cys^{35})hMOG$_{1-117}$(His)$_6$ (I)	-	1 (1 ng)
H_2O	18.75	20.25
Final volume	25	25

The amount of each enzyme and DNA was calculated according to the manufacturer's instructions. The reactions were incubated for 3 hours at 37°C. An aliquot of each reaction was loaded into an 1.5% Agarose gel containing Sybr Safe (Life Technologies), together with the not-digested form of the plasmids. The gel was run at 90 V for 1 hour.

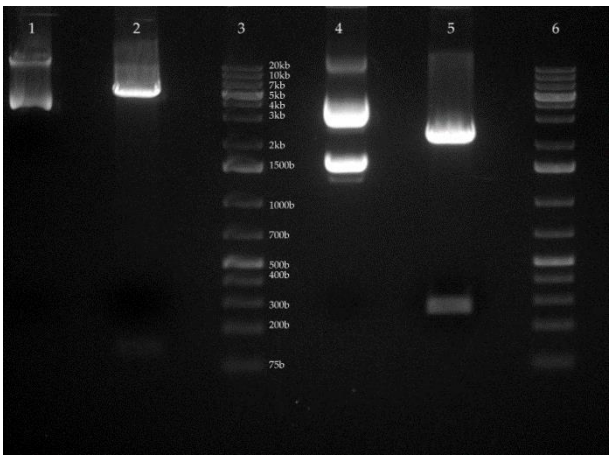

1) pET-22b (8ul TE buffer, 2ul DNA, 2ul Loading buffer 6X)
2) Double digested pET-22b (entire reaction + 2,5ul Loading buffer 10X)
3) GeneRuler 1kb Plus DNA Ladder (3 ul)
4) pMAT-(TEVconsensus)-(Cys^{35})hMOG$_{1-117}$(His)$_6$ (8ul TE buffer, 2ul DNA, 2ul Loading buffer 6X)
5) Double digested pMAT-(TEVconsensus)-(Cys^{35})hMOG$_{1-117}$(His)$_6$ (entire reaction + 2,5ul Loading buffer 10X)
6) GeneRuler 1kb Plus DNA Ladder (3 ul)

DNA fragments of interest are: pET-22b, 5364 bp and pMAT-(TEVconsensus)-(Cys^{35})hMOG$_{1-117}$(His)$_6$, 273 bp. Corresponding bands were cut from the gel and the DNA fragments were purified from agarose gel using the NucleoSpin® Gel and PCR Clean-up kit (Macherey Nagel). Obtained DNA fragments were loaded into 1.5% Agarose gel containing Sybr Safe, and then quantized

comparing the intensity of bands with GeneRuler 1kb Plus DNA Ladder. The amount of purified pET-22b is 20 ng/ul, and that of pMAT-(TEVconsensus)-(Cys^{35})hMOG$_{1\text{-}117}$(His)$_6$ is 5 ng/ul.

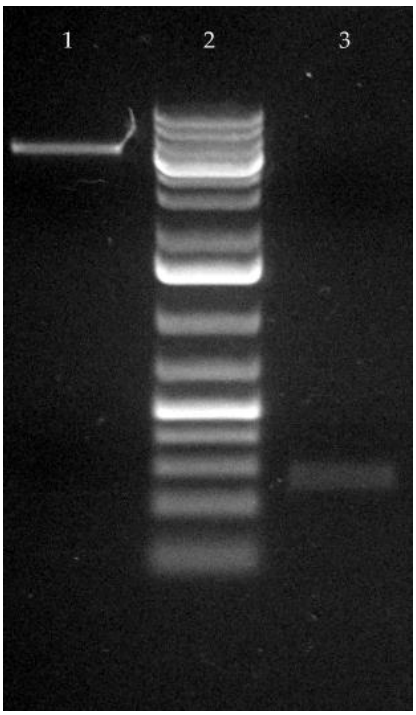

1) Double digested pET-22b, purified from Agarose gel (8ul TE buffer, 2 ul DNA, 2 ul Loading buffer 6X)

2) GeneRuler 1kb Plus DNA Ladder (6ul)

3) Double digested pMAT-(TEVconsensus)-(Cys^{35})hMOG$_{1\text{-}117}$(His)$_6$, purified from Agarose gel (4ul TE buffer, 4 ul DNA, 2 ul Loading buffer 6X)

Ligation of the digested fragments

The amount of vector and insert for the ligation reaction were chosen using the following formula:

$$x_{ng\ insert} = \frac{y_{ng\ vector} \times bp_{insert}}{bp_{vector}} \times (ratio\ insert{:}\ vector)$$

	Reaction I Vector: 40 ng (1:1)	Reaction II Vector: 80 ng (1:1)	Reaction III Vector: 40 ng (5:1)
Reagent	Volume (ul)	Volume (ul)	Volume (ul)
Vector	2	4	2
Insert	4	8	10
Ligase Buffer (Fermentas)	2	2	2
T4 Ligase (Fermentas)	2	2	2
H_2O	10	4	4
Final volume	20	20	20

Reactions were incubated at 16°C overnight.

Chemical Transformation of DH5α and XL-10 cells with ligation products

200 ul of chemically competent cells were transformed using the ligation reactions. Specifically, 5 different mixes were prepared, in order to find the best conditions:

1. DH5α cells + 10 ul of Reaction I
2. XL-10 cells + 10 ul of Reaction I
3. DH5α cells + 5 ul of Reaction II
4. XL-10 cells + 5 ul of Reaction II
5. XL-10 cells + Reaction III.

Reactions were incubated on ice for 1 hour, then heat-shocked at 42°C for 2' and incubated again on ice for at least 5'. 1 ml of LB medium was added to each reaction, and then the suspensions were incubated at 37°C for 2 hours with vigorous shaking. 100 ul of each suspension were plated on LB-Agarose plates containing Ampicillin and Nalidixic Acid. After that, reactions were centrifuged at 5000 rpm for 5'. 100 ul of each supernatant were used to resuspend the pellet, then plated on LB-Agarose plates containing Ampicillin and Nalidixic Acid. Plates were incubated at 37°C overnight.

Colony picking and Colony PCR

Colonies are visible on all the plates. 30 colonies from different plates were chosen to perform colony PCR. Briefly, each colony was picked with a sterile tip and streaked on a fresh LB-Agarose plates containing Ampicillin and Nalidixic Acid (transfer plate). Then the same tip was used to resuspend the colony in 50 ul of sterile H_2O. The suspensions were incubated at 100°C for 15', then at -20°C for 15' (heat shock). Suspensions were centrifuged at 15000 g for 3'. 2 ul of each supernatant were carefully collected and used as template for PCR. The PCR reactions were prepared as follows:

Reagent	Volume (ul)	Final Concentration
10X DreamTaq Green Buffer (Fermentas)	2.5	1X
dNTPs (Sigma Aldrich)	0.5	0.2 uM
T7 terminator primer (Jena Biosciences)	2.5	1 uM
T7 promoter primer (Jena Biosciences)	2.5	1 uM
DreamTaq DNA Polymerase (Fermentas)	0.2	
DNA template	2	
H_2O	14.8	
Final volume	25	

In addition to DNA template from the colonies, negative controls were added (pET-22b and H_2O). Thermocycler was set as follows:

1. 95°C for 3'
2. 95°C for 30"
3. 55°C for 30"
4. 72°C for 30"

   } 35 cycles
5. 72°C for 5'
6. 12°C ∞

Samples were loaded on 1% Agarose gel. The expected band is 453 bp (pET-22b negative control: 309 bp).

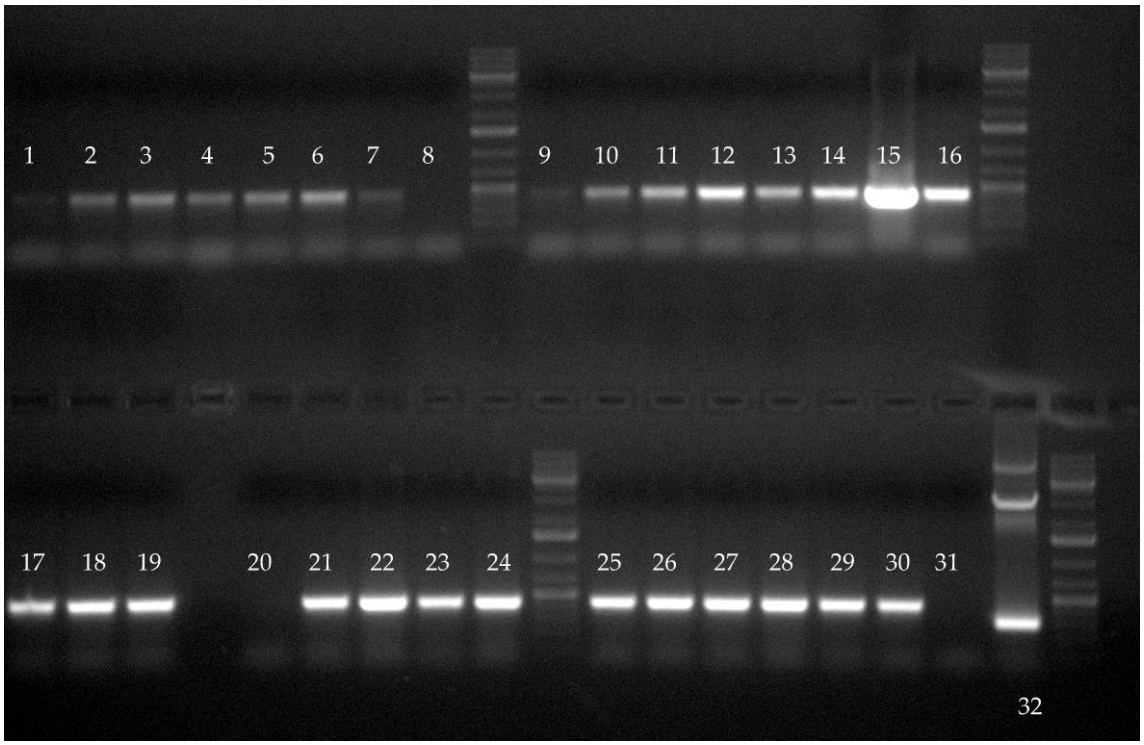

PCR reactions:

1-30 – template = colony; 31 – no template; 32 – template = pET-22b

Miniprep of the ligation product

Three clones (#15, 16 and 22) were chosen for Midiprep. Corresponding colonies from transfer plate were inoculated in 10 ml of LB-medium containing Ampicillin and Nalidixic Acid, then incubated at 37°C overnight with vigorous shaking. Each PC was divided in 2 aliquots of 5 ml and processed according Miniprep protocol (Qiagen). Plasmids were eluted with 50 ul of EB buffer.

Ligation validation: Double digestion and PCR of the prepped plasmids

Prepped plasmids were double-digested using NdeI and XhoI (NEB), using the following protocol:

Reagent	Volume (ul)
Buffer 4 (10X)	2.5
BSA (100X)	0.25
NdeI	0.5
XhoI	0.5
Plasmid	1 ng
H_2O	18.75
Final volume	25

The amount of each enzyme and DNA was calculated according to the manufacturer's instructions. Reactions were incubated for 3 hours at 37°C. An aliquot of each reaction was loaded into an 1.5% Agarose gel containing Sybr Safe, together with the not-digested form of the plasmids. The gel was run at 90 V for 1 hour. Plasmids were also tested by PCR using T7 terminator and T7 promoter primers. PCR mixes were prepared as follows:

Reagent	Volume (ul)	Final Concentration
10X DreamTaq Green Buffer	2.5	1X
dNTPs	1	0.2 uM
T7 terminator primer	1.25	0.5 uM
T7 promoter primer	1.25	0.5 uM
DreamTaq DNA Polymerase	0.2	
Plasmid	0.5	
H_2O	18.3	
Final volume	25	

pET-22b was processed as negative control. Thermocycler was set as follows:

1. 95°C for 3'
2. 95°C for 30" ⎫
3. 55°C for 30" ⎬ 35 cycles
4. 72°C for 30" ⎭
5. 72°C for 5'
6. 12°C ∞

Samples were loaded on 1% Agarose gel. The expected band is 453 bp (negative control: 309 bp).

Ligation validation: Sequencing of the amplicons

Bands corresponding to the insert were cut from Agarose gel and purified from agarose gel using the NucleoSpin® Gel and PCR Clean-up kit. Obtained DNA fragments were loaded into 1.5% Agarose gel containing Sybr Safe, and then quantized comparing the intensity of bands with GeneRuler 1kb Plus DNA Ladder. Samples were digested with XhoI to confirm the identity of the sequences, using the following reaction:

Reagent	Volume (ul)
Buffer 4 (10X)	2.5
BSA (100X)	0.25
XhoI	0.5
DNA fragment	5
H_2O	16.75
Final volume	25

After 1 hour of incubation at 37°C, samples were loaded on 2% Agarose gel. Full-lenght band is 453 bp, while the digested fragments are 359 bp and 94 bp. Three of six samples were sent to Eurofins MWG Operon to be sequenced using the commercial primers T7 promoter and T7 terminator. Exact match between of the obtained sequence and the desired one was confirmed using BLAST (Basic Local Alignment Search Tool).

Chemical transformation of BL21Gold(DE3) cells with pET-22b-(TEVconsensus)-(Cys^{35})hMOG$_{1\text{-}117}$(His)$_6$

200 ul of chemically competent cells were transformed using the ligation product #15A, that is pET-22b-(TEVconsensus)-(Cys^{35})hMOG$_{1\text{-}117}$(His)$_6$. Specifically, 3 different mixes were prepared, in order to find the best conditions:

1. BL21Gold(DE3) + 2.5 ul of plasmid
2. BL21Gold(DE3) + 1.5 ul of plasmid
3. BL21Gold(DE3) + 1 ul of plasmid

Reactions were incubated on ice for 1 hour, then heat-shocked at 42°C for 2' and incubated again on ice for at least 5'. 1 ml of LB medium was added to each reaction, and then the suspensions were incubated at 37°C for 2 hours with vigorous shaking. 100 ul of each suspension were plated on LB-Agarose plates containing Ampicillin. After that, reactions were centrifuged at 5000 rpm for 5'. 100 ul of each supernatant were used to resuspend the pellet, then plated on LB-Agarose plates containing Ampicillin. Plates were incubated at 37°C overnight.

Colony picking and Colony PCR

Colonies are visible on all the plates. 13 colonies from different plates were chosen to perform colony PCR. Briefly, each colony was picked with a sterile tip and streaked on a fresh LB-Agarose plates containing Ampicillin and Nalidixic Acid (transfer plate). Then the same tip was used to resuspend the colony in 50 ul of sterile H_2O. The suspensions were incubated at 100°C for 15', then at -20°C for 15' (heat shock). Suspensions were centrifuged at 15000 g for 3'. 2 ul of each supernatant were carefully collected and used as template for PCR. PCR reactions were prepared as previously described. Samples were loaded on 1% Agarose gel. Expected band is 453 bp.

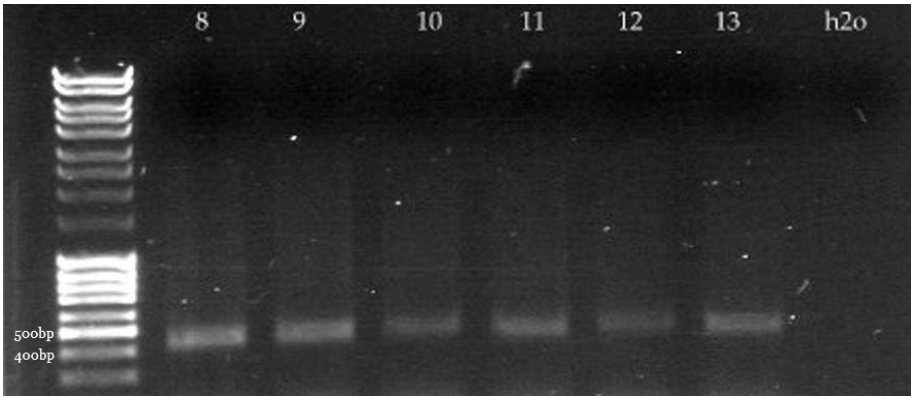

Precultures and Expression Test

6 of the 13 selected colonies were chosen to prepare PC. 5 ml of LB medium containing Ampicillin were inoculated with one single colony and incubated ON at 37°C with vigorous shaking. Then 6 ml of LB medium containing Ampicillin were inoculated with 6 ul of PC, and incubated at 37°C with vigorous shaking until an OD_{600nm} between 0.4 and 0.8 (log-phase) was reached. Afterwards, 1 ml of each suspension was collected as not-induced sample (NI) and the remaining culture was induced with 5 ul of IPTG (final concentration: 1mM) and incubated ON at 37°C with vigorous shaking. 1 ml of each induced culture was collected (I). NI and I samples were centrifuged at 17000 rpm for 30' at 4°C, then the pellet was resuspended in 50ul of Laemmli Buffer, heated at 100°C for 10' and loaded on 16% SDS-PAGE. The expected mass of (TEVconsensus)-(Cys^{35})$hMOG_{1-117}(His)_6$ is 11,678 kDa.

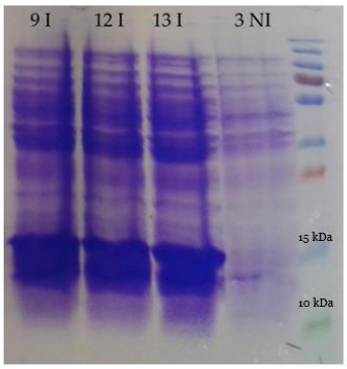

9I, 12I, 13I: IPTG-Induced samples from different precultures (ON growth after induction)

3NI: not-induced sample (collected before induction)

Evaluation of the best large-scale expression strategy

400 ml of LB medium containing Ampicillin were inoculated with 400 ul of each PC in duplicate (e.g. 1A and 1B are cultures prepared using the same PC), and incubated at 37°C with vigorous shaking until an OD_{600nm} between 0.4 and 0.8 (log-phase) was reached. Afterwards, 1 ml of each suspension was collected as not-induced sample (NI) and the remaining culture was induced with 400 ul of IPTG (final concentration: 1mM). To evaluate which is the best growth temperature for the protein over-expression, one of the culture prepared in duplicate (e.g. A serie) was incubated ON at 37°C with vigorous shaking, while the other one (e.g. B) was incubated ON at RT with vigorous shaking. 1 ml of each induced culture was collected (I). NI and I samples were centrifuged at 17000 rpm for 30' at 4°C, then the pellet was resuspended in 50ul of 5X Laemmli Buffer, heated at 100°C for 10' and loaded on 16% SDS-PAGE. The same test was performed to evaluate the best IPTG concentration (1mM or 0.5mM).

Cell Lysis and IB Disruption

Overnight cultures were centrifuged at 4000 rpm for 30' at 4°C and each pellet was resuspended in 10 ml of 20mM Tris pH 8 containing protease inhibitor (500ul of a solution obtaining dissolving a tablet of Complete, EDTA-free protease inhibitor in 2 ml of milliQ H_2O), then stored at -20°C if not immediately used for the following steps. Suspensions were sonicated (3x1', 40% amplitude, repeated twice) and centrifuged at 25000 rpm for 65' at 4°C. Supernatants (called "1st supernatant") were collected to evaluate the possible presence of the protein, and the pellets were resuspended in the same amount of Urea 8M. Sample were sonicated and centrifuged again. Supernatants (called "Urea wash") were collected to evaluate the possible presence of the protein, and the pellets were resuspended in the same amount of Urea 8M. Samples obtained were called "Solubilised IB". 20 ul of each sample were added with 5ul of 5X Laemmli Buffer, heated at 100°C for 10' and loaded on 16% SDS-PAGE.

Recombinant protein purification

Purification step was carried out using an immobilized metal ion affinity chromatography (IMAC) strategy. "Urea wash" was chosen as sample for the purification. ÄktaBasic chromatography system was used with an HisTrap FF 1 ml column (affinity column prepacked with precharged Ni Sepharose™ 6 Fast Flow, GE Healthcare). The purification protocol includes of the following steps:

1. Column equilibration: wash the column with Binding Buffer until the ABS reaches a steady baseline (generally, at least 5 CV)
2. Sample injection: using Superloop
3. Column wash: wash the column with Binding Buffer until the ABS reaches a steady baseline (generally, at least 10 CV)
4. Elution: wash the column with Elution Buffer.

Binding Buffer pH 8	
Urea	8M
NaH_2PO_4	100 mM
Tris	10 mM
NaCl	250 mM
Imidazole	20 mM

Elution Buffer pH 8	
NaH_2PO_4	100 mM
Tris	10 mM
NaCl	250 mM
Imidazole	500 mM

The presence of proteins in the different fractions (column flow, eluted fractions) was verified through 16% SDS-PAGE.

Mass Spectrometry analyses of the purified fractions

MALDI-MS analyses of the purified fractions were performed using two different matrixes: HCCA (MW range: 2-13 kDa) and sinapinic acid (5-20 kDa). Analyses were performed at Toscana Biomarkers srl, Siena.

$hMOG_{35-117}(His)_6$ cleavage trials with TEV

In order to obtain the N-terminal free Cys on the recombinant protein, different buffer and incubation conditions with TEV enzyme were tested:

1. Dilution of the protein to 1mg/ml with TEV Buffer 1. Cleavage reaction in TEV Buffer 1:
    a) @ RT for 3 h (100 ul of protein + 2 ul of TEV).
    b) @ 30°C for 3 h (100 ul of protein + 2 ul of TEV).
    c) @ 30°C for 24 h (100 ul of protein + 5 ul of TEV).
    d) @ 30°C for 24 h (100 ul of protein + 10 ul of TEV).
    e) @ 30°C for 48 h (100 ul of protein + 10 ul of TEV).

    Protein precipitation occurred in all the samples.

2. Dilution of the protein to 1mg/ml with TEV Buffer 2. Cleavage reaction in TEV Buffer 2 @ 30°C for 48 h (100 ul of protein + 10 ul of TEV), sample 4. Protein precipitation occurred.
3. Dilution of the protein to 1 mg/ml with TEV Buffer 3. Cleavage reaction @30°C ON (100ul of protein + 5 ul TEV), sample 5. Protein precipitation occurred.
4. Dilution of the protein to 1 mg/ml with TEV Buffer 4. Cleavage reaction:
    a) @30°C ON (120ul of protein + 12 ul TEV).
    b) @20°C ON (50ul of protein + 7 ul TEV).
    c) Dilution of the protein to 1mg/ml with TEV Buffer 1. Cleavage reaction in TEV Buffer 1 @ 20°C ON (100 ul of protein + 10 ul of TEV).
5. Dilution of the protein to 1 mg/ml with TEV Buffer 5. Cleavage reaction:
    a) @20°C ON (400 ul of protein + 40 ul TEV).
    b) @20°C ON (400 ul of protein + 40 ul TEV). Dialysis in buffer 1 @20°C for 24h.
    c) @20°C for 24h (400 ul of protein + 40 ul TEV). Dialysis in buffer 1 @20°C for 24h.
    d) @20°C for 48h (400 ul of protein + 40 ul TEV). Dialysis in buffer 1 @20°C for 24h.

(TEVconsensus)-(Cys^{35})$hMOG_{1-117}(His)_6$ cleavage trials with TEV: MALDI-MS analyses

Samples obtained after TEV cleavage reactions (both solutions and suspensions) were analyzed by MALDI-MS. All the analyses were performed at Toscana Biomarkers srl, Siena. Calculated masses of the two MOG form are the following:

- (TEVconsensus)-(Cys^{35})$hMOG_{1-117}(His)_6$: 11,678 kDa
- (Cys^{35})$hMOG_{1-117}(His)_6$: 10,752 kDa

(TEVconsensus)-(Cys^{35})hMOG$_{1-117}$(His)$_6$ cleavage trials with TEV: HPLC analyses

HPLC analyses on (TEVconsensus)-(Cys^{35})hMOG$_{1-117}$(His)$_6$

Analytical analyses were performed on a HPLC instrument coupled to ESI-MS using a C18 column. The viability of the test was verified using different methods on (TEVconsensus)-(Cys^{35})hMOG$_{1-117}$(His)$_6$ protein sample, modifying the elution gradient in order to find the conditions allowing to obtain a single and well-separated peak containing the recombinant protein. The solvents used were: H_2O with 0.1% TFA, ACN with 0.1% TFA. The selected method was from 30% ACN to 50% ACN in 5' at a flow rate of 0.6 mL min^{-1}.

HPLC analyses on cleavage reaction samples

Different incubation times were evaluated using the selected method on analytical HPLC. The protein was diluted to 1 mg/ml with buffer 5, then TEV was added (400 ul of protein + 40 ul TEV). The following cleavage reactions were performed:

@20°C, ON.

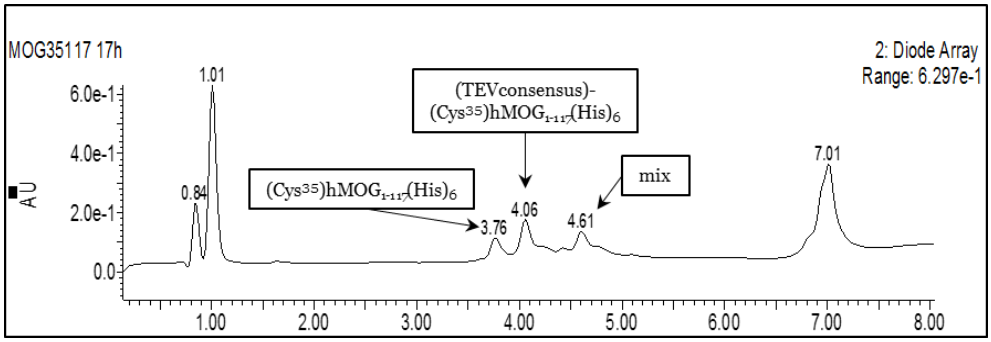

@20°C, 24h.

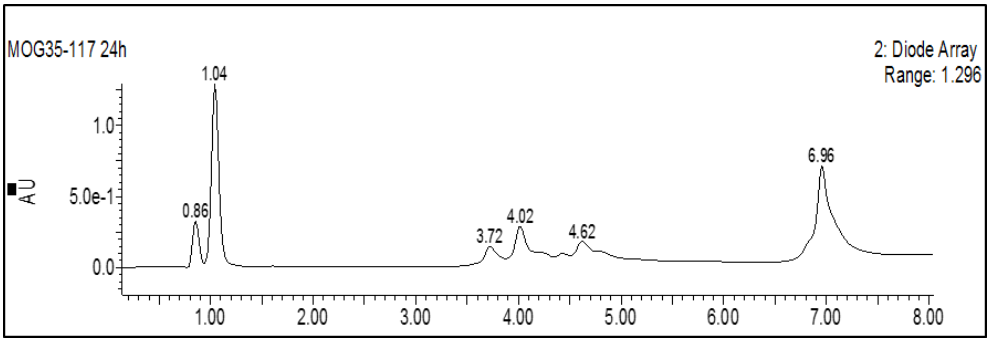

@20°C, 41h.

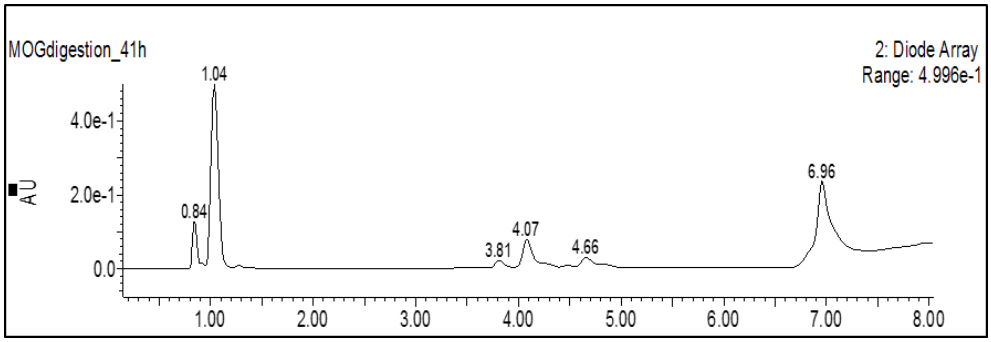

$hMOG_{35-117}(His)_6$ cleavage trials with TEV: Buffers composition

TEV Buffer 1, pH 7.5

Tris	25 mM
NaCl	250 mM
βME	14 mM

TEV Buffer 2, pH 7.5

Tris	25 mM
NaCl	250 mM
βME	28 mM

TEV Buffer 3, pH 7.5

Tris	25 mM
NaCl	250 mM
TCEP	1 mM

TEV buffer 4, pH 7.5

NaH_2PO_4	100 mM
Tris	10 mM
NaCl	250 mM
TCEP	1 mM

TEV Buffer 5, pH 7.5

Tris	25 mM
NaCl	250 mM
β-mercaptoethanol	14 mM
Urea	2 M

GENERIC METHODS

Molecular Biology Generic Methods

Sodium Dodecyl Sulphate PolyAcrilamide Gel Electrophoresis (SDS-PAGE)

Stacking gel and separating gel (in different percentages, according to the size of the proteins to be separated) were prepared as follows. Stacking gel was poured on top of the separating gel after solidification (30' at RT). Gel comb was inserted into the stacking gel, in order to allow the formation of the wells. Protein samples were diluted with 5X Laemmli Buffer and boiled at 100°C for 10'. 15 ul of each sample were loaded into a well. When all the samples were loaded, the apparatus was filled with Tris-SDS Running Buffer (250 mM Tris, 1.92 M Glycine, 1% SDS, pH 8.3), then a voltage of 150 V was applied for 1h. After the run, the gel was incubated with Staining Solution (0.1% Coomassie R250, 10% acetic acid, 40% methanol) or 1h at RT. Nonspecific bands were removed washing and the gel twice with Destaining Solution (10% acetic acid, 40% methanol) (1h incubation each).

Separating Gel, 18% - 8 ml	
Reagent	*Volume*
dd H_2O	1 ml
30% Acrylamide	4,8 ml
1.5M Tris pH 8.8	2 ml
10% SDS	80 ul
10% APS	80 ul
Temed	8 ul

Separating Gel, 16% - 8 ml	
Reagent	*Volume*
ddH_2O	1,6 ml
30% Acrylamide	4,27 ml
1.5M Tris pH 8.8	2 ml
10% SDS	80 ul
10% APS	80 ul
Temed	8 ul

Stacking Gel, 4% - 3 ml	
Reagent	*Volume*
ddH_2O	1,8 ml
30% Acrylamide	400 ul
0.5M Tris pH 6.8	750 ul
10% SDS	30 ul
10% APS	30 ul
Temed	3 ul

Tricine-PAGE

Stacking gel and separating gel were prepared as follows:

Separating Gel, 18% - 8 ml	
Reagent	*Volume*
ddH_2O	880 ul
30% Acrylamide	2,7 ml
3 M Tris pH 8,45	2 ml
Ethylene glycole	2,4 ml
10% APS	32 ul
Temed	12 ul

Stacking Gel, 5% - 4 ml	
Reagent	*Volume*
ddH_2O	2,62 ml
30% Acrylamide	375 ul
3 M Tris pH 8,45	1 ml
10% APS	16 ul
Temed	16 ul

Protein samples were diluted with 5X Laemmli Buffer (60 mM Tris-Cl pH 6.8, 2% SDS, 10% glycerol, 5% β-mercaptoethanol, 0.01% bromophenol blue) and boiled at 100°C for 10'. 15 ul of each sample were loaded into a well. When all the samples were loaded, the apparatus was filled with Tris-SDS Running Buffer, then a voltage of 200 V was applied for 1h. After the run, the gel was stained as reported for SDS-PAGE.

Agarose gel

According to the size of the DNA fragment to be separated, different Agarose percentages were selected to prepare the gel.

Recommended % Agarose	Optimum Resolution for Linear DNA
0.5	1,000–30,000bp
0.7	800–12,000bp
1.0	500–10,000bp
1.2	400–7,000bp
1.5	200–3,000bp
2.0	50–2,000bp

E.g., to prepare 30 ml of 1% agarose gel, 3 g of agarose powder were dissolved in 30 ml Tris-Acetate-EDTA Buffer, TAE (40 mM Tris, 20 mM acetic acid and 1 mM EDTA) under heating. The solution was cooled, then 3 ul of Sybr Safe were added and the mixture was poured into the instrument. Gel comb was inserted, and the gel was allowed to polymerize at RT for 1 h, then the apparatus was filled with TAE Buffer. Each DNA samples was diluted with 6X Loading Buffer and loaded into a well, then a voltage of 180V was applied for 1h. The presence of bands was revealed using an UV transilluminator.

CHAPTER 3: ROLE OF PTM IN PRIMARY BILIARY CIRRHOSIS

PRIMARY BILIARY CIRRHOSIS

Primary Biliary Cirrhosis (PBC) is an immune-mediated chronic inflammatory liver disease with slow progression. PBC is characterized by destruction of small interlobular bile ducts, gradual cholestasis and portal inflammation. Loss of bile ducts causes both decrease of bile secretion and retention of toxicants within the liver, resulting in fibrosis, cirrhosis and, ultimately, need for a liver transplantation[133]. Enhanced awareness in the diagnostic field, together with an increased knowledge of PBC pathogenesis, lead to most frequent and early diagnoses. Indeed, more than half of the diagnosed pts is asymptomatic[134]. The diagnosis can be established when two of the following criteria are met: biochemical evidence of cholestasis based on alkaline phosphatase elevation; presence of serum anti-mitochondrial Ab (AMA) of the IgG class by indirect immunofluorescence (IIF); histological evidence of non-suppurative destructive cholangitis and destruction of interlobular bile ducts on bioptic tissue[135].

PBC etiology can be defined multifactorial, as it was widely hypothesized that the disease is triggered by environmental exposure in the context of a genetic background permissible for autoimmunity development[136]. Indeed, variation in geographical prevalence, presence of disease clustering, and seasonal differences in disease diagnosis provide evidence for a crucial environmental role in PBC development. Evidence for the strong impact of genetic factors is provided by the overlap with other AID[137], the high monozygotic twin concordance (about 60%)[6,138], and the increased sibling risk of AMA positivity[139] and PBC development[140]. Furthermore, GWAS identified independent association with genes of known immunological function[141–143]. To note, many of the PBC-associated loci overlap with signals obtained for other AID, suggesting that these genetic differences may be linked to autoimmunity. Although genetic factors play an important role in the development of complex autoimmune disease, it is becoming apparent that environmental exposures are equally important. Indeed, progression and disease severity are variable among affected monozygotic twins, and the concordance between dizygotic twins is nearly 0%[136]. It is reasonable to hypothesize that environmental factors may ultimately induce tolerance breakdown through a variety of mechanisms in genetically susceptible individuals. Effectively, xenobiotics contribution to PBC pathogenesis may be due to potential direct cellular effect (leading to apoptosis or oncosis), and/or chemical modification of native proteins, causing neo-Ag formation, while viruses or bacteria may evoke a molecular mimicry mechanism. For example, several peptides and proteins from bacteria commonly associated with PBC (including *E. coli*, *Novosphingobium aromaticivorans*, and *Lactobacillus delbrueckii*) were shown to strongly cross-react with AMA and activate T-cell clones from PBC patients[144–146], disclosing how PBC could be due to exposure to bacterial Ag.

PBC immunopathogenesis: the key role of anti-mitochondrial Ab

Even if factors leading to PBC remain poorly understood, the disease is considered a model AID[147,148]. Indeed, the high specificity of the bile ducts damage is a unique and critical feature of PBC, and suggests the occurrence of an intense autoimmune response directed against biliary epithelial cells. This hypothesis is supported by the presence of MHC class II Ag on the biliary epithelium and lymphoid infiltration in the portal tract[148]. Furthermore, PBC has a serological hallmark signature, represented by AMA, highly disease-specific auto-Ab found in 90-95% of pts and less than 1% of healthy controls[149].

Numerous studies aimed to understand the molecular immunopathogenic mechanisms underlying the disease were performed since the 50s, when a PBC serum was found to react with tissue extracts by complement fixation[150]. In 1965 the reactant was located to mitochondria by IIF and called M2[151]. The first attempts of M2 molecular characterization were achieved 20 years later by Gershwin *et al.*, which identified the reactant with a family of proteins of 48-74 kDa by both immunoblotting and molecular cloning[149], and Yeaman *et al.*, which showed that M2 is the E2 component of the mammalian pyruvate dehydrogenase complex[152]. Subsequently, both Van de Water *et al.* and Coppel *et al.* confirmed that M2 is represented by multiple subunits of the 2-oxo-acid dehydrogenase complex[153,154], which is located in the inner mitochondrial membrane and is responsible of the oxidative decarboxylation of keto-acid substrates[155]. In particular, the targets of AMA are represented by:

- dihydrolipoamide acetyltransferase (E2 component of the pyruvate dehydrogenase complex, PDC-E2), which is the most frequently detected;
- dehydrogenase dihydrolipoyl transacylase (E2 subunit of the branched-chain 2-oxo-acid dehydrogenase, BCKD-E2);
- dihydrolipoamide succinyltransferase (E2 component of the oxo-glutarate dehydrogenase complex, OGDC-E2);
- dihydrolipoamide dehydrogenase binding protein or E3-binding protein (E3-BP)[147].

It is important to note that AMA auto-Ag share a substantial homology, having a common highly-conserved N-terminal domain containing a lipoylated Lys residue (Figure 37)[148].

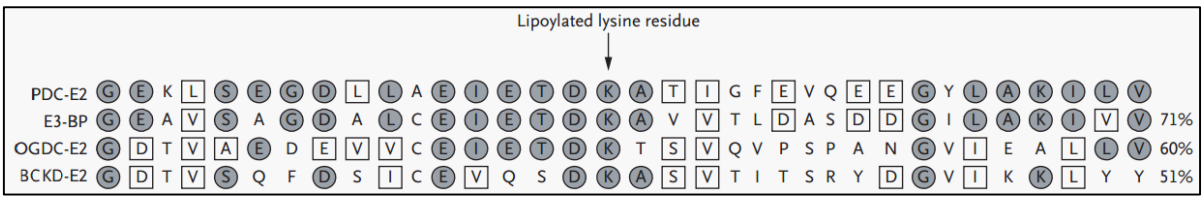

Figure 37: Lipoyl domain homology of mitochondrial auto-Ag

The specifically localized damage at the intrahepatic bile ducts and the ubiquitous auto-Ag expression lead to the PBC paradox[149]. In order to explain this phenomenon, it was hypothesized that the peculiar biliary epithelial cells metabolic processing of AMA Ag during apoptosis may attract the immune response on bile-duct cells (Figure 38). In particular, three observations on the PDC-E2 Ag demonstrate the importance of these differences in understanding PBC immunopathogenesis:

1. PDC-E2 can be recognized by auto-Ab depending on the attachment of glutathione to the lipoylated Lys during apoptosis[156];
2. differently from other cell types, epithelial cells do not attach glutathione to PDC-E2 lipoyl-Lys group during apoptosis[157];
3. specific modifications of the inner lipoyl domain of the PDC-E2 have shown to be immunoreactive when tested with pts serum, suggesting the importance of lipoyl-Lys moiety status[158].

Studies on cultured human intrahepatic biliary epithelium cells (HIBEC) confirmed that the autoimmune injury in PBC is a consequence of the unique characteristics of HIBEC during apoptosis[159], and subsequently it was demonstrated that biliary apotopes and AMA are able to activate innate immune responses in mature monocyte-derived macrophages cultures[160]. These findings provide further evidences to the hypothesis of a specific apoptotic mechanism responsible for the strictly localized PBC autoimmune response.

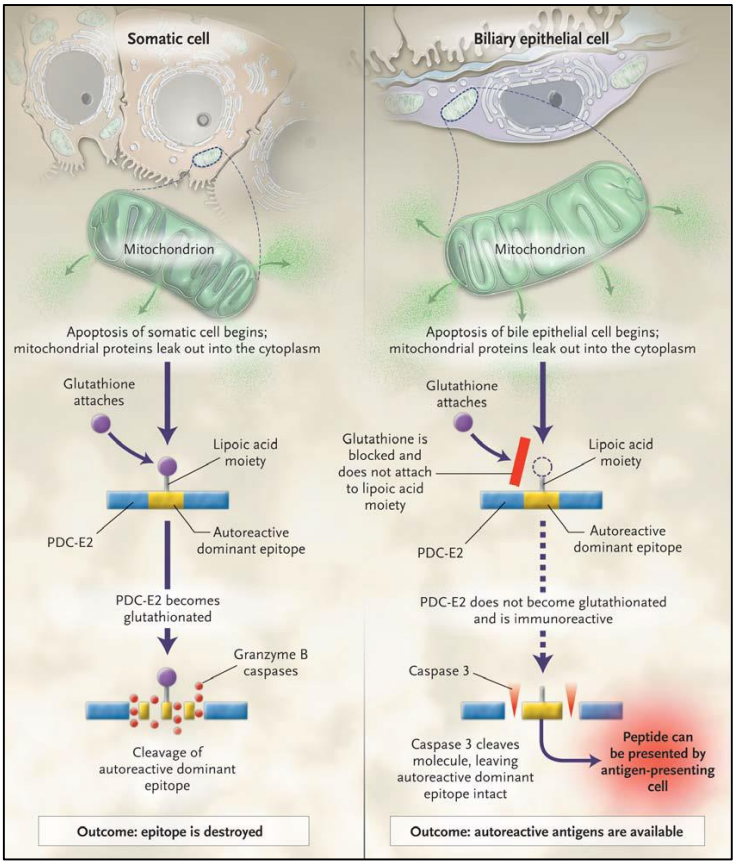

Figure 38: Properties of Apoptosis in Somatic Cells and Biliary Epithelial Cells[148].

Although it is widely demonstrated that PDC-E2 is main target of AMA, the definition of its immunodominant epitope is still controversial (as shown in Table 5). PDC-E2 was originally mapped digesting the corresponding cDNA clone with restriction endonucleases and subcloning the obtained fragments into frame-shifted expression vectors. The clone encoding for the main immunogenic region was identified by immunoblot assays with PBC pts sera. Subsequently, to precisely define the epitope, peptides encompassing distinct hydrophilic peaks within this region were synthesized and tested by ELISA, leading to the identification of the immunodominant epitope the highly conserved Aa surrounding the lipoyl-Lys residue in position 173 (K^{173}), and in particular to the 20 Aa linear peptide AEIETDKATIGFEVQEEGYL corresponding to Aa 167-186 within hPDC-E2[153]. The putative relevance of lipoic cofactor was further disclosed in another study, which reported the presence of a minor epitope associated with the outer lipoyl domain (Aa 1-80)[161] (Figure 39). Lipoyl domains are fundamental for PCD-E2 function in pyruvic acid metabolism, acting as acceptor of acetyl groups formed by the oxidative decarboxylation of pyruvate and transferring them to coenzyme A (Figure 40). Even though the previously mentioned studies represent the basis for the hypothesis of an involvement of lipoic acid in the AMA Ab recognition, it is important to stress that they have not taken into account the lipoylation status of the employed Ag.

Figure 39: Aa sequence of PDC-E2 [162].

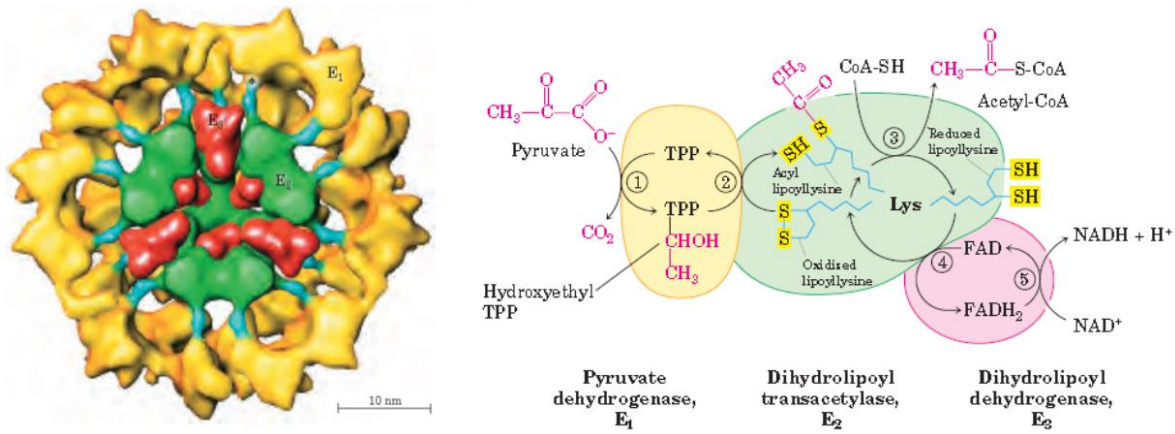

Figure 40: On the left, 3D image of PDC complex, showing the subunit structure: E1, pyruvate dehydrogenase; E2, dihydrolipoyl transacetylase; and E3,dihydrolipoyl dehydrogenase. The core (green) consists of 60 molecules of E2, arranged in 20 trimers to form a pentagonal dodecahedron. The lipoyl domain of E2 (blue) reaches outward to touch the active sites of E1 molecules (yellow) arranged on the E2 core. A number of E3 subunits (red) are also bound to the core, where the swinging arm on E2 can reach their active sites. An asterisk marks the site where a lipoyl group is attached to the lipoyl domain of E2. On the right, the oxidative decarboxylation of pyruvate to acetyl-CoA by the PDC complex.

The identification of the main immunogenic region with hPDC-E2(167-186) was questioned by Braun *et al.*[162]. In this work, 33 synthetic overlapping peptides covering the entire length of PDC-E2 were tested by SP-ELISA. The authors showed that the reactivity of PBC sera with peptides containing the immunodominant epitope in both inner and outer lipoyl domain was rather low, although significantly higher than that of NBD. In contrast, up to 74% of the PBC sera reacted with the two peptides within the catalytic domain (Aa 407-431 and 475-499) and the peptide 101-125 in the first hinge region. Sera from AMA- PBC pts hardly reacted with any of the peptides. In addition, they evaluated the function of lipoic acid synthesizing the immunodominant peptide 167-184 in both unlipoylated and lipoylated form. In order to find out whether Ab may recognize a conformational epitope, either peptide was also coupled with ovalbumin (OVA). For this purpose, it was necessary to add a Cys at the C-terminal end, which had to be substituted by a Lys for coupling the LA-conjugated. Compared with the unconjugated analogues, the OVA conjugates exhibited stronger reactivity. However, most sera showed high reactivity also with OVA alone, disclosing a huge limitation of this study. After subtracting the reactivity to OVA alone from the OVA-coupled peptides, 44% of PBC sera had IgG response to the unlipoylated (OVA-167-184) peptide and 22% to the lipoylated peptide (OVA-167-184-LA). IgM were found in 57% and 31%, respectively. Therefore, the higher Ab response was detected by the unlipoylated peptide (Figure 41).

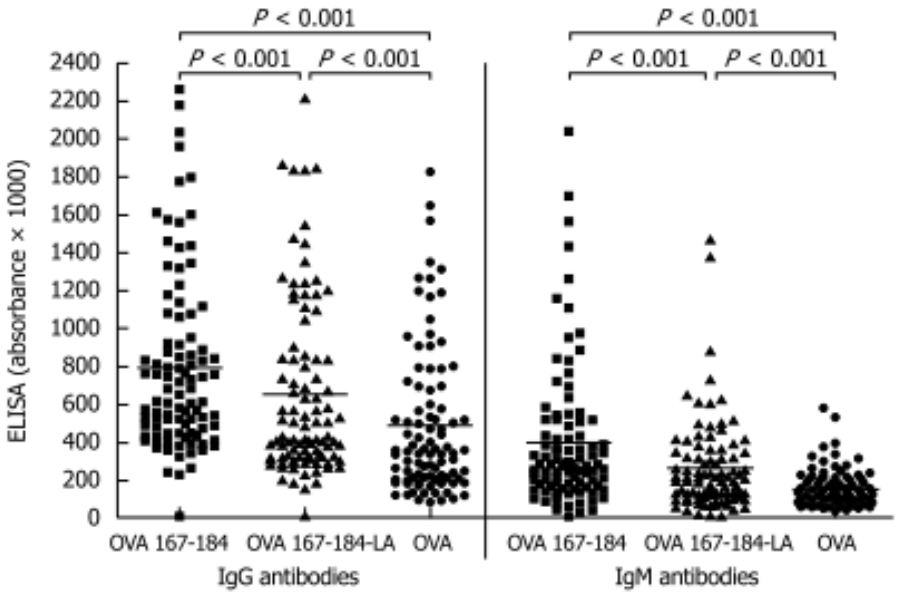

Figure 41: Data distribution of IgG (left) and IgM (right) reactivity of PBC sera with OVA-167-184, OVA-167-184-LA and OVA alone.

Significance of lipoic acid cofactor in Ab recognition

The identification of the main immunogenic region with the inner lipoyl domain of PDC-E2 prompted the investigation on the role of lipoic acid cofactor. From a conformational point of view, a study on *Bacillus stearothermophylus* PCD-E2 lipoyl domain disclosed that lipoylation does not impose any conformational change on the secondary structure of the protein[163]. If the same condition occurs in the human analog, this would imply that the Ab recognition of the lipoylated form is not a consequence of any conformational change imposed by the lipoate attachment, but involves the lipoate group *per se*[164]. The resolution of the 3D structure of lipoylated recombinant hPDC-$E2_{132-208}$ by Howard *et al.* revealed that the inner lipoyl domain is characterized by a β-barrel containing two antiparallel β-sheet, each of which contains three major strands and one minor strand. Intriguingly, they hypothesized that the lipoylated K^{173} is prominently exposed at the top of a tight type I β-turn (Figure 42)[165], but without verifying the lipoylation status of the recombinant protein. This serious issue represents a crucial limitation of this study for two reasons. Firstly, the 3D structure obtained in this study may not represent the native one. Secondly, although they documented the K^{173} localization on the tip of the β-turn, the prominent exposition of lipoic acid is not demonstrated, as the presence of lipoylation may affect both conformation and folding of the domain, resulting in a different 3D structure.

Figure 42: Representation of recombinant hPDC-$E2_{132-208}$ polypeptide fold hypothesized by Howard. Lipoylation site is indicated together with the type I β turn (black). The β sheet containing K^{173} residue is shown in dark grey; β sheet containing N- and C-terminal residues is shown in light grey.

Since the main immunogenic region of PCD-E2 was identified with the inner lipoyl domain of the protein, the involvement of lipoyc acid in the IgG auto-Ab response was intensely examined. Unfortunately, the use of inhomogeneous and not well characterized Ag preparations led to an intricate situation. Indeed, these studies employed PDC-E2 of different origin (bacterial, human, rat), using the whole protein or a sub-domain, obtained by extraction or produced by molecular biology, and even short peptide fragments, prepared by chemical synthesis and, in one case, conjugated to an irrelevant proteins (such as OVA), to mimic the native Ag. Therefore, a univocal conclusion was not reached yet, as outlined by some of the most remarkable studies summarized in Table 5, and the role of lipoic acid in PBC autoimmunity is still matter of debate.

Authors (year)	**Ag description**	**Lipoate attachment is required for Ab recognition?**
Gershiwn *et al.* (1987)[149]	Fused polypeptide (obtained by screening of rat liver cDNA library) expressed in *E.coli.*	Lipoylation status was not taken into account during the Ag characterization.
Van de Water *et al.* (1988)[153]	Synthetic peptides of rPDC-E2 (mapping of the fused polypeptide obtained by Gershwin[149]).	Lipoylation status was not taken into account during the Ag characterization.
Coppel *et al.* (1988)[154]	Recombinant hPDC-E2 of unknown lipoylation state expressed in *E.coli.*	Lipoylation status was not taken into account during the Ag characterization.
Mutimer *et al.* (1989)[166]	Extractive PDC-E2 from bovine heart.	Lipoylation status was not taken into account during the Ag characterization.
Fussey *et al.* (1990)[161]	Lipoylated, unlipoylated and octanoylated PDC-E2 extracted from *E.coli*	Yes (also octanoylated protein detects Ab)
Leung *et al.* (1990)[167]	Recombinant hPDC-E2 of unknown lipoylation state. Ag was engineered by site directed mutagenesis, substituting K^{173} to make new unlipoylatable isoforms, which are as immunogenic as the wild type.	No
Tuaillon *et al.* (1992)[168]	Lipoylated and unlipoylated synthetic octadecapeptides conjugated with OVA. Racemic lipoic acid is directly coupled to the side chain of Lys.	Yes
Quinn *et al.* (1993)[164]	Lipoylated and unlipoylated recombinant hPDC-E2 inner lipoyl domain expressed in *E.coli.* Lipoylation was performed *in vitro* using racemic mixture.	Yes
Koike et al. (1998)[169]	PDC-E2 from porcine heart, enzimatically delipoylated and re-lipoylated.	No
Bruggraber, *et al.* (2003)[157]	• Free lipoic acid • Recombinant lipoylated hPDC-E2 • PDC-E2 unrelated carrier bound lipoate.	Yes (Reactivity is specific for conjugated form of lipoyc acid, irrespective of the protein carrier)
Braun, *et al.* (2010)[162]	• Lipoylated and unlipoylated synthetic hPDC-E2(167-184) • Lipoylated and unlipoylated synthetic hPDC-E2(167-184) conjugated with OVA.	No

Table 5: Summary of the literature on lipoic acid involvement in PBC autoimmunity.

According to the popular assumption of xenobiotics as trigger for PBC, it was hypothesized that the exposure to certain compounds may cause aberrant modifications on lipoic acid, leading to neo-epitope uncovering. The susceptibility of lipoic acid to non-natural alteration may be explained considering its prominent exposition on the outer surface of the protein[165]. Furthermore, lipoic acid is able to rotate with respect to the PDC-E2 molecule by means of its "swinging arm", allowing the accessibility of its dithiolane ring for reductive acylation[170,171]. This conformational change, together with the existence of multiple conformations of lipoyl domain during the reductive acylation[170], is required for acyl transfer mechanism, but renders the cofactor vulnerable to modifications. Indeed, it was shown that PDC-E2 conjugated to some synthetic small molecules able to mimic lipoic acid displays highly specific reactivity to AMA+ PBC sera, at levels often higher than the native molecule[172,173]. In this context, one of the most relevant work is that of Amano *et al.*[174], which concerns the replacement of lipoic acid on synthetic PDC-E2(169-183) by 107 different xenobiotics. They showed that 33/107 xenobiotics have significantly higher IgG reactivity against PBC sera compared with NBD, and one of the compounds, 2-octinoyc acid (Figure 43), is more reactive than the native lipoylated peptide. Interestingly, the methyl ester of this molecule is one of the oldest artificial flavoring and was widely used since the 1900s in perfumed cosmetics for its violet scent. Other relevant findings were achieved by Leung *et al.*[175], which addressed the question whether the physiological lipoyl ring reduction renders the lipoyc acid receptive for xenobiotics modification, testing synthetic thioesters modified analogs of open-ring lipoyc acid. They verified that three of these molecules, namely 6,8-bis(acetylthio)octanoic acid (SAc), 8-(acetylthio)octanoic acid and 6,8-bis(propionylthio)octanoic acid (Figure 43), showed highly reactivity to AMA+ sera compared to the native lipoylated protein. These data suggest that xenobiotics alterations of the lipoyl S-S linkage during physiological electron transfer could break immunological tolerance to PDC-E2, according to the former hypothesis that the oxidative state of PDC-E2 may affect its immunogenicity[156]. In the same study it was demonstrated that purified anti-SAc-bovine serum albumin (BSA) conjugate Ab are of the IgM type, and are able to recognize both SAc-BSA and recombinant PDC-E2, while purified anti-recombinant PDC-E2 Ab are of the IgG type and recognize only PDC-E2. Based on these results, the presence of the following process may be argued:

1. The initial exposure to chemicals leads to a primary IgM specific immune response against the exogenous Ag;
2. Subsequently, the similarity between the lipoyl domain of PDC-E2 and the xenobiotic generates a cross-reactive response to the self-Ag, causing self-tolerance breakdown to the native protein;
3. In the end, the affinity maturation and isotype switching processes lead to a secondary IgG immune response to the native protein[176].

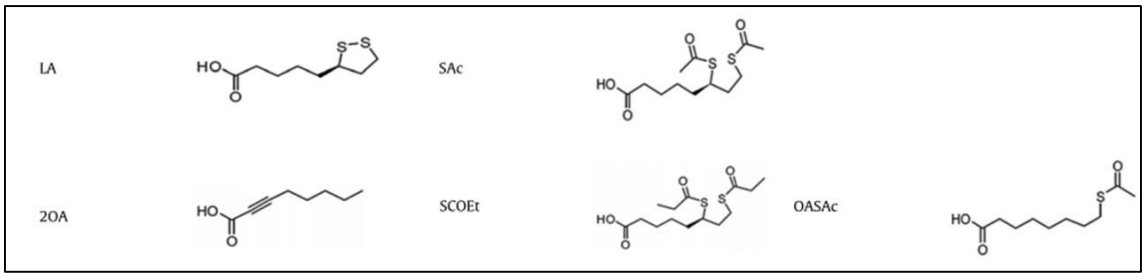

Figure 43: Chemical structure of lipoic acid (LA) and related xenobiotc compounds. SAc = 6,8-bis(acetylthio)octanoic acid; 2OA = 2-octinoyc acid; SCOEt = 6,8-bis(propionylthio)octanoic acid; OASAc=8(acetylthio)octanoic acid.

In a few words, the hypothesis of lipoic acid as minimal epitope candidate in the case of PBC was deeply investigated, but remains highly controversial. The assumption of a role of lipoic acid in PBC immunopathogenesis is supported by both cofactor localization[165] and oxidized state during pyruvate decarboxylation[170], which make it an easy target for auto-Ab and aberrant chemical modifications due to xenobiotic exposure. However, the presence of inhomogeneous data on this topic led to a confusing situation that needs further clarifications.

AIM OF THE WORK

PBC is a chronic liver AID characterized by the presence of highly specific serum AMA in 95% of pts. The current diagnostic tool for AMA detection is based on IIF detection of serum IgG targeting the so-called M2 Ag, which is represented by a pool of various, not fully characterized Ag. Indeed, AMA test is performed using whole tissues from rat kidney as Ag substrate, enabling the detection on a heterogeneous Ab population directed against an undefined complex set of proteins. This unclear situation may be resolved through a precise molecular definition of the immunodominant epitope(s), which may provide critical insights into the molecular basis of PBC immunology and ethiopathogenesis. The main immunogenic region of AMA was mapped to the inner lipoyl domain of PDC-E2, and in particular to the Aa residues surrounding the lipoylated K^{173} of the linear peptide AEIETDKATIGFEVQEEG, corresponding to PDC-E2(167-184)[153]. The importance of the lipoyl-Lys seems to be confirmed by its relevant localization within the protein, on the tip of a type I β-turn[165]. It was also speculated that the lipoic acid itself is prominently exposed on the β-turn, but since the structural studies were performed without verifying the lipoylation status of the analyzed protein this is only one of the possible hypothesis. In addition to the doubts of its structural localization, to date also the role of lipoic acid *per se* and of the lipoylation on the immunodominant peptide is still debated for several reasons. First, different Ag preparations, including peptides, recombinants and conjugated molecules, were use. Second, the length and origin (bacterial, human, rat) of the PDC-E2 sequences employed is extremely heterogeneous. Third, the assays used for anti-PDC-E2 detection range from immunoblot to IIF. Last but not least, some studies have not taken into account the lipoylation status of the probes.

In this scenario, we decided to characterize the PDC-E2 immunodominat region (Aa 167-184) from a molecular point of view. We focused our attention on both lipoylation and aberrant PTM that may occur on this region, using well-characterized synthetic peptide probes resulting from the human sequence. These peptides were used as antigenic probes in SP-ELISA to detect Ab in PBC pts sera. The project addressed the following issues:

1. <u>Role of lipoic acid and its chiral center</u>

   Lipoic acid is an essential cofactor of many enzyme complex, and its role is crucial in aerobic metabolism. As the C6 of the molecule is chiral, lipoic acid exists as two enantiomers, (*R*)-lipoic acid and (*S*)-lipoic acid (Figure 44), and as a racemic mixture (*R/S*)-lipoic acid. Only the (*R*)-enantiomer exists in nature. To date, the role of the two enantiomers and/or the racemic mixture in PBC immunopathogenesis was not taken into account. For this purpose, we developed a SPPS strategy aimed to introduce both the natural and non-natural enantiomers of lipoic acid on the immunodominant epitope in a controlled fashion. Using this methodology, we synthesized and characterized [(*R*)-Lipoamide-Lys^{173}]PDC-E2(167-186)-KKKK and [(*S*)-Lipoamide-Lys^{173}]PDC-E2(167-186)-KKKK. To elucidate the significance of lipoic acid, the unlipoylated form of the peptide was also synthesized: [Lys^{173}]PDC-E2(167-186)-KKKK. In

order to enhance the solubility of PDC-E2(167-186) derived peptides, and to allow the coating on the ELISA plate, a 4-Lys tag (KKKK) was added to the C terminus of all the PDC-E2(167-186) peptides.

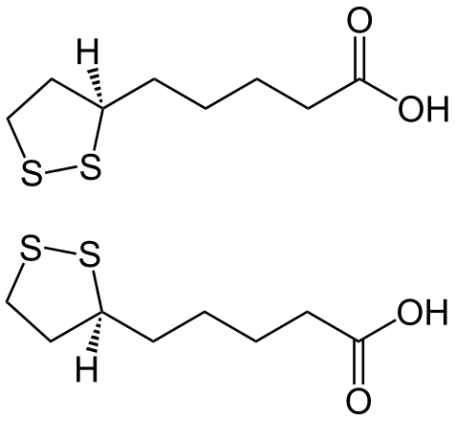

Figure 44: (*R*)-lipoic acid (top) and (*S*)-lipoic acid (down)

2. Role of K^{173} lipoylation and relevance of K^{173} hypothetical exposition on the tip of the β-turn

   In order to clarify the role of the presence of lipoyl-modified Lys residue on the immunodominant sequence, and the importance of its presumed exposition on the β-turn in the Ab recognition, we inserted the lipoylated Lys on the tip of a scaffold β-turn peptide sequence. We selected the 21-mer peptide CSF114, as we previously demonstrated its ability to expose optimally post-translationally modified residues on the tip of a type I' β-turn (corresponding to position 7) as irrelevant peptide sequence[177]. Analogues of CSF114 bearing the same PTM of hPDC-E2 peptides were designed: [(*R*)-Lipoamide-Lys^7]CSF114, [(*S*)-Lipoamide-Lys^7]CSF114 and [Lys^7]CSF114.

3. Relevance of N-glucosylation in PBC autoimmunity

   The involvement of aberrant N-glucosylation in autoimmunity and the role of Asn(Glc) as minimal epitope exposed on a type I' β-turn structure was previously demonstrated[36,37]. In order to assess a possible role of glucosylation in PBC autoimmunity, we synthesized an analog of PDC-E2 peptide containing the minimal epitope Asn(Glc) exposed on the tip of the β-turn (same position of the natural lipoylated Lys): [Asn^{173}(Glc)]PDC-E2(167-186)-KKKK. The specificity of the response against Glc was evaluated synthesizing also the peptide bearing an N-acetyl-glucosamine (GlcNAc) on Asn residue: [Asn^{173}(GlcNAc)]PDC-E2(167-186)-KKKK. To further clarify the relevance of glucosylation, the corresponding unglucosylated peptide (with the Lys → Asn mutation) was synthesized: [Asn^{173}]PDC-E2(167-186)-KKKK. Finally, we investigated a possible role of Asn(Glc) independently from the specific sequence of PDC-E2, we prepared and tested analogues of CSF114 with the same PTM of hPDC-E2 peptides: [Asn7(Glc)]CSF114, [Asn^7(GlcNAc)]CSF114 and [Asn^7]CSF114 .

Further to the molecular characterization of the PDC-E2 immunodominant region, we evaluated the possible diagnostic relevance of the previously mentioned peptides (summarized in Table 6). For this purpose, we tested the synthetic probes as Ag in SP-ELISA, comparing the results obtained in the PBC cohort with other control diseases, such as Rheumatoid Arthritis (RA) and Scleroderma (SSC), and NBD.

PDC-E2 series	**CSF114 Series**
[(*R*)-Lipoamide-Lys^{173}]PDC-E2(167-186)-KKKK	[(*R*)-Lipoamide-Lys^{7}]CSF114
[(*S*)-Lipoamide-Lys^{173}]PDC-E2(167-186)-KKKK	[(*S*)-Lipoamide-Lys^{7}]CSF114
[Lys^{173}]PDC-E2(167-186)-KKKK	[Lys^{7}]CSF114
[Asn^{173}(Glc)]PDC-E2(167-186)-KKKK	[Asn^{7}(Glc)]CSF114
[Asn^{173}(GlcNAc)]PDC-E2(167-186)-KKKK	[Asn^{7}(GlcNAc)]CSF114
[Asn^{173}]PDC-E2(167-186)-KKKK	[Asn^{7}]CSF114

Table 6: Summary of the peptides used in the PBC study [§].
All the peptides were synthesized by SPPS at the SOSCO Laboratory (*Universitè de Cergy Pontoise*, France).

[§] Rentier, C., **Pacini, G.,** Nuti, F., Peroni, E., Rovero, P., Papini, A. M.,Synthesis of diastereomerically pure Lys(Nε-lipoyl) building-blocks and their use in Fmoc/tBu solid phase synthesis of lipoyl-containing peptides for diagnosis of paciprimary biliary cirrhosis. *Journal of Peptide Sciences*, submitted.

RESULTS & DISCUSSION

Importance of lipoyc acid and its chiral center

[(*R*)-Lipoamide-Lys^{173}]PDC-E2(167-186)-KKKK, [(*S*)-Lipoamide-Lys^{173}]PDC-E2(167-186)-KKKK and [Lys^{173}]PDC-E2(167-186)-KKKK were tested for both IgG and IgM on a cohort of 65 PBC pts using SP-ELISA. IgM on [(*S*)-Lipoamide-Lys^{173}]PDC-E2(167-186)-KKKK were tested on a smaller cohort.

Results obtained display an Ab response against all the peptides tested (Figure 45). In particular, a paired t test confirmed that values obtained for the (*R*)- and (*S*)-enantiomers are comparable (P= 0.499 in the case of IgG and P= 0.367 for IgM), allowing us to assume that the lipoic acid chirality on the C6 has no influence on the Ab recognition.

The presence of a response against [Lys^{173}]PDC-E2(167-186)-KKKK enables to hypothesize that a PTM (namely, a de-lipoylation) can uncover a neo-epitope.

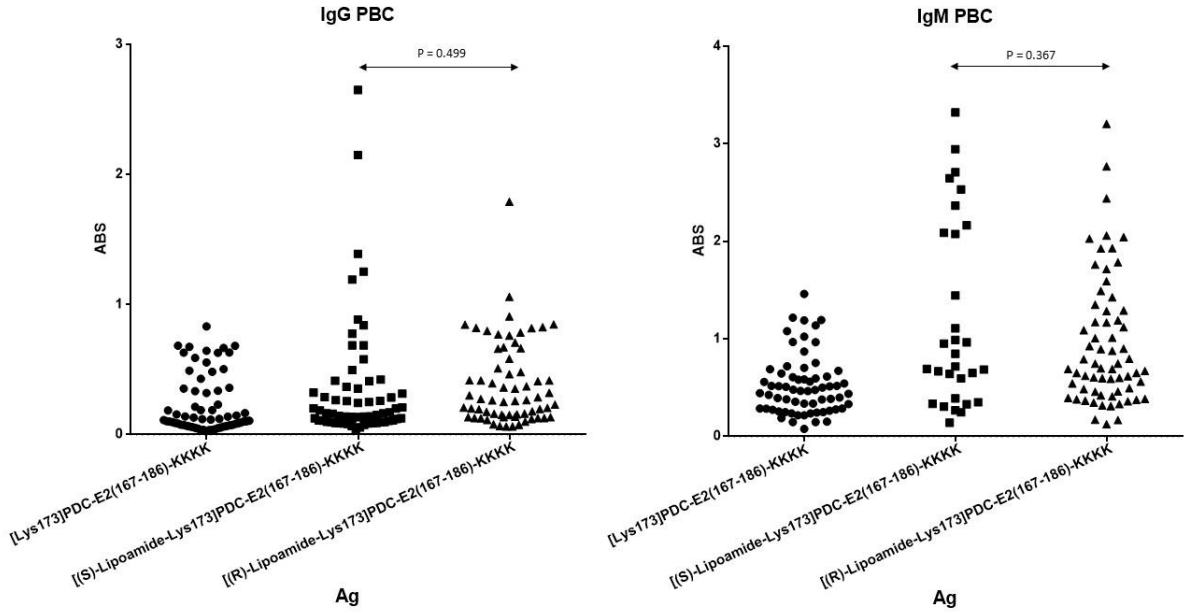

Figure 45: IgG (left) and IgM (right) data distribution of PBC sera against [Lys^{173}]PDC-E2(167-186)-KKKK, [(*S*)-Lipoamide-Lys^{173}]PDC-E2(167-186)-KKKK and [(*R*)-Lipoamide-Lys^{173}]PDC-E2(167-186)-KKKK. P-values obtained in paired t tests are shown.

Role of lipoyl-K^{173} and the relevance of K^{173} exposition on the tip of the β-turn

Results obtained with [(*R*)-Lipoamide-Lys^{173}]PDC-E2(167-186)-KKKK, [(*S*)-Lipoamide-Lys^{173}]PDC-E2(167-186)-KKKK and [Lys^{173}]PDC-E2(167-186)-KKKK were compared with the one achieved with CSF114 corresponding analogues: [(*R*)-Lipoamide-Lys7]CSF114, [(*S*)-Lipoamide-Lys7]CSF114 and [Lys7]CSF114. All the peptides were tested for both IgG and IgM on a cohort of 65 PBC pts using SP-ELISA. IgM on [(*S*)-Lipoamide-Lys^{173}]PDC-E2(167-186)-KKKK were tested on a smaller cohort.

A paired t test confirmed that the absorbance values observed against CSF114 series are lower than the one obtained with the corresponding PDC-E2 analogues (Figure 46). These findings enable us to speculate that K^{173} (both lipoylated and unlipoylated) exposed on the type I' β-turn irrelevant peptide sequence is not able to detect Ab in PBC pts, and therefore that the Aa residues surrounding the lipoyl-Lysine are required for Ab recognition.

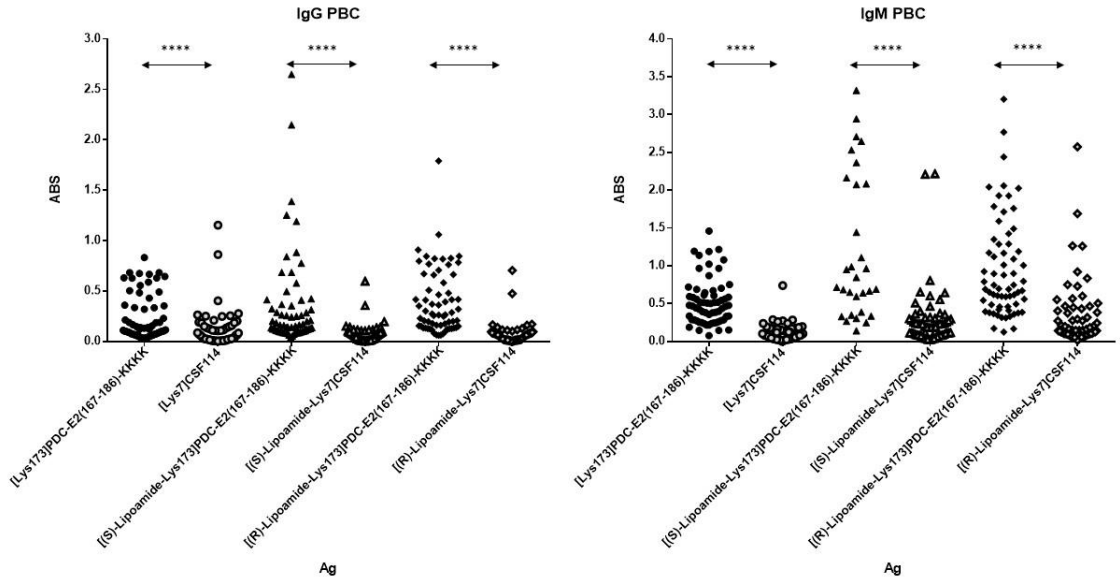

Figure 46: IgG (left) and IgM (right) data distribution of PBC sera against [Lys^{173}]PDC-E2(167-186)-KKKK, [Lys^{7}]CSF114, [(*S*)-Lipoamide-Lys^{173}]PDC-E2(167-186)-KKKK, [(*S*)-Lipoamide-Lys^{7}]CSF114, [(*R*)-Lipoamide-Lys^{173}]PDC-E2(167-186)-KKKK and [(*R*)-Lipoamide-Lys^{7}]CSF114. P-values obtained in paired t tests are shown: **** P < 0,0001.

Relevance of N-glucosylation in PBC autoimmunity

[Asn^{173}(Glc)]PDC-E2(167-186)-KKKK, [Asn^{173}]PDC-E2(167-186)-KKKK, [Asn^{7}(Glc)]CSF114 and [Asn^{7}]CSF114 were tested for both IgG and IgM on a cohort of 65 PBC pts using SP-ELISA.

Results obtained (Figure 47) display a high and specific response in the case of [Asn^{173}(Glc)]PDC-E2(167-186)-KKKK, uncovering the hypothesis of an involvement of aberrant N-glucosylation in the immunopathogenesis of PBC.

To verify the specificity of the Ab response detected against glucose, [Asn^{173}(GlcNAc)]PDC-E2(167-186)-KKKK and [Asn^{173}(GlcNAc)]CSF114 were tested on a smaller cohort of sera (n=7).

Results obtained show that the higher titers detected in both CSF114 and PDC-E2 series concerns [Asn(Glc)] peptides (Figure 48). We can assume that the response is [Asn(Glc)]-specific, as [Asn(GlcNAc)] peptides are unable to recognize Ab in PBC pts sera. It is important to note that [Asn^{173}(Glc)]PDC-E2(167-186)-KKKK could also mimic a different self Ag bearing an aberrant N-glucosylation. For this purpose, further investigations on the involvement of N-glucosylation in PBC are required, such as the characterization of anti-[Asn^{173}(Glc)]PDC-E2(167-186)-KKKK Ab isolated from pts sera and the assessment of the cross-reactivity between these Ab and the other PDC-E2 antigenic probes.

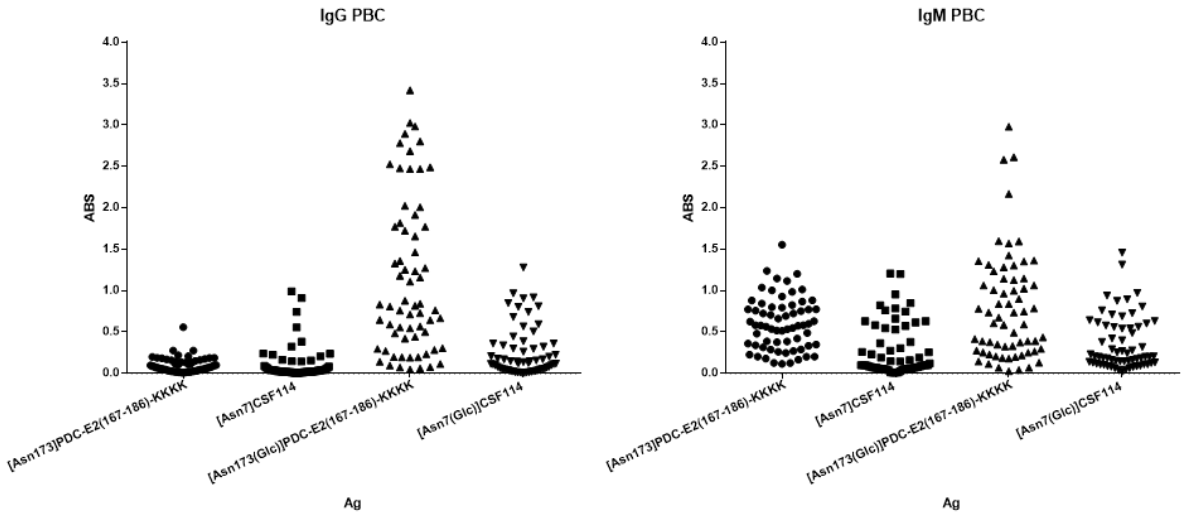

Figure 47: IgG (left) and IgM (right) data distribution of PBC sera against [Asn^{173}]PDC-E2(167-186)-KKKK, [Asn^{7}]CSF114, [Asn^{173}(Glc)]PDC-E2(167-186)-KKKK and [Asn^{7}(Glc)]CSF114.

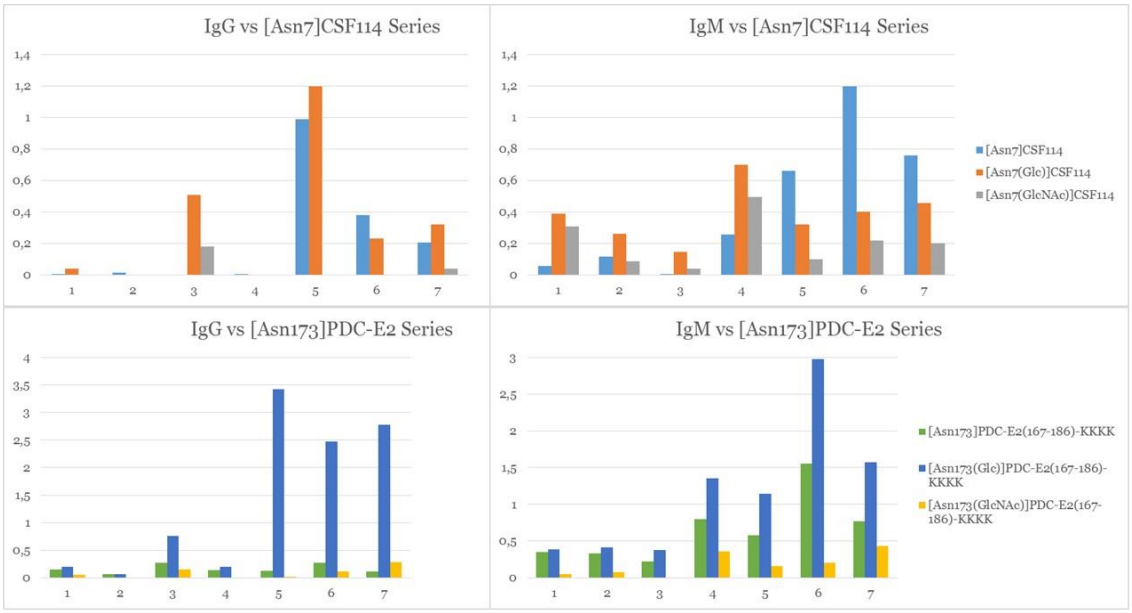

Figure 48: Comparison between [Asn], [Asn(Glc)] and [Asn(GlcNAc)] results for both IgG (left) and IgM (right).

Search of an antigenic probe able to recognize disease-specific auto-Ab in PBC pts sera

The antigenic probes summarized in Table 6 were tested as antigenic probes in SP-ELISA, in order to identify auto-Ab in pts sera as disease BM. Disease-specificity of the detected Ab was evaluated comparing the results obtained in PBC pts with NBD cohort using a cutoff value calculated as (mean value of NBD) + 3*(standard deviation of NBD). Data distribution of all the tests are shown in Supplementary Data.

Unpaired t tests with Welch's correction confirmed that the difference between the results obtained for PBC pts and for NBD are statistically significant for all the Ag. Furthermore, we included 3 different cohorts of disorders as pathological control groups: RA, SSC and other not-hepatic AID (OAID). The most interesting results were achieved using the PDC-E2 peptide series (Figure 49). Comparing PBC data with NBD through cutoff value allowed us to identify [Lys^{173}]PDC-E2(167-186)-KKKK as the most relevant antigenic probe for IgM detection. This peptide is able to recognize 63% of PBC pts, even if with lower titers compared with the lipoylated peptide [(*R*)-Lipoamide-Lys^{173}]PDC-E2(167-186)-KKKK, which is able to discriminate 37% of pts (Figure 50). PBC-specificity of the detected Ab was confirmed using 3 different pathologic control cohorts: RA (n=22), SSC (n=12) and OAID (n=47). In particular, we obtained 0% positivity percentage for IgM against the unlipoylated PDC-E2 peptide in both RA and SSC cohorts, while OAID have 23% of positivity (Figure 51). This finding enabled us to hypothesize that [Lys^{173}]PDC-E2(167-186)-KKKK may represent the target of auto-Ab response in the case of PBC. The disease specificity of detected Ab is confirmed by the comparison with all the three pathological control cohorts. Such a result is remarkable, as RA is characterized by high levels of circulating auto-Ab, in particular rheumatoid factors, cross-reactive Ab that may cause interference in solid phase assays. SSC was selected as control disease because it is often associated with PBC, suggesting a common genetic background for the two disorders. SSC sera included in this study, however, are AMA negative and contain auto-Ab of other specificities, not reactive with the PDC-E2 sequences.

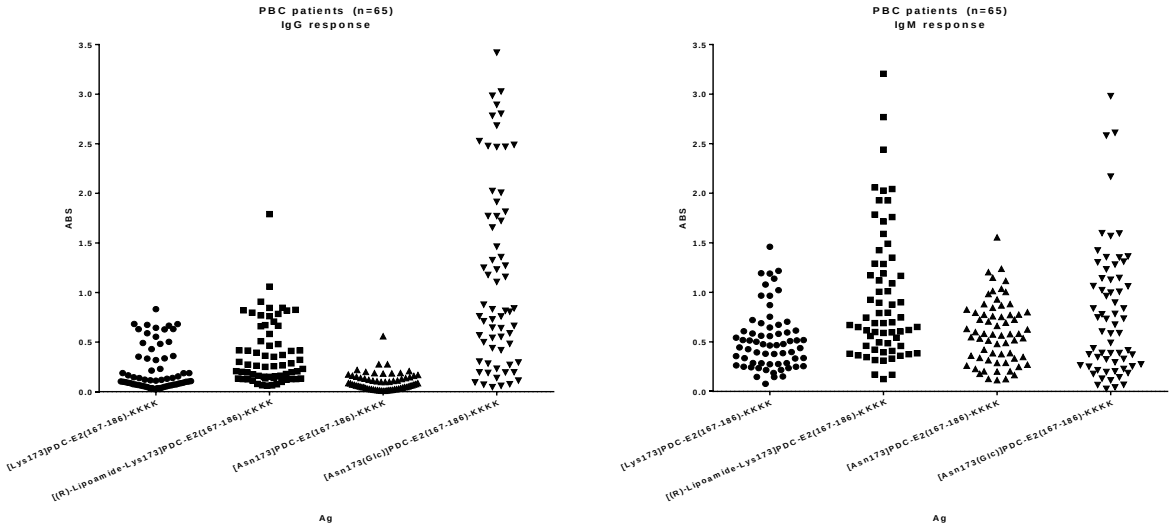

Figure 49: IgG (left) and IgM (right) data distribution of PBC sera against [Lys^{173}]PDC-E2(167-186)-KKKK, [(*R*)-Lipoamide-Lys^{173}]PDC-E2(167-186)-KKKK, [Asn^{173}]PDC-E2(167-186)-KKKK and [Asn^{173}(Glc)]PDC-E2(167-186)-KKKK

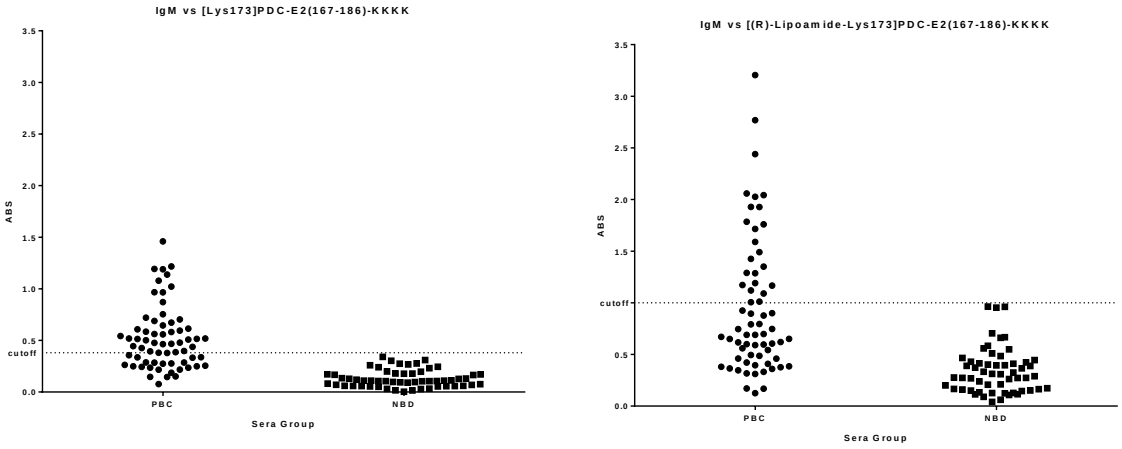

Figure 50: IgM data distribution of PBC pts and NBD against [Lys^{173}]PDC-E2(167-186)-KKKK (left), and [(*R*)-Lipoamide-Lys^{173}]PDC-E2(167-186)-KKKK (right). Dotted line indicate the cutoff value.

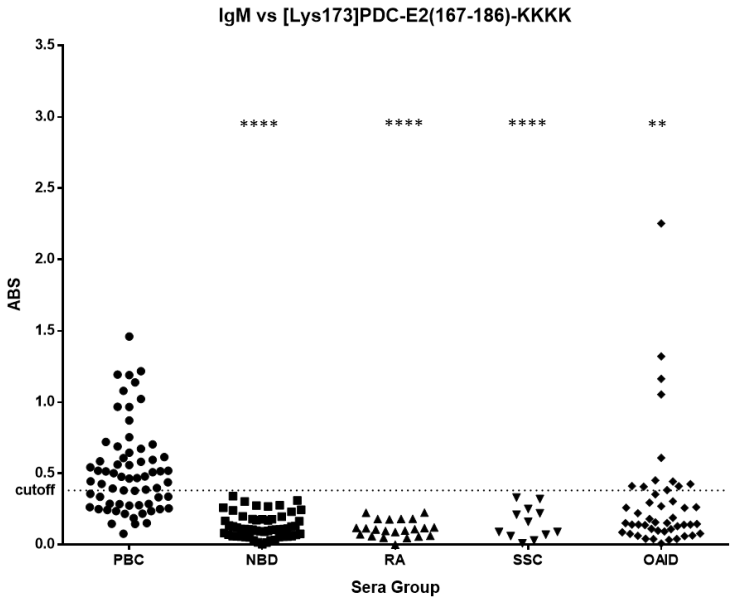

Figure 51: IgM data distribution of PBC pts against [Lys^{173}]PDC-E2(167-186)-KKKK compared with control cohorts: NBD, RA, SSC and OAID.
Dotted line indicate the cutoff value.
P-values obtained comparing PBC pts with control cohorts are shown:
****** P < 0,0001; ** P 0.001 to 0.01 .**

CONCLUSIONS

PBC is one of the few AID having available a not-invasive diagnostic tool, i.e. serum AMA detection. However, since AMA are not present in all pts, the diagnostic procedure includes also a control of alkaline phosphatase elevation, and/or histological analyses on bioptic tissue[135]. AMA detection procedure is executed by IIF (a not-automated, subjective and labor-intensive technique) on whole tissues from rat kidney as Ag substrate. This enables the detection of a heterogeneous Ab population, directed against an undefined complex of various, not fully characterized proteins, the so-called M2 Ag. The absence of a precise molecular definition of the immunodominant epitope(s) led to an intricate situation, which results in a lack of characterization of the immunopathogenic mechanism triggering and pursuing PBC. Indeed, the research in the PBC field was strictly focused on the identification of the main immunogenic region of AMA, without considering that the diagnostic test reveals Ab toward a pool of proteins.

In the late 80s, the main immunogenic region was mapped to the inner lipoyl domain of PDC-E2, and specifically to the Aa residues surrounding the lipoylated K^{173} of the linear peptide AEIETDKATIGFEVQEEG, corresponding to PDC-E2(167-184)[153]. Therefore, the importance of both lipoyl-Lys and lipoic acid *per se* were extensively debated, but without reaching a conclusion, particularly due to the use of inhomogeneous Ag preparations and sequences. Furthermore, some studies have not taken into account the lipoylation status of the probes, resulting in even more confusion. Even the conformational study performed by Howard *et al.*[165], which resolved the 3D structure of recombinant $hPDC\text{-}E2_{132\text{-}208}$ speculating the exposition of lipoic acid at the top of a tight type I β-turn (Figure 42), was performed without verifying the lipoylation status of the protein. This could have led to the obtainment of a structure that not correspond to the native one, as the presence of lipoic acid may influence both conformation and folding. To elucidate this point, circular dichroism spectroscopy studies on our synthetic peptides [(*R/S*)-Lipoamide-Lys^{173}]PDC-E2(167-186)-KKKK and [Lys^{173}]PDC-E2(167-186)-KKKK were performed by Prof. Alfonso Carotenuto (University of Naples "Federico II"). Preliminary results disclosed that lipoylation actually affects the conformation of the peptides (data not shown), although it should be taken into account that peptides have a different conformational behavior compared with full-length proteins, encouraging us to deepen the structural differences between lipoylated and unlipoylated probes.

In this context, we decided to clarify the situation characterizing PDC-E2 immunodominat region (Aa 167-184) from a molecular point of view. We focused our attention on both lipoylation and aberrant PTM that may occur on this region, using well-defined synthetic hPDC-E2 peptide probes, which were used as antigenic probes in SP-ELISA to detect Ab in PBC pts sera.

Firstly, we examined the problem of lipoic acid chirality, which until now was never addressed. We elucidated that the chirality on the C6 has no influence on the Ab recognition, as the Ab responses detected toward (*R*)- and (*S*)-enantiomers are comparable.

Secondly, we clarified the relevance of K^{173} lipoylation and hypothetical exposition on the β-turn in the Ab recognition inserting it on the tip of a optimized scaffold β-turn peptide sequence, $CSF114^{177}$. We tested analogues of CSF114, disclosing that the absorbance values observed against CSF114 series are lower than the one obtained with the corresponding hPDC-E2 analogues. Based on these results, we speculate that Lys (both lipoylated and unlipoylated) exposed on the type I' β-turn irrelevant peptide sequence is not able to detect Ab in PBC pts, and therefore that the Aa residues surrounding Lys are required for Ab recognition.

Thirdly, as we previously demonstrated the involvement of aberrant N-glucosylation in autoimmunity and the role of Asn(Glc) as minimal epitope exposed on a type I' β-turn structure[36,37], we decided to explore the putative relevance of this PTM in PBC. Therefore, we tested an analog of hPDC-E2 peptide containing the minimal epitope Asn(Glc) exposed on the tip of the β-turn (same position of the natural lipoylated Lys). Results were compared with the unglucosylated analogue (bearing a Lys → Asn mutation), uncovering the hypothesis of an involvement of aberrant N-glucosylation in the immunopathogenesis of PBC. The specificity of the response against Glc was assessed testing a peptide bearing a GlcNAc on Asn residue, which gave lower titers compared with Glc peptide. These results allow us to assume the presence of a Glc-specific response in PBC sera. We investigated also the possibility of a role of Asn(Glc) independently from the specific sequence of hPDC-E2 testing analogues of CSF114. Preliminary data display a high and specific response in the case of [Asn^{173}(Glc)]PDC-E2(167-186)-KKKK, uncovering the hypothesis of an involvement of aberrant N-glucosylation in the immunopathogenesis of PBC, which however requires further clarification.

In addition to the molecular characterization of the PDC-E2 immunodominant region, we evaluated the possible diagnostic relevance of the previously mentioned peptides, in order to identify auto-Ab in pts sera as disease BM (summarized in Table 6). For this purpose, we tested the synthetic probes as Ag in SP-ELISA, comparing the results obtained in the PBC cohort with other control diseases, such as RA, SSC, OAID and NBD. Disease-specificity of the detected Ab was evaluated comparing the results obtained in PBC pts with NBD cohort using a cutoff value calculated as (mean value of NBD) + 3*(standard deviation of NBD). Comparing PBC data with NBD through cutoff value allowed us to identify [Lys^{173}]PDC-E2(167-186)-KKKK as the most relevant antigenic probe for IgM detection. This peptide recognized 63% of PBC pts sera, even if with lower titers compared with the lipoylated peptide [(*R*)-Lipoamide-Lys^{173}]PDC-E2(167-186)-KKKK, which is able to discriminate 37% of pts. PBC-specificity of the detected Ab was confirmed using pathologic control cohorts: we obtained 0% positivity percentage for IgM against the unlipoylated PDC-E2 peptide in both RA and SSC cohorts, while OAID have 23% of positivity.

Based on the obtained results, we hypothesized that an aberrant PTM, namely a de-lipoylation, may uncover a neo-epitope, triggering PBC autoimmune reaction. Inner mitochondrial proteins may become the target of an autoimmune response by several possible mechanisms, including

abnormalities in structure: altered or abnormal enzyme forms may be degraded at an increased rate, leading to amplified presentation at the surface.

The de-lipoylation reaction may be enzymatically performed by a lipoamidase (Lpa). For example, the presence of an Lpa was described in *Enterococcus faecalis*, a gut bacterium capable to do a commensal-to-pathogen switch in particular conditions. Expression and cloning of Lpa allowed to demonstrate its ability to release lipoyc acid from lipoylated intact proteins both *in vivo* and *in vitro*[178,179]. Intriguingly, *Enterococcus faecalis* is responsible of urinary tract infections, and the occurrence of this pathology is strictly associated with PBC as reproducible risk factor[180,181]. Based on these observations, it is possible to hypothesize the occurrence of a pathological de-lipoylation of PDC-E2 operated by *Enterococcus faecalis* as trigger for PBC.

Even if hPDC-E2 includes two lipoyl domains (Figure 52), a de-lipoylation of the protein could lead to a failure of the PDC function or even to an enzymatic inactivation. Genetic PDC-E2 deficiency results in lactic acidosis as well as neurological dysfunction in infancy and early childhood[182], symptoms that are not included in the clinical presentation of PBC pts.

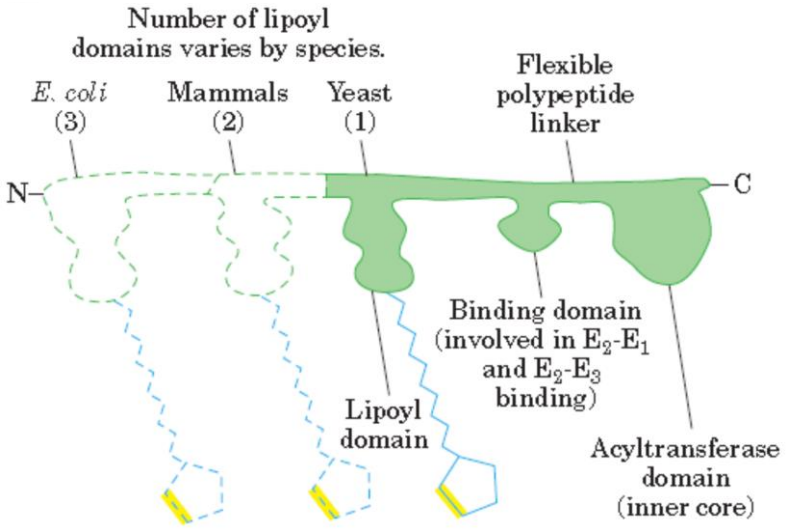

Figure 52: PDC-E2 domains in different species: E.coli, mammals, yeast.

However, both Van de Water[183] and Uibo[184] demonstrated the AMA ability to inhibit the catalytic function of PDC by binding to the residues surrounding the lipoyl-Lys on PDC-E2, which is the core of the enzymatic reaction. Specifically, they incubated PBC pts sera with commercial PDC in a medium containing the reagents required for the enzymatic reaction, and quantified the NADH production by spectrophotometrical measurement at 340 nm. Intriguingly, the degree of enzymatic inhibition was directly proportional to the pts ABS value detected in ELISA. It was also demonstrated that PBC pts sera pre-absorbed with the recombinant Ag lost the ability to inhibit the enzyme activity. Results obtained with control sera are comparable with the one achieved

incubating the reaction mixture without sera. Therefore, the presence of AMA *per se* affects the enzyme functionality. Based on this statement, it is possible to hypothesize that the presence of an aberrant modification on PDC-E2, which may lead to an enzyme malfunction, is compatible with the disorder.

Testing [Lys^{173}]PDC-E2(167-186)-KKKK, we obtained 63% of positivity in PBC pts, which may seem a relatively significant result compared with the 95% detected by the routine assay. However, it must be kept in mind that the IIF assay measures the response directed toward a mixture of tissue Ag trough a complicated and time-consuming method. Our simple, single-Ag detection enabled to identify a population of PBC pts, with high specificity compared with control cohorts. Indeed, the significance of our result is emphasized not only by the 0% positivity obtained testing NBD, RA and SSC control cohorts, but also by the fact that RA is characterized by high levels cross-reactive Ab, and SSC is often associated with PBC. It will be of great interest to investigate the clinical features of the positive pts compared with the negative one, to disclose if our assay is able to discriminate a clinically defined subgroup of PBC pts, characterized by pathological peculiarity. Further investigations will be carried out to identify other candidate Ag to be added to the selected one, in order to develop a multi-Ag assay capable to discriminate a higher percentage of pts. In this way, we may obtain a new diagnostic tool characterized by:

- Molecular characterization of the Ag;
- Low invasivity for the pts;
- Ease of execution (with feasibility of automating) and high reproducibility of the assay, which gave clearly interpretable results.

Concluding, these results allowed us to hypothesize a molecular mechanism responsible for PBC triggering, and pave the way for further studies aimed both at understanding the pathological insights of PBC and at developing a more advantageous and significant diagnostic assay.

MATERIALS & METHODS

Serum samples

50 AMA+ and 15 AMA- serum samples were analyzed as PBC pts group (n=65). 56 NBD serum samples were used as healthy control group. Samples were tested in triplicate with a single dilution (1:100) in FBS Buffer.

Antigens

Antigenic probes used in this study are listed in Table 6. All the sequences were synthesized at the SOSCO Laboratory (*Universitè de Cergy Pontoise*, France) using SPPS strategy.

Enzyme-Linked Immunosorbent Assay (ELISA)

1ug/well of Ag (peptide or protein) were dissolved in Coating Buffer (12mM Na_2CO_3, 35mM $NaHCO_3$, pH 9.6), then 100 ul of solution were dispensed in each well of 96-well Maxisorp plates. Plates were incubated @4°C ON. Subsequently, plates were washed 3 times with Washing Buffer (0,9% NaCl, 0,01% Tween 20), and blocked 1 h at RT with 100ul/well of FBS Buffer (10% FBS in Washing Buffer). FBS Buffer were removed, and 100ul/well of diluted sera sample (1:100 in FBS Buffer) were dispensed. Blank wells were included in all the plates, and were obtained using FBS Buffer instead of serum. Plates were incubated @4°C ON, and then washed 3 times with Washing Buffer. 100ul/well of secondary Ab diluted in FBS Buffer (hIgG 1:8000 and hIgM 1:1200) were dispensed, and plates were incubated 3 h at RT. Plates were washed 3 times with Washing Buffer, then 100ul/well of Substrate Solution (1mg/ml p-PNP in Substrate Buffer: 1M Diethanolamine, 1mM MgCl2, pH 9.8) were dispensed. Plates were incubated for 15'-40', and then ABS at 405 nm of each well was red with a spectrophotometer. ABS value for each serum was calculated as (mean ABS of triplicate) – (mean ABS of blank triplicate).

SUPPLEMENTARY DATA

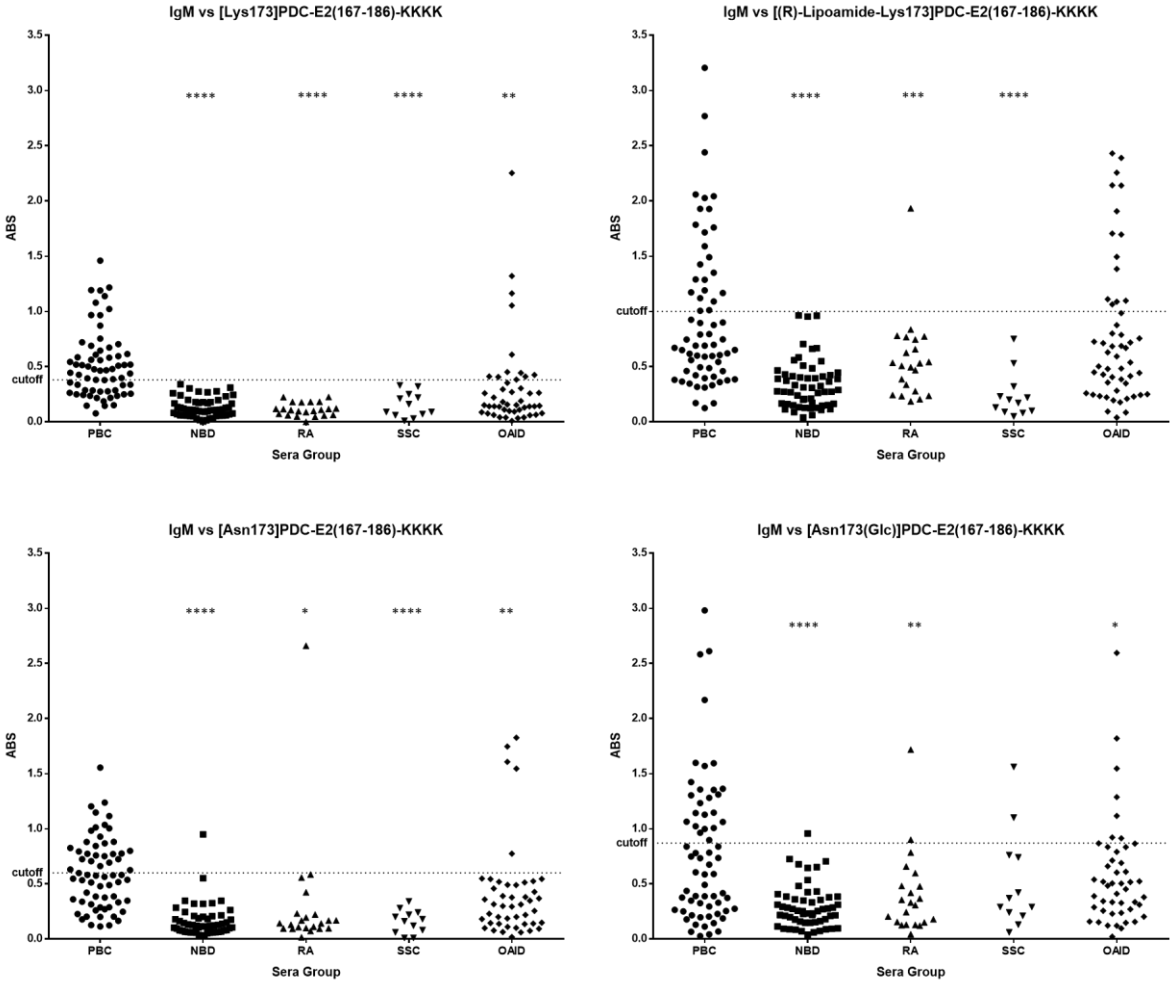

Supplementary figure 1: IgM data distribution of PBC pts and control cohorts against PDC-E2 peptides. Dotted line indicate the cutoff value. P-values obtained comparing PBC pts with control cohorts are shown: **** P < 0,0001; *** P 0.0001 to 0.001; ** P 0.001 to 0.01; * P 0.01 to 0.05.

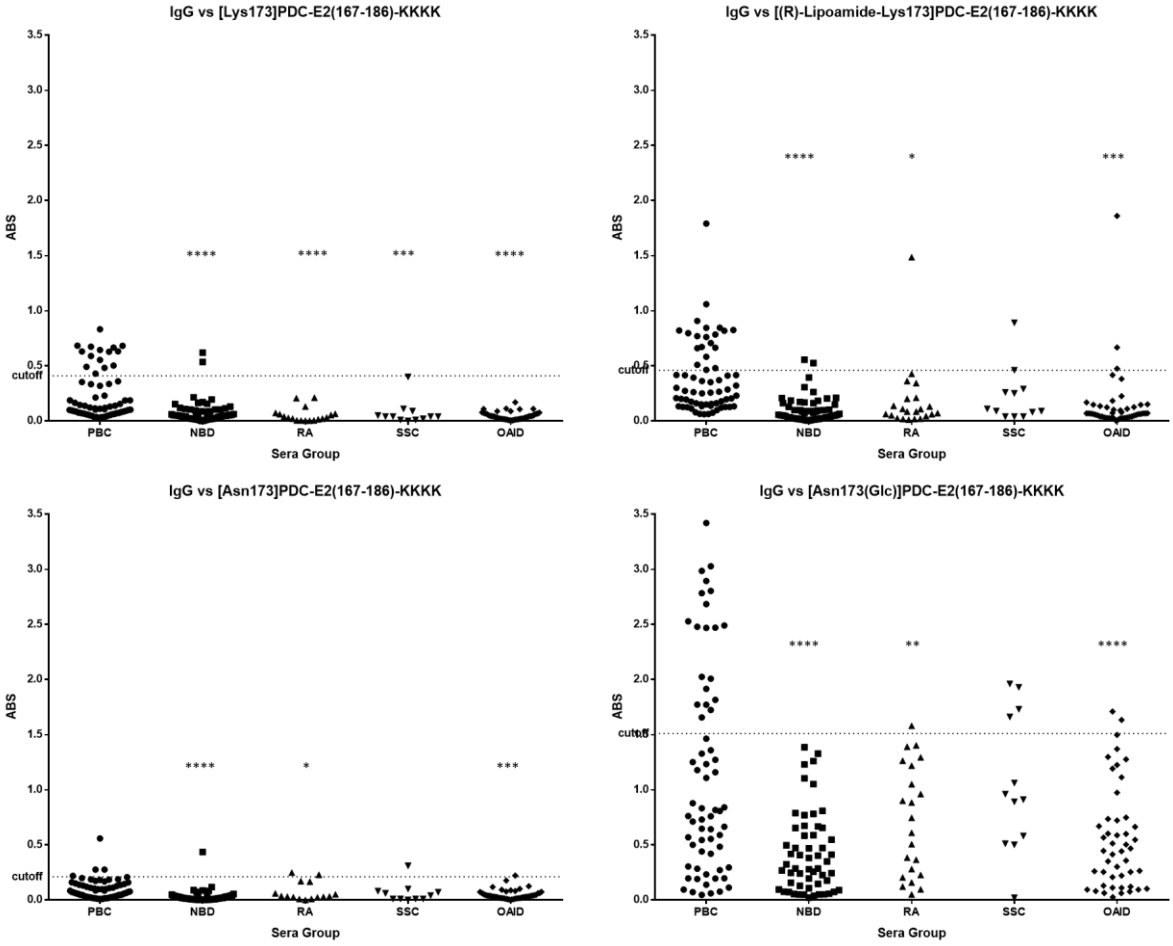

Supplementary figure 2: IgG data distribution of PBC pts and control cohorts against PDC-E2 peptides. Dotted line indicate the cutoff value.
P-values obtained comparing PBC pts with control cohorts are shown:
****** P < 0,0001; *** P 0.0001 to 0.001; ** P 0.001 to 0.01; * P 0.01 to 0.05.**

BIBLIOGRAPHY

1. Cho, J. H. & Gregersen, P. K. Genomics and the multifactorial nature of human autoimmune disease. *N. Engl. J. Med.* **365,** 1612–23 (2011).

2. Cooper, G. S., Bynum, M. L. K. & Somers, E. C. Recent insights in the epidemiology of autoimmune diseases: improved prevalence estimates and understanding of clustering of diseases. *J. Autoimmun.* **33,** 197–207 (2009).

3. Jacobson, D. L., Gange, S. J., Rose, N. R. & Graham, N. M. Epidemiology and estimated population burden of selected autoimmune diseases in the United States. *Clin. Immunol. Immunopathol.* **84,** 223–243 (1997).

4. Beeson, P. B. Age and sex associations of 40 autoimmune diseases. *Am. J. Med.* **96,** 457–462 (1994).

5. Hu, Z.-D. & Deng, A.-M. Autoantibodies in pre-clinical autoimmune disease. *Clin. Chim. Acta.* **437,** 14–18 (2014).

6. Selmi, C., Invernizzi, P., Miozzo, M., Podda, M. & Gershwin, M. E. Primary biliary cirrhosis: Does X mark the spot? *Autoimmun. Rev.* **3,** 493–499 (2004).

7. Selmi, C. *et al.* Mechanisms of environmental influence on human autoimmunity: A national institute of environmental health sciences expert panel workshop. *J. Autoimmun.* **39,** 272–284 (2012).

8. Anderton, S. M. Post-translational modifications of self antigens: Implications for autoimmunity. *Curr. Opin. Immunol.* **16,** 753–758 (2004).

9. Doyle, H. A. & Mamula, M. J. Post-translational protein modifications in antigen recognition and autoimmunity. *Trends Immunol.* **22,** 443–9 (2001).

10. Doyle, H. A. & Mamula, M. J. Posttranslational modifications of self-antigens. *Ann. N. Y. Acad. Sci.* **1050,** 1–9 (2005).

11. Doyle, H. A., Yang, M. L., Raycroft, M. T., Gee, R. J. & Mamula, M. J. Autoantigens: Novel forms and presentation to the immune system. *Autoimmunity* **47,** 220–233 (2014).

12. Mamula, M. J. *et al.* Isoaspartyl Post-translational Modification Triggers Autoimmune Responses to Self-proteins. *J. Biol. Chem.* **274,** 22321–22327 (1999).

13. Lehmann, P. V, Forsthuber, T., Miller, A. & Sercarz, E. E. Spreading of T-cell autoimmunity to cryptic determinants of an autoantigen. *Nature* **358,** 155–157 (1992).

14. Kidd, B. A. *et al.* Epitope spreading to citrullinated antigens in mouse models of autoimmune arthritis and demyelination. *Arthritis Res. Ther.* **10,** R119 (2008).

15. Walsh, S. J. & Rau, L. M. Autoimmune diseases: a leading cause of death among young and middle-aged women in the United States. *Am. J. Public Health* **90,** 1463–6 (2000).

16. Cooper, G. S. & Stroehla, B. C. The epidemiology of autoimmune diseases. *Autoimmun. Rev.* **2,** 119–125 (2003).

17. Cohen, I. R. Biomarkers, self-antigens and the immunological homunculus. *J. Autoimmun.* **29,** 246–9 (2007).

18. Papini, A. M. The use of post-translationally modified peptides for detection of biomarkers of immune-mediated diseases. *J. Pept. Sci.* **15,** 621–8 (2009).

19. Bizzaro, N. Autoantibodies as predictors of disease: the clinical and experimental evidence. *Autoimmun. Rev.* **6,** 325–33 (2007).

20. Bizzaro, N. The predictive significance of autoantibodies in organ-specific autoimmune diseases. *Clin. Rev. Allergy Immunol.* **34,** 326–31 (2008).

21. Leslie, D., Lipsky, P. & Notkins, A. L. Autoantibodies as predictors of disease. *J. Clin. Invest.* **108,** 1417–22 (2001).

22. Berger, T. & Reindl, M. Biomarkers in multiple sclerosis: role of antibodies. *Dis. Markers* **22,** 207–212 (2006).

23. Nothaft, H. & Szymanski, C. M. Protein glycosylation in bacteria: sweeter than ever. *Nat. Rev. Microbiol.* **8,** 765–778 (2010).

24. Wacker, M. *et al.* N-linked glycosylation in Campylobacter jejuni and its functional transfer into E. coli. *Science* **298,** 1790–1793 (2002).

25. Linton, D. *et al.* Functional analysis of the Campylobacter jejuni N-linked protein glycosylation pathway. *Mol. Microbiol.* **55,** 1695–1703 (2005).

26. Kowarik, M. *et al.* Definition of the bacterial N-glycosylation site consensus sequence. *EMBO J.* **25,** 1957–1966 (2006).

27. Gross, J. *et al.* The Haemophilus influenzae HMW1 adhesin is a glycoprotein with an unusual N-linked carbohydrate modification. *J. Biol. Chem.* **283,** 26010–26015 (2008).

28. Grass, S., Lichti, C. F., Townsend, R. R., Gross, J. & St. Geme, J. W. The haemophilus influenzae HMW1c protein is a glycosyltransferase that transfers hexose residues to asparagine sites in the HMW1 adhesin. *PLoS Pathog.* **6,** 1–9 (2010).

29. Chen, R. Bacterial expression systems for recombinant protein production: E. coli and beyond. *Biotechnol. Adv.* **30,** 1102–1107 (2012).

30. Dawson, P. E., Muir, T. W., Clark-Lewis, I. & Kent, S. B. Synthesis of proteins by native chemical ligation. *Science* **266,** 776–779 (1994).

31. Dawson, P. E. & Kent, S. B. Synthesis of native proteins by chemical ligation. *Annu. Rev. Biochem.* **69,** 923–960 (2000).

32. Hackeng, T. M., Griffin, J. H. & Dawson, P. E. Protein synthesis by native chemical ligation: expanded scope by using straightforward methodology. *Proc. Natl. Acad. Sci. U. S. A.* **96,** 10068–10073 (1999).

33. Gan, S. D. & Patel, K. R. Enzyme Immunoassay and Enzyme-Linked Immunosorbent Assay. *J. Invest. Dermatol.* **133,** 1–3 (2013).

34. Mazzucco, S. *et al.* A synthetic glycopeptide of human myelin oligodendrocyte glycoprotein to detect antibody responses in multiple sclerosis and other neurological diseases. *Bioorganic Med. Chem. Lett.* **9,** 167–172 (1999).

35. Carotenuto, A., D'Ursi, A. M., Nardi, E., Papini, A. M. & Rovero, P. Conformational analysis of a glycosylated human myelin oligodendrocyte glycoprotein peptide epitope able to detect antibody response in multiple sclerosis. *J. Med. Chem.* **44,** 2378–2381 (2001).

36. Lolli, F. *et al.* An N-glucosylated peptide detecting disease-specific autoantibodies, biomarkers of multiple sclerosis. *Proc. Natl. Acad. Sci. U. S. A.* **102,** 10273–10278 (2005).

37. Lolli, F. *et al.* The glycopeptide CSF114(Glc) detects serum antibodies in multiple sclerosis. *J. Neuroimmunol.* **167,** 131–137 (2005).

38. Papini, A. M. Simple test for multiple sclerosis. *Nat. Med.* **11,** 13 (2005).

39. Kikonomou, K. G., Zachou, K. & Dalekos, G. N. Alpha-actinin: A multidisciplinary protein with important role in B-cell driven autoimmunity. *Autoimmun. Rev.* **10,** 389–396 (2011).

40. Pandey, S. *et al.* Alpha actinin is specifically recognized by Multiple Sclerosis autoantibodies isolated using an N-glucosylated peptide epitope. *Mol. Cell. Proteomics* **12,** 277–82 (2013).

41. Brunner, C., Lassmann, H., Waehneldt, T. V, Matthieu, J. M. & Linington, C. Differential ultrastructural localization of myelin basic protein, myelin/oligodendroglial glycoprotein, and 2',3'-cyclic nucleotide 3'-phosphodiesterase in the CNS of adult rats. *J. Neurochem.* **52,** 296–304 (1989).

42. Johns, T. G. & Bernard, C. C. A. The structure and function of myelin oligodendrocyte glycoprotein. *J. Neurochem.* **72,** 1–9 (1999).

43. Pham-Dinh, D. *et al.* Characterization and expression of the cDNA coding for the human myelin/oligodendrocyte glycoprotein. *J. Neurochem.* **63,** 2353–2356 (1994).

44. Hemmer, B., Archelos, J. J. & Hartung, H.-P. New concepts in the immunopathogenesis of multiple sclerosis. *Nat. Rev. Neurosci.* **3,** 291–301 (2002).

45. Kroepfl, J. F., Viise, L. R., Charron, A. J., Linington, C. & Gardinier, M. V. Investigation of myelin/oligodendrocyte glycoprotein membrane topology. *J. Neurochem.* **67,** 2219–2222 (1996).

46. Breithaupt, C. *et al.* Structural insights into the antigenicity of myelin oligodendrocyte glycoprotein. *Proc. Natl. Acad. Sci. U. S. A.* **100,** 9446–51 (2003).

47. Clements, C. S. *et al.* The crystal structure of myelin oligodendrocyte glycoprotein, a key autoantigen in multiple sclerosis. *Proc. Natl. Acad. Sci. U. S. A.* **100,** 11059–64 (2003).

48. Slavin, A. J., Johns, T. G., Orian, J. M. & Bernard, C. C. Regulation of myelin oligodendrocyte glycoprotein in different species throughout development. *Dev. Neurosci.* **19,** 69–78 (1997).

49. Linnington, C., Webb, M. & Woodhams, P. A novel myelin-associated glycoprotein defined by a mouse monoclonal antibody. *J. Neuroimmunol.* **6,** 387–396 (1984).

50. Schluesener, H. J., Sobel, R. A., Linington, C. & Weiner, H. L. A monoclonal antibody against a myelin oligodendrocyte glycoprotein induces relapses and demyelination in central nervous system autoimmune disease. *J. Immunol.* **139,** 4016–4021 (1987).

51. Lassmann, H., Brück, W. & Lucchinetti, C. F. The immunopathology of multiple sclerosis: An overview. in *Brain Pathol.* **17,** 210–218 (2007).

52. Lin, C. H., Kadakia, S. & Frieri, M. New insights into an autoimmune mechanism, pharmacological treatment and relationship between multiple sclerosis and inflammatory bowel disease. *Autoimmun. Rev.* **13,** 114–116 (2014).

53. Denic, A. *et al.* The relevance of animal models in multiple sclerosis research. *Pathophysiology* **18,** 21–29 (2011).

54. Van der Star, B. J. *et al.* In vitro and in vivo models of multiple sclerosis. *CNS Neurol. Disord. Drug Targets* **11,** 570–88 (2012).

55. Miller, D., Barkhof, F., Montalban, X., Thompson, A. & Filippi, M. Clinically isolated syndromes suggestive of multiple sclerosis, part I: Natural history, pathogenesis, diagnosis, and prognosis. *Lancet Neurol.* **4,** 281–288 (2005).

56. Milo, R. & Miller, A. Revised diagnostic criteria of multiple sclerosis. *Autoimmun. Rev.* **13,** 518–524 (2014).

57. Ramagopalan, S. V., Dobson, R., Meier, U. C. & Giovannoni, G. Multiple sclerosis: risk factors, prodromes, and potential causal pathways. *Lancet Neurol.* **9,** 727–739 (2010).

58. Fraussen, J., Claes, N., de Bock, L. & Somers, V. Targets of the humoral autoimmune response in multiple sclerosis. *Autoimmun. Rev.* (2014). doi:10.1016/j.autrev.2014.07.002

59. Fraussen, J. *et al.* B cell characterization and reactivity analysis in multiple sclerosis. *Autoimmun. Rev.* **8,** 654–658 (2009).

60. Somers, K., Govarts, C., Stinissen, P. & Somers, V. Multiplexing approaches for autoantibody profiling in multiple sclerosis. *Autoimmun. Rev.* **8,** 573–579 (2009).

61. Cole, S. R., Beck, R. W., Moke, P. S., Kaufman, D. I. & Tourtellotte, W. W. The predictive value of CSF oligoclonal banding for MS 5 years after optic neuritis. Optic Neuritis Study Group. *Neurology* **51,** 885–887 (1998).

62. Reindl, M., Khalil, M. & Berger, T. Antibodies as biological markers for pathophysiological processes in MS. *J. Neuroimmunol.* **180,** 50–62 (2006).

63. Quandt, J. a *et al.* Myelin basic protein-specific TCR/HLA-DRB5*01:01 transgenic mice support the etiologic role of DRB5*01:01 in multiple sclerosis. *J. Immunol.* **189,** 2897–908 (2012).

64. Rao, P. & Segal, B. M. Experimental autoimmune encephalomyelitis. *Methods Mol. Biol.* **900,** 363–380 (2012).

65. Gran, B., O'Brien, K., Fitzgerald, D. & Rostami, A. Experimental Autoimmune Encephalomyelitis. *Handb. Neurochem. Mol. Neurobiol. A. Lajtha. Springer Heidelb.* 19 (2007).

66. Libbey, J. E. & Fujinami, R. S. Experimental autoimmune encephalomyelitis as a testing paradigm for adjuvants and vaccines. *Vaccine* **29,** 3356–3362 (2011).

67. Wingerchuk, D. M., Hogancamp, W. F., O'Brien, P. C. & Weinshenker, B. G. The clinical course of neuromyelitis optica (Devic's syndrome). *Neurology* **53,** 1107–1114 (1999).

68. Cree, B. A. C., Goodin, D. S. & Hauser, S. L. Neuromyelitis optica. *Semin. Neurol.* **22,** 105–122 (2002).

69. De Seze, J. Neuromyelitis optica. *Arch. Neurol.* **60,** 1336–1338 (2003).

70. Weinshenker, B. G. Neuromyelitis optica: what it is and what it might be. *Lancet* **361,** 889–890 (2003).

71. Wingerchuk, D. M., Lennon, V. A., Pittock, S. J., Lucchinetti, C. F. & Weinshenker, B. G. Revised diagnostic criteria for neuromyelitis optica. *Neurology* **66,** 1485–1489 (2006).

72. Lennon, V. A. *et al.* A serum autoantibody marker of neuromyelitis optica: Distinction from multiple sclerosis. *Lancet* **364,** 2106–2112 (2004).

73. Pittock, S. J. *et al.* Brain abnormalities in neuromyelitis optica. *Arch. Neurol.* **63,** 390–396 (2006).

74. Pittock, S. J. *et al.* Neuromyelitis optica brain lesions localized at sites of high aquaporin 4 expression. *Arch. Neurol.* **63,** 964–968 (2006).

75. Wingerchuk, D. M., Lennon, V. A., Lucchinetti, C. F., Pittock, S. J. & Weinshenker, B. G. The spectrum of neuromyelitis optica. *Lancet Neurol.* **6,** 805–815 (2007).

76. Keegan, M. *et al.* Relation between humoral pathological changes in multiple sclerosis and response to therapeutic plasma exchange. *Lancet* **366,** 579–582 (2005).

77. Lassmann, H. Multiple sclerosis: Lessons from molecular neuropathology. *Exp. Neurol.* (2013). doi:10.1016/j.expneurol.2013.12.003

78. Na, S. Y. *et al.* Naïve CD8 T-cells initiate spontaneous autoimmunity to a sequestered model antigen of the central nervous system. *Brain* **131,** 2353–2365 (2008).

79. Saxena, A. *et al.* Cutting edge: Multiple sclerosis-like lesions induced by effector CD8 T cells recognizing a sequestered antigen on oligodendrocytes. *J. Immunol.* **181,** 1617–1621 (2008).

80. Linington, C., Bradl, M., Lassmann, H., Brunner, C. & Vass, K. Augmentation of demyelination in rat acute allergic encephalomyelitis by circulating mouse monoclonal antibodies directed against a myelin/oligodendrocyte glycoprotein. *Am. J. Pathol.* **130,** 443–454 (1988).

81. Bornstein, M. B. & Appel, S. H. Tissue culture studies of demyelination. *Ann. N. Y. Acad. Sci.* **122,** 280–286 (1965).

82. Hughes, D. & Field, E. J. Myelinotoxicity of serum and spinal fluid in multiple sclerosis: a critical assessment. *Clin. Exp. Immunol.* **2,** 295–309 (1967).

83. Lumsden, C. E. The immunogenesis of the multiple sclerosis plaque. *Brain Res.* **28,** 365–390 (1971).

84. Lebar, R., Boutry, J. M., Vincent, C., Robineaux, R. & Voisin, G. A. Studies on autoimmune encephalomyelitis in the guinea pig. II. An in vitro investigation on the nature, properties, and specificity of the serum-demyelinating factor. *J. Immunol.* **116,** 1439–1446 (1976).

85. Lebar, R., Lubetzki, C., Vincent, C., Lombrail, P. & Boutry, J. M. The M2 autoantigen of central nervous system myelin, a glycoprotein present in oligodendrocyte membrane. *Clin. Exp. Immunol.* **66,** 423–434 (1986).

86. Appel, S. H. & Bornstein, M. B. The Application of Tissue Culture to the Study of Experimental Allergic Encephalomyelitis. *J. Exp. Med.* **119,** 303–312 (1964).

87. Bornstein, M. B. & Appel, S. G. The application of tissue culture to the study of experimental allergic encephalomyelitis. I. Pattern of demyelination. *J. Neuropathol. Exp. Neurol.* **20,** 141–147 (1961).

88. Grundke-Iqbal, I., Raine, C. S., Johnson, A. B., Brosnan, C. F. & Bornstein, M. B. Experimental allergic encephalomyelitis. Characterization of serum factors causing demyelination and swelling of myelin. *J. Neurol. Sci.* **50,** 63–79 (1981).

89. Lassmann, H., Kitz, K. & Wisniewski, H. M. In vivo effect of sera from animals with chronic relapsing experimental allergic encephalomyelitis on central and peripheral myelin. *Acta Neuropathol.* **55,** 297–306 (1981).

90. Lassmann, H., Stemberger, H., Kitz, K. & Wisniewski, H. M. In vivo demyelinating activity of sera from animals with chronic experimental allergic encephalomyelitis. Antibody nature of the demyelinating factor and the role of complement. *J. Neurol. Sci.* **59,** 123–137 (1983).

91. Linington, C. & Lassmann, H. Antibody responses in chronic relapsing experimental allergic encephalomyelitis: correlation of serum demyelinating activity with antibody titre to the myelin/oligodendrocyte glycoprotein (MOG). *J. Neuroimmunol.* **17,** 61–69 (1987).

92. Von Büdingen, H. C. *et al.* Immune responses against the myelin/oligodendrocyte glycoprotein in experimental autoimmune demyelination. *J. Clin. Immunol.* **21,** 155–170 (2001).

93. Bettadapura, J., Menon, K. K., Moritz, S., Liu, J. & Bernard, C. C. Expression, purification, and encephalitogenicity of recombinant human myelin oligodendrocyte glycoprotein. *J. Neurochem.* **70,** 1593–1599 (1998).

94. Genain, C. P. *et al.* Antibody facilitation of multiple sclerosis-like lesions in a nonhuman primate. *J. Clin. Invest.* **96,** 2966–2974 (1995).

95. Storch, M. K. *et al.* Autoimmunity to myelin oligodendrocyte glycoprotein in rats mimics the spectrum of multiple sclerosis pathology. *Brain Pathol.* **8,** 681–694 (1998).

96. Storch, M. K. *et al.* Cortical demyelination can be modeled in specific rat models of autoimmune encephalomyelitis and is major histocompatibility complex (MHC) haplotype-related. *J. Neuropathol. Exp. Neurol.* **65,** 1137–1142 (2006).

97. Peters, A. *et al.* Th17 Cells Induce Ectopic Lymphoid Follicles in Central Nervous System Tissue Inflammation. *Immunity* **35,** 986–996 (2011).

98. Von Büdingen, H. C. *et al.* Frontline: Epitope recognition on the myelin/oligodendrocyte glycoprotein differentially influences disease phenotype and antibody effector functions in autoimmune demyelination. *Eur. J. Immunol.* **34,** 2072–2083 (2004).

99. Marta, C. B., Oliver, A. R., Sweet, R. a, Pfeiffer, S. E. & Ruddle, N. H. Pathogenic myelin oligodendrocyte glycoprotein antibodies recognize glycosylated epitopes and perturb oligodendrocyte physiology. *Proc. Natl. Acad. Sci. U. S. A.* **102,** 13992–7 (2005).

100. Brehm, U., Piddlesden, S. J., Gardinier, M. V. & Linington, C. Epitope specificity of demyelinating monoclonal autoantibodies directed against the human myelin oligodendrocyte glycoprotein (MOG). *J. Neuroimmunol.* **97,** 9–15 (1999).

101. Ichikawa, M., Johns, T. G., Adelmann, M. & Bernard, C. C. Antibody response in Lewis rats injected with myelin oligodendrocyte glycoprotein derived peptides. *Int. Immunol.* **8,** 1667–74 (1996).

102. Lalive, P. H. Auto antibodies in inflammatory demyelinating diseases of the central nervous system. *Swiss Med Wkly.* **138,** 692–707 (2008).

103. Mayer, M. C. & Meinl, E. Glycoproteins as targets of autoantibodies in CNS inflammation: MOG and more. *Ther. Adv. Neurol. Disord.* **5,** 147–159 (2012).

104. Reindl, M., Di Pauli, F., Rostásy, K. & Berger, T. The spectrum of MOG autoantibody-associated demyelinating diseases. *Nat. Rev. Neurol.* **9,** 455–61 (2013).

105. Xiao, B. G., Linington, C. & Link, H. Antibodies to myelin-oligodendrocyte glycoprotein in cerebrospinal fluid from patients with multiple sclerosis and controls. *J. Neuroimmunol.* **31,** 91–96 (1991).

106. Reindl, M. *et al.* Antibodies against the myelin oligodendrocyte glycoprotein and the myelin basic protein in multiple sclerosis and other neurological diseases: a comparative study. *Brain* **122,** 2047–56 (1999).

107. Gaertner, S., de Graaf, K. L., Greve, B. & Weissert, R. Antibodies against glycosylated native MOG are elevated in patients with multiple sclerosis. *Neurology* **63,** 2381–2383 (2004).

108. O'Connor, K. C. *et al.* Antibodies from inflamed central nervous system tissue recognize myelin oligodendrocyte glycoprotein. *J. Immunol.* **175,** 1974–1982 (2005).

109. Zhou, D. *et al.* Identification of a pathogenic antibody response to native myelin oligodendrocyte glycoprotein in multiple sclerosis. *Proc. Natl. Acad. Sci. U. S. A.* **103,** 19057–19062 (2006).

110. Lalive, P. H. *et al.* Antibodies to native myelin oligodendrocyte glycoprotein are serologic markers of early inflammation in multiple sclerosis. *Proc. Natl. Acad. Sci. U. S. A.* **103,** 2280–2285 (2006).

111. Menge, T., von Budingen, H. C., Lalive, P. H. and & Genain, C. P. Relevant antibody subsets against MOG recognize conformational epitopes exclusively exposed in solid-phase ELISA. *Eur J Immunol* **37,** 3229–3239 (2007).

112. McLaughlin, K. A. *et al.* Age-dependent B cell autoimmunity to a myelin surface antigen in pediatric multiple sclerosis. *J. Immunol.* **183,** 4067–4076 (2009).

113. Klawiter, E. C. *et al.* Elevated intrathecal myelin oligodendrocyte glycoprotein antibodies in multiple sclerosis. *Arch. Neurol.* **67,** 1102–1108 (2010).

114. Kuhle, J. *et al. Lack of association between antimyelin antibodies and progression to multiple sclerosis. N. Engl. J. Med.* **356,** 371–378 (2007).

115. Pelayo, R. *et al.* Antimyelin antibodies with no progression to multiple sclerosis. *N Engl J Med* **356,** 426–428 (2007).

116. O'Connor, K. C. *et al.* Self-antigen tetramers discriminate between myelin autoantibodies to native or denatured protein. *Nat. Med.* **13,** 211–217 (2007).

117. Di Pauli, F. *et al.* Temporal dynamics of anti-MOG antibodies in CNS demyelinating diseases. *Clin. Immunol.* **138,** 247–254 (2011).

118. Gori, F. *et al.* IgG and IgM antibodies to the refolded MOG1-125 extracellular domain in humans. *J. Neuroimmunol.* **233,** 216–220 (2011).

119. Tenembaum, S. N. Emerging concepts in pediatric-onset multiple sclerosis and related disorders. *Curr. Opin. Pediatr.* **22,** 726–730 (2010).

120. Lalive, P. H. *et al.* Highly reactive anti-myelin oligodendrocyte glycoprotein antibodies differentiate demyelinating diseases from viral encephalitis in children. *Mult. Scler.* **17,** 297–302 (2011).

121. Pröbstel, A. K. *et al.* Antibodies to MOG are transient in childhood acute disseminated encephalomyelitis. *Neurology* **77,** 580–588 (2011).

122. Chou, I.-J., Whitehouse, W. P., Wang, H.-S., Tanasescu, R. & Constantinescu, C. S. Diagnostic modalities in multiple sclerosis: perspectives in children. *Biomed. J.* **37,** 50–9 (2014).

123. Karni, A., Bakimer-Kleiner, R., Abramsky, O. & Ben-Nun, A. Elevated levels of antibody to myelin oligodendrocyte glycoprotein is not specific for patients with multiple sclerosis. *Arch. Neurol.* **56,** 311–315 (1999).

124. Lindert, R. B. *et al.* Multiple sclerosis: B- and T-cell responses to the extracellular domain of the myelin oligodendrocyte glycoprotein. *Brain* **122,** 2089–2099 (1999).

125. Egg, R., Reindl, M., Deisenhammer, F., Linington, C. & Berger, T. Anti-MOG and anti-MBP antibody subclasses in multiple sclerosis. *Mult. Scler.* **7,** 285–289 (2001).

126. Berger, T. *et al.* Antimyelin antibodies as a predictor of clinically definite multiple sclerosis after a first demyelinating event. *N. Engl. J. Med.* **349,** 139–145 (2003).

127. Vojdani, A., Vojdani, E. & Cooper, E. Antibodies to myelin basic protein, myelin oligodendrocytes peptides, alpha-beta-crystallin, lymphocyte activation and cytokine production in patients with multiple sclerosis. *J. Intern. Med.* **254,** 363–374 (2003).

128. Kennel De March, A. *et al.* Anti-myelin oligodendrocyte glycoprotein B-cell responses in multiple sclerosis. *J. Neuroimmunol.* **135,** 117–125 (2003).

129. Lampasona, V. *et al.* Similar low frequency of anti-MOG IgG and IgM in MS patients and healthy subjects. *Neurology* **62,** 2092–2094 (2004).

130. Mantegazza, R. *et al.* Anti-MOG autoantibodies in Italian multiple sclerosis patients: Specificity, sensitivity and clinical association. *Int. Immunol.* **16,** 559–565 (2004).

131. Wang, H. *et al.* Myelin oligodendrocyte glycoprotein antibodies and multiple sclerosis in healthy young adults. *Neurology* **71,** 1142–1146 (2008).

132. Menge, T., Lalive, P. H., von Büdingen, H.-C. & Genain, C. P. Conformational epitopes of myelin oligodendrocyte glycoprotein are targets of potentially pathogenic antibody responses in multiple sclerosis. *J. Neuroinflammation* **8,** 161 (2011).

133. Hohenester, S., Oude-Elferink, R. P. J. & Beuers, U. Primary biliary cirrhosis. *Semin. Immunopathol.* **31,** 283–307 (2009).

134. Prince, M. I., Chetwynd, A., Craig, W. L., Metcalf, J. V & James, O. F. W. Asymptomatic primary biliary cirrhosis: clinical features, prognosis, and symptom progression in a large population based cohort. *Gut* **53,** 865–870 (2004).

135. Lindor, K. D. *et al.* Primary Biliary Cirrhosis. *Hepatology* **50,** 291– 307 (2009).

136. Selmi, C. *et al.* Primary biliary cirrhosis in monozygotic and dizygotic twins: Genetics, epigenetics, and environment. *Gastroenterology* **127,** 485–492 (2004).

137. Selmi, C., Meroni, P. L. & Gershwin, M. E. Primary biliary cirrhosis and Sjögren's syndrome: Autoimmune epithelitis. *J. Autoimmun.* **39,** 34–42 (2012).

138. Invernizzi, P., Selmi, C., Mackay, I. R., Podda, M. & Gershwin, M. E. From bases to basis: Linking genetics to causation in primary biliary cirrhosis. *Clin. Gastroenterol. Hepatol.* **3,** 401–410 (2005).

139. Lazaridis, K. N. *et al.* Increased prevalence of antimitochondrial antibodies in first-degree relatives of patients with primary biliary cirrhosis. *Hepatology* **46,** 785–792 (2007).

140. Jones, D. E. J., Watt, F. E., Metcalf, J. V., Bassendine, M. F. & James, O. F. W. Familial primary hiliary cirrhosis reassessed: A geographically-based population study. *J. Hepatol.* **30,** 402–407 (1999).

141. Liu, X. *et al.* Genome-wide meta-analyses identify three loci associated with primary biliary cirrhosis. *Nat. Genet.* **42,** 658–660 (2010).

142. Mells, G. F. *et al.* Genome-wide association study identifies 12 new susceptibility loci for primary biliary cirrhosis. *Nat Genet* **43,** 329–332 (2011).

143. Nakamura, M. *et al.* Genome-wide association study identifies TNFSF15 and POU2AF1 as susceptibility loci for primary biliary cirrhosis in the Japanese population. *Am. J. Hum. Genet.* **91,** 721–728 (2012).

144. Selmi, C. *et al.* Patients With Primary Biliary Cirrhosis React Against a Ubiquitous Xenobiotic-Metabolizing Bacterium. *Hepatology* **38,** 1250–1257 (2003).

145. Bogdanos, D. P. *et al.* Microbial mimics are major targets of crossreactivity with human pyruvate dehydrogenase in primary biliary cirrhosis. *J. Hepatol.* **40,** 31–39 (2004).

146. Selmi, C., De Santis, M., Cavaciocchi, F. & Gershwin, M. E. Infectious agents and xenobiotics in the etiology of primary biliary cirrhosis. *Dis. Markers* **29,** 287–299 (2010).

147. Gershwin, M. E. *et al.* Primary biliary cirrhosis: an orchestrated immune response against epithelial cells. *Immunol. Rev.* **174,** 210–25 (2000).

148. Kaplan, M. M. & Gershwin, M. E. Primary biliary cirrhosis. *N. Engl. J. Med.* **353,** 1261–73 (2005).

149. Gershwin, M. E., Mackay, I. A. N. R. & Coppel, R. L. Identification and specificity of a cDNA encoding the 70 Kd mitochondrial antigen recognized in primary biliary cirrhosis. 3525–3531 (1987).

150. Mackay, I. R. Primary biliary cirrhosis showing a high titer of autoantibody. *N Engl J Med* **258,** 185–87 (1958).

151. Walker, J., Doniach, D., Roitt, I. & Scherlock, S. Serological tests in diagnosis of primary biliary cirrhosis. *Lancet* **i,** 827–31 (1965).

152. Yeaman, S. J. *et al.* Primary biliary cirrhosis: identification of two major M2 mitochondrial autoantigens. *Lancet* **1,** 1067–1070 (1988).

153. Van de Water, J., Gershwin, M. E., Leung, P. S., Ansari, A. & Coppel, R. L. The Autoepitope Of The 74-Kd Mitochondrial Autoantigen Of Primary Biliary Cirrhosis Corresponds To The Functional Site Of Dihydrolipoamide Acetyltransferase. *J. Exp. Med.* **167,** 1791–1799 (1988).

154. Coppel, R. L. *et al.* Primary structure of the human M2 mitochondrial autoantigen of primary biliary cirrhosis: dihydrolipoamide acetyltransferase. *Proc. Natl. Acad. Sci. U. S. A.* **85,** 7317–21 (1988).

155. Moteki, S. *et al.* Epitope mapping and reactivity of autoantibodies to the E2 component of 2-oxoglutarate dehydrogenase complex in primary biliary cirrhosis using recombinant 2-oxoglutarate dehydrogenase complex. *Hepatology* **23,** 436–444 (1996).

156. Odin, J. A., Huebert, R. C., Casciola-Rosen, L., LaRusso, N. F. & Rosen, A. Bcl-2-dependent oxidation of pyruvate dehydrogenase-E2, a primary biliary cirrhosis autoantigen, during apoptosis. *J. Clin. Invest.* **108,** 223–232 (2001).

157. Bruggraber, S. *et al.* Autoreactivity to lipoate and a conjugated form of lipoate in primary biliary cirrhosis. *Gastroenterology* **6,** 1705–13 (2003).

158. Allina, J. *et al.* T cell targeting and phagocytosis of apoptotic biliary epithelial cells in primary biliary cirrhosis. *J Autoimmun* **27,** 232–241 (2006).

159. Lleo, A. *et al.* Apotopes and the biliary specificity of primary biliary cirrhosis. *Hepatology* **49,** 871–879 (2009).

160. Lleo, A. *et al.* Biliary apotopes and anti-mitochondrial antibodies activate innate immune responses in primary biliary cirrhosis. *Hepatology* **52,** 987–996 (2010).

161. Fussey, S. P. *et al.* Reactivity of primary biliary cirrhosis sera with Escherichia Coli dihydrolipoamide acetyltransferase (E2p): characterization of the main immunogenic region. *Proc. Natl. Acad. Sci. U. S. A.* **87,** 3987–91 (1990).

162. Braun, S. Catalytic domain of PDC-E2 contains epitopes recognized by antimitochondrial antibodies in primary biliary cirrhosis. *World J. Gastroenterol.* **16,** 973 (2010).

163. Dardel, F., Laue, E. D. & Perham, R. N. Sequence-specific H-NMR assignments and secondary structure of the lipo yl domain of the Bacillus stearothermophilus pyruvate dehydrogenase multienzyme complex. **209,** 203–209 (1991).

164. Quinn, J. *et al.* Lipoylated and unlipoylated domains of human PDC-E2 as autoantigens in primary biliary cirrhosis: Significance of lipoate attachment. *Hepatology* **18,** 1384–1391 (1993).

165. Howard, M. J. *et al.* Three-dimensional structure of the major autoantigen in primary biliary cirrhosis. *Gastroenterology* **115,** 139–46 (1998).

166. Mutimer, D. J. *et al.* Frequency of IgG and IgM autoantibodies to four specific M2 mitochondrial autoantigens in primary biliary cirrhosis. *Hepatology* **10,** 403–407 (1989).

167. Leung, P. S., Iwayama, T., Coppel, R. L. & Gershwin, M. E. Site-directed mutagenesis of lysine within the immunodominant autoepitope of PDC-E2. *Hepatology* **12,** 1321–1328 (1990).

168. Tuaillon, N., Andre, C., Briand, J. P., Penner, E. & Muller, S. A lipoyl synthetic octadecapeptide of dihydrolipoamide acetyltransferase specifically recognized by anti-M2 autoantibodies in primary biliary cirrhosis. *J. Immunol.* **148,** 445–50 (1992).

169. Koike, K., Ishibashi, H. & Koike, M. Immunoreactivity of porcine heart dihydrolipoamide acetyl- and succinyl-transferases (PDC-E2, OGDC-E2) with primary biliary cirrhosis sera: characterization of the autoantigenic region and effects of enzymatic delipoylation and relipoylation. *Hepatology* **27,** 1467–74 (1998).

170. Jones, D. D., Stott, K. M., Howard, M. J. & Perham, R. N. Restricted motion of the lipoyl-lysine swinging arm in the pyruvate dehydrogenase complex of Escherichia coli. *Biochemistry* **39,** 8448–8459 (2000).

171. Vijayakrishnan, S. *et al.* Solution structure and characterisation of the human pyruvate dehydrogenase complex core assembly. *J. Mol. Biol.* **399,** 71–93 (2010).

172. Long, S. a *et al.* Immunoreactivity of organic mimeotopes of the E2 component of pyruvate dehydrogenase: connecting xenobiotics with primary biliary cirrhosis. *J. Immunol.* **167,** 2956–63 (2001).

173. Naiyanetr, P. *et al.* Electrophile-modified lipoic derivatives of PDC-E2 elicits anti-mitochondrial antibody reactivity. *J. Autoimmun.* **37,** 209–216 (2011).

174. Amano, K. *et al.* Chemical xenobiotics and mitochondrial autoantigens in primary biliary cirrhosis: identification of antibodies against a common environmental, cosmetic, and food additive, 2-octynoic acid. *J. Immunol.* **174,** 5874–5883 (2005).

175. Leung, P. S. C. *et al.* Environment and primary biliary cirrhosis: electrophilic drugs and the induction of AMA. *J. Autoimmun.* **41,** 79–86 (2013).

176. Chen, R. C. Y. *et al.* Antimitochondrial antibody heterogeneity and the xenobiotic etiology of primary biliary cirrhosis. *Hepatology* **57,** 1498–1508 (2013).

177. Carotenuto, A. *et al.* Conformation - Activity Relationship of Designed Glycopeptides as Synthetic Probes for the Detection of Autoantibodies , Biomarkers of Multiple Sclerosis. *J. Med. Chem.* 5072–5079 (2006).

178. Jiang, Y. & Cronan, J. E. Expression cloning and demonstration of Enterococcus faecalis lipoamidase (pyruvate dehydrogenase inactivase) as a Ser-Ser-Lys triad amidohydrolase. *J. Biol. Chem.* **280,** 2244–56 (2005).

179. Spalding, M. D. & Prigge, S. T. The amidase domain of lipoamidase specifically inactivates lipoylated proteins in vivo. *PLoS One* **4,** e7392 (2009).

180. Kouroumalis, E. Environmental agents involved in the cause of primary biliary cirrhosis. *Dis. Markers* **29,** 329–36 (2010).

181. Uibo, R., Kisand, K., Yang, C.-Y. & Gershwin, M. E. Primary biliary cirrhosis: a multi-faced interactive disease involving genetics, environment and the immune response. *APMIS* **120,** 857–71 (2012).

182. Head, R. A. *et al.* Clinical and genetic spectrum of pyruvate dehydrogenase deficiency: Dihydrolipoamide acetyltransferase (E2) deficiency. *Ann. Neurol.* **58,** 234–241 (2005).

183. Van de Water, J. *et al.* Detection of autoantibodies to recombinant mitochondrial proteins in patients with primary biliary cirrhosis. *N. Engl. J. Med.* **320,** 1377–1380 (1989).

184. Uibo, R. *et al.* Inhibition of enzyme function by human autoantibodies to an autoantigen pyruvate dehydrogenase E2: different epitope for spontaneous human and induced rabbit autoantibodies. *Clin. Exp. Immunol.* **80,** 19–24 (1990).

ABBREVIATIONS

AID	Autoimmune Disease	Ig	Immunoglobulin
Aa	Aminoacid	IIF	Indirect Immunofluorescence
Ab	Antibody	K	Lys
ABS	Absorbance	kDa	kilo Daltom
Ag	Antigen	mAb	Monoclonal Ab
AMA	Anti-Mitochondrial Antibodies	MBP	Myelin Basic Protein
APC	Antigen Presenting Cell	MHC	Major Histocompatibility Complex
AQP4	Aquaporin-4	MOG	Myelin Oligodendrocyte Glycoprotein
BCKD-E2	Dehydrogenase Dihydrolipoyl Transacylase	mRNA	Messenger RNA
BM	Biomarker	MS	Multiple Sclerosis
BSA	Bovine Serum Albumin	NBD	Normal Blood Donors
C.jejuni	*Campylobacter jejuni*	NCL	Native Chemical Ligation
cDNA	Complementary DNA	NMO	Neuromyelitis Optice
CDR	Complementarity Determining Regions	OD	Optical Density
CIS	Clinically Isolated Syndrome	OGDC-E2	Dihydrolipoamide Succinyltransferase
CNS	Central Nervous System	OND	Other Neurological Disorders
CSF	Cerebrospinal Fluid	OVA	Ovalbumin
E.coli	*Escherichia coli*	PBC	Primary Biliary Cirrhosis
E3BP	Dihydrolipoamide Dehydrogenase Binding Protein	PDC-E2	Dihydrolipoamide Acetyltransferase
EAE	Experimental Autoimmune Encephalomyelitis	PPMS	Primary Progressive MS
ELISA	Enzyme-Linked Immunosorbent Assay	PTM	Post-Translational Modification
FACS	Fluorescence-Activated Flow Cytometry	pts	Patients
FBS	Fetal Bovine Serum	RA	Rheumatoid Arthritis
Glc	Glucose	RRMS	Relapsing-Remitting MS
GlcNAc	N-Acetyl-Glucosamine	SLE	Systemic Lupus Erytemathosus
GWAS	Genome-Wide Association Studies	SP-ELISA	Solid Phase ELISA
H.infulenzae	*Haemophilus influenzae*	SPMS	Secondary Progressive MS
HIBEC	Human Intrahepatic Biliary Epithelium Cells	SPPS	Solid-Phase Peptide Synthesis
HLA	Human Leukocyte Antigen	SSC	Scleroderma
HMW1	High-Molecular-Weight Adhesin 1	TEV	*Tobacco Etch Virus*
IB	Inclusion Bodies	ul	microliter